GENETIC VARIATION IN THE VOLTAGE-GATED POTASSIUM CHANNEL GENES *KCNV2* AND *KCNB1* CONTRIBUTES TO EPILEPSY SUSCEPTIBILITY

By

Benjamin Jorge

Dissertation

Submitted to the Faculty of the

Graduate School of Vanderbilt University

In partial fulfillment of the requirements

for the degree of

DOCTOR OF PHILOSOPHY

In

Neuroscience

December 2014

Nashville, Tennessee

Approved:

Jennifer Kearney, Ph.D.

Alfred George, Jr., M.D.

Kevin Ess, M.D., Ph.D.

Douglas Mortlock, Ph.D.

To my son, Oliver,

“Do not be too timid and squeamish about your actions. All life is an experiment… What if you do fail, and get fairly rolled in the dirt once or twice? Up again, you shall never be so afraid of a tumble.”

-Ralph Waldo Emerson

To my wife, Paige,

In this grand experiment, you are the discovery of a lifetime.

ACKNOWLEDGEMENTS

Thank you, Dr. Jennifer Kearney, for all of the time and effort you have invested in me as my mentor. You are an excellent scientist and a wonderful person, and I am truly grateful for all that I have learned from you, both professionally and personally. I will always consider you a close friend.

Thank you to the members of my dissertation committee for all that each of you has contributed to my development as a scientist. Thank you, Dr. Al George, for serving as the chair of my dissertation committee, for co-sponsoring my NINDS NRSA grant, and for helping to establish the productive collaboration between our labs. Thank you, Dr. Kevin Ess, for providing me with invaluable clinical experiences as my clinical mentor in the Certificate Program in Molecular Medicine. Thank you, Dr. Doug Mortlock, for your genetic insights and for taking me on as a post-doc in your lab. I look forward to working with you.

Thank you to all of the members of the Kearney lab, both past and present. Thank you Sarah Bergren, Rebecca Somershoe, and Elizabeth Rutter, for your foundational work on the *KCNV2* project. Thank you Dr. Nicole Hawkins for helping me to navigate my way through graduate school and for being a great friend. Thank you Alison Miller for your contributions to the PNAS paper and for all your hard work as lab manager to keep the lab up and running. Thank you Dr. Jeffrey Calhoun for your input on my dissertation. Thank you Clint McCollom and Jae Maeng for your help in the lab. Thanks to everyone for making the lab a wonderful place to work.

Thank you to all of the members of the George lab for the friendly interactions that we've had over the past few years as collaborators. Thank you Jennifer Kunic for your willingness to share equipment and reagents. Thank you Dr. Courtney Campbell, Dr. Carlos Vanoye, and Kevin Bersell for your contributions to the PNAS and Annals of Neurology papers. Thank you Dr. Chris Thompson for all of your encouragement, for teaching me cell culture techniques, and for working with me to optimize the hippocampal cell culture protocol. Thank you Dr. Lyndsey Anderson for helping me with cell-surface biotinylation and for being one of the most thoughtful people I know.

Thank you to Dr. Christina Gurnett, Dr. Ali Torkamani, Dr. Robert Bjork, Jr., Dr. Jennifer Friedman, Dr. Cinnamon Bloss, Julie Cohen, Dr. Siddharth Gupta, and Dr. Sakkubai Naidu for your contributions to the PNAS and Annals of Neurology papers.

This work was funded by: the National Institute of Mental Health Neuroscience Training Grant (T32 MH64913-10), the HHMI/VUMC Certificate Program in Molecular Medicine, the Epilepsy Foundation of America Pre-doctoral Research Training Fellowship, the Ruth L. Kirschstein Pre-Doctoral National Research Service Award (F31 NSO83097-02), and Dr. Jennifer Kearney's (R01 NSO53792) funding.

Thank you to all of the coordinators and support staff of the Vanderbilt Graduate School, the Vanderbilt Integrated Graduate Program, the Vanderbilt Neuroscience Program, and the VUMC/HHMI Certificate Program in Molecular Medicine for making my graduate school experiences possible.

Finally, thank you to my family for your steadfast love and support.

TABLE OF CONTENTS

LIST OF TABLES

LIST OF FIGURES

LIST OF ABBREVIATIONS

General Abbreviations

129	129S6/SvEvTac Strain
B6	C57BL/6J strain
BFNC	Benign familial neonatal convulsions
BFNIS	Benign familial neonatal-infantile seizures
BWA	Burrows-Wheeler Aligner
CDG	congenital disorders of glycosylation
CNV	Copy number variant
CPK	Creatine phosphokinase
CGH	Comparative genomic hybridization
CSF	Cerebrospinal fluid
DS	Dravet Syndrome
EEG	Electroencephalogram
EGTA	Ethylene glycol tetraacetic acid
GATK	Genome analysis toolkit
GTCS	Generalized tonic-clonic seizures
GABA	Gamma-aminobutyric acid
GEFS+	Generalized epilepsy with febrile seizures plus
ICE-GTC	Intractable childhood epilepsy with generalized tonic-clonic seizures
Moe 1	Modifier of Epilepsy 1, chromosome 11

Moe 2	Modifier of Epilepsy 2, chromosome 19
NCL	neuronal ceroid lipfuscinosis
$NMDG^+$	N-methyl-D-glucamine
NSE	Neuron specific enolase
qRT-PCR	Quantitative RT-PCR
RACE	Rapid amplification of cDNA ends
RPA	RNase protection assay
SNP	Single nucleotide polymorphism
SNV	Single nucleotide variant
SJL	SJL/J strain
SUDEP	Sudden unexpected death in epilepsy
TSS	Transcription start site
UTR	Untranslated region
VLCFA	very long chain fatty acids
WES	Whole exome sequencing
WGS	Whole genome sequencing

Gene Abbreviations

ALG13	UDP-N-acetylglucosaminyltransferase subunit
ARX	Aristaless related homeobox
BAHCC1	BAH domain and coiled-coil containing 1
CDKL5	Cyclin-dependent kinase-like 5
CHD2	Chromodomain helicase DNA binding protein 2
FOXG1	Forkhead box G1

GABRA1	GABA A receptor, alpha 1
GABRA3	GABA A receptor, alpha 3
GRIN2A	Glutamate receptor, ionotroic, N-methyl D-aspartate 2A
HCN1	Hyperpolarization activated cyclic nucleotide-gated potassium channel
HRNBP3	RNA binding protein, FOX-1 homolog
KCNA1	Potassium voltage-gated channel, subfamily A, member 1
KCNAB2	Potassium voltage-gated channel, subfamily B, beta member 2
KCNB1	Potassium voltage-gated channel, subfamily B, member 1
KCND2	Potassium voltage-gated channel, subfamily D, member 2
KCNH2	Potassium voltage-gated channel, subfamily H, member 2
KCNQ2	Potassium voltage-gated channel, subfamily Q, member 2
KCNQ3	Potassium voltage-gated channel, subfamily Q, member 3
KCNV2	Potassium voltage-gated channel, subfamily V, member 2
MECP2	Methyl CpG binding protein 2 (Rett syndrome)
MLST8	MTOR associated protein, LST8 homolog
NLRP1	NLR family, pyrin domain containing 1
SCN1A	Sodium channel, voltage-gated, type 1, α subunit
SCN2A	Sodium channel, voltage-gated, type 2, α subunit
SCN3A	Sodium channel, voltage-gated, type 3, α subunit
SCN8A	Sodium channel, voltage-gated, Type 8, α subunit
STXBP1	Syntaxin binding protein 1

SYNGAP1	Synaptic Ras GTPase activating protein 1

Mouse Alleles

Q54	*Scn2a*^{Q54}

CHAPTER I

INTRODUCTION

Epilepsy

Epilepsy is a common neurological disease characterized by an enduring predisposition to generate epileptic seizures, as determined by the occurrence of: 1) two or more unprovoked seizures separated by at least 24 hours, 2) one unprovoked seizure with a probability of recurrence greater than 60%, or 3) the diagnosis of an epilepsy syndrome [1, 2]. Representing an estimated 0.5% of the global disease burden and 1% of days lost due to ill health, epilepsy affects over 50 million people, and is the fourth most common neurological disease in the United States behind migraine, stroke, and Alzheimer's disease [3-8]. With a 3% lifetime incidence, an estimated 1 in 26 people will develop epilepsy, costing the U.S. economy approximately 12.5 billion dollars annually [5, 9-13].

In addition to seizures, there are a number of comorbidities associated with epilepsy including: depression, anxiety, and other psychiatric disorders; hyperlipidemia; hypertension; asthma; and psychosocial problems such as poor academic performance, increased drug abuse, and difficulties obtaining and maintaining employment [14-16]. People with epilepsy have an increased risk of premature mortality, either as a direct consequence of epilepsy (e.g. status epilepticus), sudden unexpected death in epilepsy (SUDEP), seizure related accidents, or as a result of epilepsy-associated comorbidities [5, 17-19]. In resource-poor countries, as many as 90% of people with epilepsy do not receive

adequate treatment, and in developed countries, approximately 30% of patients do not achieve remission of seizures despite access to current therapies [9, 16, 20].

Epilepsy is a spectrum disease encompassing more than 30 different syndromes, which range in severity from relatively mild to catastrophic and may be classified according to: seizure type(s); age of onset; progressive nature; electroencephalogram (EEG) patterns; associated interictal signs and symptoms; pathophysiologic mechanisms, anatomical substrates, etiological categories; or genetic basis [21-23]. On the mild end of the spectrum are syndromes like benign familial neonatal-infantile seizures (BFNIS), which is characterized by afebrile seizures that spontaneously remit within the first year of life without neurological sequelae (OMIM 607745). On the other end of the spectrum are the epileptic encephalopathies in which epileptic activity begins early in life, results in severe neurological and cognitive impairment, and is generally refractory to standard antiepileptic drugs [22, 24-27]. These include: early myoclonic encephalopathy, Ohtahara syndrome, West syndrome, Dravet syndrome (DS), myoclonic status in nonprogressive encephalopathies, Lennox-Gastaut syndrome, Landau-Kleffner syndrome, and epilepsy with continuous spike-waves during slow-wave sleep [28].

Epilepsy is a multifactorial disease, the underlying causes of which can be broadly defined as either structural/metabolic (e.g. stroke, trauma, cortical malformations, infection, and disorders like tuberous sclerosis, which are associated with an increased risk of epilepsy) or genetic [26]. With numerous

epidemiological studies in twins and family pedigrees offering compelling evidence for epilepsy heritability and the discovery of some of the genes involved in monogenic epilepsy syndromes, the majority of epilepsy cases are now considered to be genetic in origin [29-44]. Although only 1 to 2% of genetic epilepsies are believed to be monogenic, the discovery of many of the genes involved in monogenic epilepsy syndromes over the last two decades has greatly improved our understanding of the molecular pathogenesis of epilepsy [35]. Most of these genes encode components of neuronal signaling, including nicotinic acetylcholine and gamma-aminobutyric acid (GABA) receptors, chloride channels, and of particular importance, voltage-gated sodium and potassium channels [35, 45-48].

Voltage-Gated Sodium Channels

Voltage-gated sodium channels contribute to neuronal excitability by initiating and propagating action potentials [49]. Upon membrane depolarization, a conformational change occurs in the channel via the movement of charged residues in the voltage-sensing domain. This activates the channel and allows sodium ions to enter the neuron through the channel pore, further depolarizing the membrane and activating additional sodium channels. The simultaneous activation of multiple sodium channels produces the rising phase of an action potential. Sodium channel α subunits are composed of four homologous domains (I-IV), each consisting of six α-helical transmembrane segments (S1-S6) flanked by cytoplasmic amino and carboxy-termini [50]. The first four transmembrane

segments (S1-S4) comprise the voltage-sensing domain, the main component of which is a stretch of hydrophobic and basic residues in S4 that provide the membrane voltage-sensing mechanism [51]. The S5 and S6 segments form the pore domain through which sodium passes. Within the pore domain, located in the membrane-reentrant pore loop between S5 and S6, is a selectivity filter that contains two conserved amino acid motifs, which are critical for sodium selectivity [49, 52].

There are four sodium channel α subunits expressed throughout the central nervous system. Nav1.1 channels (encoded by *SCN1A*) and Nav1.3 channels (encoded by *SCN3A*) are primarily localized to neuronal cell bodies [53]. Nav1.2 channels (encoded by *SCN2A*) are expressed on dendrites and unmyelinated or pre-myelinated axons, and Nav1.6 channels (encoded by *SCN8A*) are located on axon initial segments, dendrites, and nodes of Ranvier [53, 54].

Voltage-Gated Sodium Channels and Epilepsy

Epilepsy-associated mutations have been reported in each of the neuronal voltage-gated sodium channel α subunits. In the interest of brevity, only *SCN1A* and *SCN2A*, the two channels associated with the most mutations, will be highlighted here. Mutations in the *SCN1A* gene, encoding the α subunit of the type I voltage-gated sodium channel (Nav1.1), are the leading cause of monogenic epilepsies with nearly 900 mutations identified in patients with various epilepsy syndromes including febrile seizures, genetic (generalized) epilepsy with

febrile seizures plus (GEFS+), Lennox-Gastaut and DS or its variants (intractable childhood epilepsy with generalized tonic-clonic seizures (ICE-GTC), and severe myoclonic epilepsy, borderline) [35, 42-44, 55-60]. *SCN1A* mutations are extremely heterogenous, with mutations distributed over nearly every part of the channel and very few sites of re-mutations observed [44, 61]. Over 650 distinct, heterozygous *SCN1A* mutations have been identified in patients with DS, accounting for approximately 85% of the patients tested [55]. Over 90% of these mutations arise *de novo*, and approximately half are nonsense or frameshift mutations that result in protein truncation, demonstrating the haploinsufficiency of *SCN1A* [44, 59].

Heterozygous *Scn1a*$^{K0/+}$ knockout mouse models exhibit phenotypes with features similar to those observed in DS patients, including frequent, spontaneous seizures, cognitive and motor deficits, and premature lethality [62-65]. Hippocampal GABAergic interneurons from *Scn1a*$^{K0/+}$ postnatal day 13-14 mice exhibit reduced sodium current density, while hippocampal pyramidal neuron current density remains unchanged from wild-type [62]. However, at postnatal day 21-24 there is enhanced sodium current density in hippocampal pyramidal neurons as well as suppressed sodium current density from GABAergic interneurons [66]. This enhancement is accompanied by more frequent firing of spontaneous and evoked action potentials and conincides with the time at which *Scn1a*$^{K0/+}$ mortality peaks [66]. Thus, it appears that a reduction in GABAergic inhibition and a secondary intensification of neuronal excitability contribute to the *Scn1a*$^{K0/+}$ phenotype.

Over 20 missense mutations have been identified in the paralogous sodium channel gene *SCN2A* in patients with BFNIS and GEFS+ [55]. More recently, *de novo* missense *SCN2A* mutations were identified in patients with epileptic encephalopathies including DS and Ohtahara syndrome, and one nonsense mutation with an apparent dominant negative effect was reported in a patient with intractable epilepsy and severe mental decline [55, 64, 67-70]. A common mechanism by which *SCN2A* contributes to epilepsy susceptibility remains elusive as both gain-of-function and loss-of-function mutations can result in epilepsy, but it appears that the clinical severity of the phenotype is correlated with the extent to which the biophysical function of the channel is disrupted by the mutation [55].

Scn2a^{Q54} (Q54) transgenic mice, with pan-neuronal expression of a mutant rat brain IIA sodium channel (Nav1.2), exhibit a progressive epilepsy phenotype with seizures, which originate in the hippocampus, beginning at two months of age. These seizures are accompanied by behavioral arrest, stereotyped repetitive behaviors, hippocampal cell loss and gliosis, mossy fiber sprouting, and a reduced lifespan [71]. Hippocampal slice recordings from Q54 mice demonstrate network hyperexcitability [72]. The phenotype results from a gain-of-function mutation (GAL879-881QQQ) in the S4-S5 linker region in the second domain of the channel, resulting in slowed inactivation and increased persistent sodium current in neurons isolated from the hippocampus of presymptomatic Q54 mice, implicating increased persistent sodium current as a possible mechanism for neuronal hyperexcitability [71].

Voltage-Gated Potassium Channels

Voltage-gated potassium channels, the most diverse group of ion channels, modulate neuronal excitability by regulating the resting membrane potential and controlling the shape, duration, and frequency of action potentials [73]. Although the expression patterns and functions of voltage-gated potassium channels vary greatly, most are generally closed at neuronal resting membrane potentials and open after membrane depolarization, allowing potassium to leave the cell and thus repolarizing the membrane. Four α-subunits, each analogous in structure to a single domain of a voltage-gated sodium channel, combine to form a functional potassium channel [73-76]. Similar to a voltage-gated sodium channel, the potassium channel selectivity filter also contains highly conserved amino acids that are critical for ion selectivity [77, 78]. Glycine-tyrosine-glycine (GYG) residues line the narrowest part of the potassium (K^+)-conducting pore and contribute precisely spaced backbone carbonyls which help to coordinate dehydrated K^+ ions as they move through the channel [79-81]. Alteration of these residues disrupts the pore and results in altered ion selectivity [79, 82-84].

Potassium channel α-subunits are divided into nine subfamilies (Kv1 through Kv9) according to sequence similarity [73]. Subunits comprising the Kv1 through Kv4 subfamilies form functional homotetramers when heterologously expressed, and subunits within the same subfamily can also heterotetramerize to form channels with current properties distinct from the parent subunits [85-94]. Members of the Kv5 through Kv9 subfamilies generally do not function as homotetramers [85-87]. Rather, they act as modulatory subunits, binding to Kv2

subfamily members and imparting distinct functional properties by altering current density, kinetic, and/or other gating properties [95-101].

Voltage-Gated Potassium Channels and Epilepsy

Mutations associated with epilepsy have been identified in several genes encoding voltage-gated potassium channel subunits or accessory subunits including: *KCNA1* (Kv1.1)*, KCNAB2* (Kvβ2), *KCND2* (Kv4.2), *KCNV2* (Kv8.2), *KCNQ2* (Kv7.2), *KCNQ3* (Kv7.3), and *KCNH2* (Kv11.2) [38-40, 102-121]. *KCNQ2* and *KCNQ3*, encoding the M-type potassium channel subunits Kv7.2 and Kv7.3, were among the first genes identified in association with genetic epilepsies. M-current, present in many parts of the brain, contributes to the polarization of neuronal resting membrane potentials, preventing repetitive firing and mediating spike-frequency adaption [122, 123]. Mutations in these genes, most of which result in loss-of-function or dominant-negative effects on channel function, have been associated with both benign familial neonatal convulsions (BFNC) and epileptic encephalopathy [39, 40, 124-126]. As with *SCN2A*, the clinical severity of the phenotype seems to be correlated with the degree to which the mutation impairs channel function, with a 25% reduction in M-current predicted to be sufficient to cause epilepsy [127, 128].

Consistent with the idea that reduction of Kv7.2/Kv7.3-mediated M-current results in hyperexcitability, heterozygous *Kcnq2* knock-out mice ($Kcnq2^{+/-}$) exhibit hypersensitivity to pentylenetetrazole induced seizures [129]. Additionally, knock-in mice heterozygous for BFNC mutations ($Kcnq2^{A306T/+}$ and $Kcnq3^{G311V/+}$) exhibit

reduced thresholds to electrically induced seizures, and mice homozygous for these mutations have spontaneous generalized tonic-clonic seizures concurrent with reduced M-current from CA1 hippocampal pyramidal neurons [130]. Moreover, the anti-epileptic drug ezogabine (retigabine) enhances M-current by stabilizing the open conformation of Kv7.2/Kv7.3 channels, and a structural analogue of retigabine, flupirtine, has been shown to prevent kainite-induced status epilepticus and fluorothyl-induced seizures in rats [131-134].

Genetic and Phenotypic Heterogeneity In Monogenic Epilepsies

As evidenced by the previous discussion of voltage-gated sodium and potassium channel mutations associated with epilepsy, monogenic epilepsy syndromes exhibit a considerable degree of phenotypic and genetic heterogeneity, with different mutations in the same gene resulting in different epilepsy syndromes (e.g. *SCN1A, SCN2A, KCNQ2*) and mutations in different genes resulting in similar epilepsy syndromes (e.g. *SCN1A* and *SCN2A* mutations resulting in GEFS+) [41, 55, 135-139]. Furthermore, incomplete penetrance and variable expressivity are commonly observed in families with inherited epilepsy mutations [35]. For example, among thirteen family members with an inherited GEFS+ mutation ($SCN1A^{R1648H}$) one had only febrile seizures; seven had febrile seizures and epilepsy; four had epilepsy without febrile seizures; and one was asymptomatic [42, 136]. Moreover, among the individuals who developed epilepsy, the age of onset of the first epileptic seizure varied from 3-60 years [42, 136].

Analogous to the variable expressivity observed in humans, the phenotypes of mouse models of epilepsy are often dependent on the genetic background of the mice. The heterozygous *Scn1a*$^{KO/+}$ knockout mouse model of DS exhibits no overt phenotype on the 129S6/SvEvTac (129) background, but when bred with the C57BL/6J (B6) strain, the resulting F1 generation exhibits a severe epilepsy phenotype and premature lethality [66]. The Q54 phenotype is also dependent upon the strain background of the mice with congenic B6 mice carrying the Q54 transgene (C57BL/6J.Q54) exhibiting delayed onset of seizures, decreased incidence of spontaneous seizures, and increased lifespan relative to [C57BL/6J x SJL/J]F_1.Q54 mice [140].

Genetic Modifiers

The genetic and phenotypic heterogeneity observed among the monogenic epilepsies in humans and the strain-dependent phenotypes observed among genetic mouse models of epilepsy strongly suggest that genetic modifiers influence epilepsy phenotypes. Genetic modifiers are non-allelic genes or loci that segregate independently from the primary mutation and alter its phenotypic expression, influencing penetrance, progression, age of onset, and/or clinical severity of the mutant phenotype [141]. Genetic modifier loci have been mapped in a number of neurological diseases including: cystic fibrosis, amyotrophic lateral sclerosis, Alzheimer disease, Huntington disease, tuberous sclerosis, Hirschsprung disease, and epilepsy [117, 142-148]. The identification of genetic modifiers provides insight into the complex pathophysiology of heritable diseases

and can suggest novel targets for the development of rational therapeutic strategies.

Identifying modifier genes in humans can be arduous. Unbiased genetic mapping approaches require large, well-characterized cohorts of affected individuals, and candidate gene approaches are limited by *a priori* knowledge. Genetic mouse models provide a tractable alternative to human-based strategies. The strain-dependent phenotypes of genetic mouse models recapitulate the heterogeneity observed in humans and can be exploited to identify genetic modifiers by crossing mutations onto different inbred strain backgrounds and using conventional genetic mapping approaches to isolate the loci responsible for the phenotype modification.

Our lab used this approach to identify two loci, designated *Moe 1* (Modifier of Epilepsy 1) and *Moe2* (Modifier of Epilepsy 2) on Chromosomes 11 and 19, respectively, that contribute to the strain-dependent phenotype of Q54 transgenic mice [140]. We further refined the *Moe2* interval on Chromosome 19 to a 5-Mb region using interval-specific congenic strains carrying various SJL/J (SJL)-derived segments of the *Moe2* region on the B6 background. Sequencing of brain-expressed positional candidate genes within the 5-Mb region revealed three synonymous and two non-synonymous variants (Q252R and R208H) that differed between the B6 and SJL strains in the voltage-gated potassium channel subunit subfamily V, member 2 (*Kcnv2*) [149].

KCNV2 (Kv8.2) and *KCNB1* (Kv2.1)

Kv2.1 channels (encoded by *KCNB1*) are widely expressed throughout the brain in both projection and interneurons of the hippocampus and cortex where they are the main contributors to delayed rectifier potassium current [150-155]. This current contributes to membrane repolarization after action potential firing and is an important determinant of intrinsic neuronal excitability [150, 155, 156]. Kv2.1 channels dynamically regulate neuronal excitability via delayed rectifier potassium current in response to neuronal activity. Typically localized to large clusters on somata and proximal dendrites of pyramidal neurons, under conditions of repetitive stimulation, Kv2.1 channels undergo a calcineurin-mediated dephosphorylation and assume a more uniform distribution. This change in distribution is accompanied by a hyperpolarizing shift in voltage dependence of activation and inactivation gating properties resulting in a suppression of neuronal firing [150, 156, 157]. Thus, Kv2.1 channels are important regulators of neuronal excitability.

Kcnv2 encodes Kv8.2, a modulatory voltage-gated potassium channel subunit. When expressed alone in heterologous expression systems, Kv8.2 subunits are retained in the endoplasmic reticulum, and are therefore non-functional as homotetramers [85]. Kv2.1 and Kv8.2 have similar expression patterns in the cortex, where they are expressed predominately in Layers 2/3 and 5, and in the hippocampus, where they are found in the principal excitatory neurons of the pyramidal cell layers and dentate gyrus [158-162]. Direct interaction between Kv8.2 and Kv2.1 has been demonstrated in mammalian cell

lines and in *Xenopus* oocytes, resulting in suppression of Kv2.1-mediated delayed rectifier potassium current and altered kinetic properties [85, 86, 117]. Suppression of Kv2.1-mediated delayed rectifier potassium current by Kv8.2 could predispose neurons to increased excitability by impairing membrane repolarization, especially under conditions of repetitive firing.

Summary

Epilepsy is a common neurological spectrum disease that places a tremendous burden not only on affected individuals and their families but also on society as a whole. Genetic factors contribute to the majority of epilepsy cases, and most of the genes associated with monogenic epilepsy syndromes encode components of neuronal signaling, including voltage-gated sodium and potassium channels, the coordinated activities of which are critical in determining neuronal excitability. Genetic and phenotypic heterogeneity are frequently associated with monogenic epilepsy syndromes, and strain-dependent phenotypes are common among genetic mouse models of epilepsy, suggesting that genetic modifiers influence epilepsy phenotypes. Identifying genetic modifiers that contribute to epilepsy susceptibility can enrich our understanding of epilepsy etiology, and may reveal novel therapeutic strategies. Mouse models of epilepsy provide a system in which genetic modifiers can be systematically identified.

Using the Q54 transgenic mouse model of epilepsy, our lab previously identified *Kcnv2* as a candidate modifier gene. Chapter II, modified from *Jorge et*

al., 2011, describes the validation of *Kcnv2* as a genetic modifier of epilepsy in mice and the functional characterization of two *KCNV2* variants identified in pediatric epilepsy patients.

The data described in Chapter II suggested that *Kcnv2* is a quantitative modifier of epilepsy in mice, with increased *Kcnv2* expression correlated with a more severe Q54 phenotype. We hypothesize that regulatory sequence variation in the *Kcnv2* promoter and/or 3' untranslated region (UTR) influences seizure susceptibility by altering steady-state expression levels. Chapter III describes the characterization of the *Kcnv2* promoter and 3' UTR regions. These studies provide the foundation for future studies to determine the effect of sequence variation in these regions on *Kcnv2* expression.

The identification of *Kcnv2* as a genetic modifier of epilepsy implicated alteration of delayed rectifier potassium current as a potential mechanism for increased neuronal excitability. As the primary mediator of delayed rectifier potassium current, we hypothesized that genetic variation in *KCNB1* (Kv2.1) may also contribute to epilepsy risk. Chapter IV, modified from *Torkamani et al., 2014*, describes the functional characterization of three *KCNB1* mutations that were identified in three unrelated pediatric epilepsy patients with epileptic encephalopathy by whole-exome sequencing. Chapter V is a summary of the conclusions and implications of the studies described in Chapters II-IV followed by suggestions for future directions.

CHAPTER II

VOLTAGE-GATED POTASSIUM CHANNEL KCNV2 (KV 8.2) CONTRIBUTES TO EPILEPSY SUSCEPTIBILITY*

Introduction

Epilepsy is a common neurological disorder affecting approximately 1% of the population worldwide [4, 163, 164]. Over the last 15 years, a number of genes responsible for monogenic epilepsy have been identified. Most of the responsible genes are components of neuronal signaling, including voltage-gated ion channels [165]. Mutations in the voltage-gated sodium channel genes *SCN1A* and *SCN2A* are responsible for several types of human epilepsy, including GEFS+, DS, and BFNIS [44]. More than 700 *SCN1A* mutations have been reported to date, making this gene the most frequently identified cause of monogenic epilepsy. Approximately 20 *SCN2A* mutations have been reported in patients with BFNIS, GEFS+, and DS [44]. Variable expressivity is a common feature of monogenic epilepsy caused by ion channel mutations, suggesting that genetic modifiers may influence clinical severity [55].

Q54 transgenic mice are a model of sodium channel-dependent epilepsy. These mice express a gain-of-function mutation in *Scn2a* that results in

---

* Modified from: Jorge, B.S., et al., *Voltage-gated potassium channel KCNV2 (Kv8.2) contributes to epilepsy susceptibility.* Proceedings of the National Academy of Sciences, 2011. **108**(13): p. 5443-5448.

progressive epilepsy that begins with brief, spontaneous partial motor seizures [71]. As they age, Q54 mice exhibit more frequent partial seizures, as well as secondarily generalized seizures, and have a reduced lifespan. Excitatory hippocampal pyramidal neurons from Q54 mice display elevated persistent current that is predicted to increase neuronal excitability and contribute to seizure generation [71]. Severity of the epilepsy phenotype in Q54 is highly dependent on genetic background. The phenotype is less severe on the resistant strain (B6), with delayed seizure onset and improved survival, compared with the susceptible strain (SJL) [140]. We previously mapped two modifier loci that influence the difference in severity between these two strains: *Moe1* on chromosome 11 and *Moe2* on chromosome 19 [140]. Previous linkage analysis identified *Kcnv2* as a strong candidate for the *Moe2* locus [149]. *Kcnv2* encodes the voltage-gated potassium channel Kv8.2, which is a silent subunit as a homotetramer. Kv8.2 can form functional heterotetramers with Kv2 subunits and influence membrane translocation and channel properties [85, 86]. Members of the Kv2 family are expressed in the nervous system and underlie the neuronal delayed rectifier K+ current, which is important for limiting membrane excitability, particularly under conditions of repetitive stimulation [150]. In the hippocampus, which is a region of particular importance for seizure generation, Kv2.1 is the major contributor to the delayed rectifier potassium current [166] and colocalizes with Kv8.2 in hippocampal pyramidal neurons [167].

To test the contribution of strain-dependent variation in *Kcnv2* to epilepsy susceptibility, we characterized the functional effects of previously identified

nonsynonymous coding variants and compared transcript levels between strains. We also evaluated the *in vivo* effect of *Kcnv2* variants in transgenic mice. To determine whether the human ortholog contributes to human epilepsy, we screened epilepsy patients for genetic variation in *KCNV2*. Our studies demonstrate *Kcnv2* transgene-mediated transfer of seizure susceptibility in mice, as well as human variants that alter delayed rectifier K^+ currents. These results implicate *KCNV2* as an epilepsy gene in mice and humans.

Materials and Methods

Transgene Constructs

The *Kcnv2* open reading frame was amplified by RT-PCR from mouse brain RNA and cloned into a neuron specific enolase (NSE) transgene expression construct as previously described [71]. The transgene contains the 4-kb promoter fragment from the rat NSE gene that includes 2.8 kb of flanking sequence, exon 1, intron 1, and 6 bp of noncoding sequence from exon 2, and the SV40 late polyadenylation sequence [168]. Constructs were confirmed by sequencing before transgene microinjection.

Animals

All experimental protocols were approved by the Vanderbilt University Institutional Animal Care and Use Committee, in accordance with the National Institutes of Health Guide for the Care and Use of Laboratory Animals. Q54 transgenic mice [Tg(Eno2-Scn2a1*)Q54Mm] congenic on the B6 background (B6.Q54) were established as described and are maintained by continued backcrossing of hemizygous transgenic males to B6 females. Transgenic mice carrying a B6 *Kcnv2* cDNA [Tg(Kcnv2B)1Jak] or SJL *Kcnv2* cDNA [Tg(Kcnv2S)1Jak] were generated by pronuclear injection into B6 fertilized oocytes in the University of Michigan Transgenic Animal Core or the Vanderbilt University Transgenic Mouse/ESC Shared Resource. Transgenic founders were identified by PCR genotyping as described below. Each founder was crossed to strain B6 to generate an independent transgenic line, and lines were maintained by continued backcrossing of transgenic hemizygotes to B6. We generated two lines that carry the SJL *Kcnv2* cDNA transgene (Kcnv2-S1, S2) and two lines that carry the B6 cDNA transgene (Kcnv2-B1, B2). We crossed B6.Kcnv2 transgenic mice to B6.Q54 mice to generate double-transgenic mice and single-transgenic littermate controls for experiments. Offspring of all genotypes were obtained at the expected Mendelian ratios.

Genotyping

Genotyping of Q54 mice was performed as previously described [140]. *Kcnv2* transgenics were identified by PCR genotyping of genomic DNA using

primers located in intron 1 of NSE and in the *Kcnv2* cDNA. These primers amplify a 935-bp band from the *Kcnv2* cDNA transgene.

Phenotyping

Mice were tail biopsied on postnatal day 14 and genotyped. We used the same phenotyping paradigm that was used for mapping of the *Moe2* locus [140, 149]. Briefly, *Q54*;*Kcnv2* double-transgenic mice and single-transgenic littermates were observed for visible seizures during 30-min observation periods at 3, 4.5, and 6 wk of age. Mice were transferred to a clean observation cage [7.75 in (width) × 12 in (depth) × 6.5 in (height)] just before the observation session. All observations occurred between 1300 hours and 1600 hours. Videotaped observation sessions were analyzed offline by a blinded observer using Observer XT behavioral coding software (Noldus). Assessment of visible partial motor seizures was based on prior extensive video-EEG monitoring that demonstrated coincident stereotyped behavioral and EEG abnormalities [71]. Animals exhibiting one or more seizures during the observations were classified as having seizures (average frequency, three per 30 min). The proportion of mice with a seizure frequency of one or more per 30 min by 6 wk of age was compared between genotypes using Fisher's exact test ($n \geq 14$ per group).

Quantitative RT-PCR

For comparing relative *Kcnv2* levels in strains B6 and SJL, hippocampi were dissected from 8-wk-old B6 and SJL mice (n = 7 per strain). For assessment of *Kcnv2* transcript levels in transgenic mice, whole-brain RNA was isolated from 10- to 12-wk-old *Kcnv2* transgenic mice and nontransgenic littermates (n = 5 per line). RNA was isolated using the RNeasy kit (Qiagen). Real-time RT-PCR was performed as previously described [149]. Briefly, real-time PCR was performed in triplicate using QuantiTect SYBR Green PCR mix (Qiagen) on an ABI 7900HT system. All reported assays exhibited a single peak in dissociation analysis and no detectable signal in no-RT controls. Relative transcript levels were assessed using the $2^{-\Delta\Delta CT}$ method [169] with TATA binding protein as a reference gene (Qiagen QuantiTect Assay QT00198443). Statistical comparison between groups was made by the pairwise fixed reallocation randomization test [170].

Plasmids and Cell Transfection

A full-length mouse Kv8.2 cDNA was generated by RT-PCR of mouse brain RNA and cloning into the pIRES2-smGFP mammalian expression vector, which contains the CMV promoter, an IRES-2 element, and soluble modified GFP (DF/HCC DNA Resource Core, EvNO00025960). A full-length mouse Kv2.1 cDNA clone was obtained from Open Biosystems (clone ID 5363843) and cloned into a modified pIRES2-DsRed vector (BD Biosciences-Clontech), in which we substituted the fluorescent protein cDNA with that of DsRed-MST (provided by

Dr. Andras Nagy, University of Toronto, Toronto, Canada). A full-length human Kv8.2 cDNA clone was obtained from Open Biosystems (clone ID 40025518) and cloned into the pIRES2-smGFP vector. Mutations were introduced into Kv8.2 using the QuikChange Site-Directed Mutagenesis system (Agilent Technologies). Human Kv2.1 was amplified by RT-PCR from human brain total RNA (Clontech) and cloned into pIRES2-DsRed-MST. All clones were sequenced in their entirety to confirm their identity before transfection.

Expression of Kv8.2 and Kv2.1 constructs in CHO cells was achieved by transient plasmid transfection using FUGENE-6 (Roche) in which 1 μg of total cDNA was transfected with a mass ratio of 1:1. To study the pore-forming Kv2.1 subunit in the absence of Kv8.2, cells were transfected with pIRES2-DsRed-MST-Kv2.1 in combination with nonrecombinant pIRES2-smGFP vector. After transfection, cells were incubated for 48 h before use in electrophysiological experiments.

Electrophysiology

Whole cell patch clamp recordings were performed as previously described [171], except the pipette solution was modified to contain lower K^+ concentration to improve voltage-control (modified pipette solution, in mM: K^+ aspartate 55, N-methyl-D-glucamine 55, aspartic acid 55, $CaCl_2$ 1, Hepes 10, EGTA 11, $MgCl_2$ 1, and K_2ATP 5, pH 7.3). Whole-cell currents were measured from −80 to +60 mV (in 10-mV steps) from a holding potential of −80 mV. Data were collected for each experimental condition from at least three transient

transfections and analyzed and plotted using a combination of Clampfit (Molecular Devices) and SigmaPlot 2000 (Systat Software). Statistical analyses were carried out using SigmaStat 2.03 (Systat Software), and *P* values are provided in the figures or listed in the figure legends. Statistical significance among two groups was determined using unpaired Student's *t* test, and one-way ANOVA followed by Tukey post test was performed when comparing more than two groups. Whole-cell currents were normalized for membrane capacitance, and results are expressed as mean ± SEM. The number of cells used for each experimental condition is given in the figure legends.

Human KCNV2 Mutation Screening

Research was approved by the local institutional review boards. Consent and DNA samples were obtained from study subjects. The two coding exons of *KCNV2* were amplified from genomic DNA, and variants were identified by CSGE and sequencing using previously described methods [172]. *SCN1A* and *SCN2A* were screened by PCR amplification and sequencing of the 26 coding exons. NINDS neurologically normal control panels NDPT079 and NDPT093 (Coriell Cell Repository) were screened for the R7K and M285R variants using custom Taqman assays on an ABI 7900HT system (Applied Biosystems).

Statistical Analysis

Values are expressed as mean ± SEM. Comparisons of mean differences between groups were made by unpaired two-tailed Student *t* test or one-way ANOVA unless otherwise stated. Comparisons of proportions were made by Fisher's exact test. For qRT-PCR results, comparisons between groups were made by the pairwise fixed reallocation randomization test [170]. $P < 0.05$ was considered statistically significant.

Results

Functional Analysis of Kcnv2 Variants in the Mouse

We previously identified two nonsynonymous coding variants in *Kcnv2* that differ between the resistant B6 and susceptible SJL strains and hypothesized that functional effects of these variants may explain the differences in seizure susceptibility. Strain SJL carries the Kv8.2 amino acid substitutions R205H and Q252R [149]. We compared the functional effects of the B6 and SJL isoforms of Kv8.2 on potassium currents by coexpression with mouse Kv2.1 in a heterologous expression system. Channel cDNAs were cotransfected into CHO cells, and whole-cell currents were measured in the whole-cell configuration of the patch clamp technique [173]. Expression of mouse Kv2.1 (mKv2.1) alone produced large voltage-dependent potassium currents, and coexpression with the B6 or SJL isoforms of Kv8.2 (B6-Kv8.2, SJL-Kv8.2) resulted in significant

suppression of K^+ current density (mKv2.1 alone, 326.1 ± 30.8 pA/pF, n = 8; mKv2.1 + B6-Kv8.2, 84.5 ± 5.3 pA/pF, n = 7, P < 0.001; mKv2.1 + SJL-Kv8.2, 157.1 ± 29.1 pA/pF, n = 7, P < 0.005) (Fig. 2.1). Coexpression of mKv2.1 with B6-Kv8.2 produced significantly greater suppression than SJL-Kv8.2 for voltage steps between 0 mV and +60 mV (Fig. 2.1). Further, B6-Kv8.2, but not SJL-Kv8.2, had a significant effect on the kinetics of activation that was limited to a single test potential (0 mV) without a corresponding change in voltage dependence (Fig. 2.2). Neither Kv8.2 isoform differed in the magnitude of cumulative inactivation evoked by moderate-frequency pulse trains (Fig. 2.3), but SJL-Kv8.2 did evoke a greater time-dependent decay in whole-cell current (Fig. 2.1C). However, given their colocalization in excitatory neurons, the differences in biophysical properties of Kv2.1/B6-Kv8.2 and Kv2.1/SJL-Kv8.2 heterotetrameric channels do not provide a clear and compelling explanation for strain differences in epilepsy severity in Q54 mice.

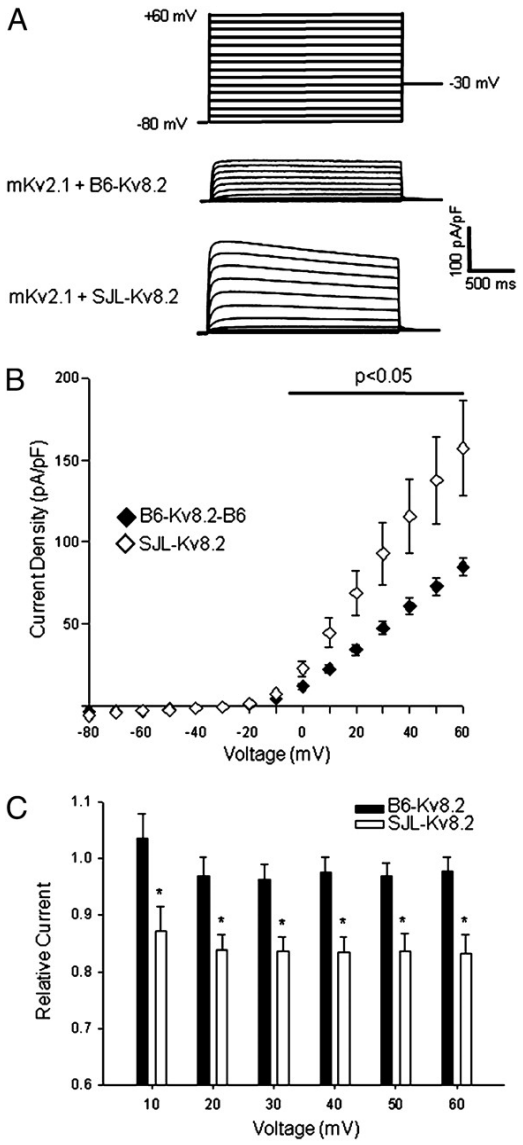

Figure 2.1 Functional Consequences of Amino Acid Sequence Variants in Mouse *Kcnv2*

(A) Averaged whole-cell current traces normalized to membrane capacitance recorded from CHO cells expressing mKv2.1 in combination with either B6-Kv8.2 or SJL-Kv8.2 (n = 7 for each condition). (B) Current density–voltage relationships for mKv2.1 coexpressed with the two Kv8.2 isoforms. Current was measured at 1,990 ms after start of the test pulse then normalized to membrane capacitance. (C) Extent of time-dependent whole-cell current decay illustrated by the ratio of steady-state current (measured at 1,990 ms) to instantaneous current (measured at 100 ms).

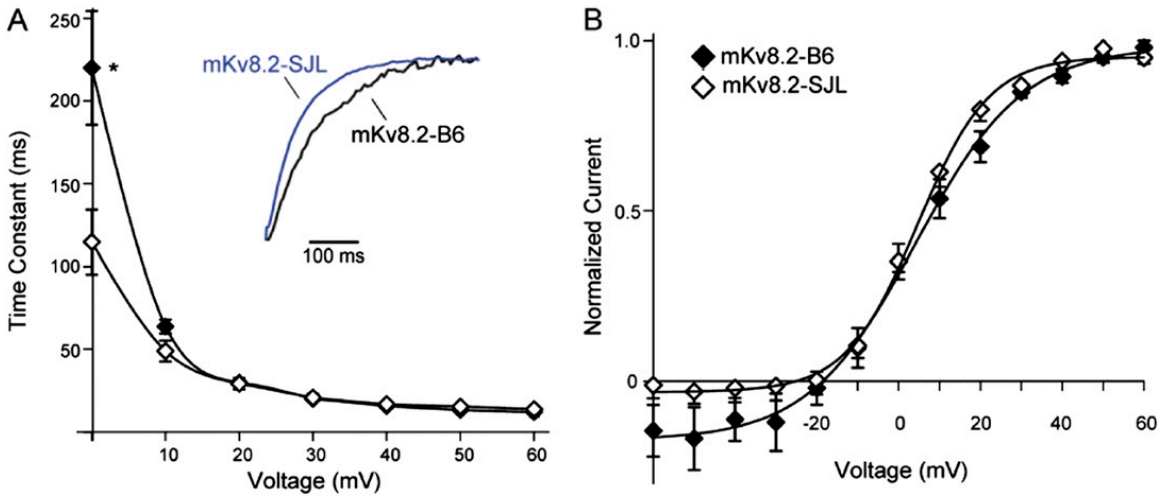

Figure 2.2 Biophysical Properties of mKv2.1 Channels Coexpressed with mKv8.2 Subunits

(A) Voltage dependence of activation time constants for mKv2.1 coexpressed with Kv8.2 isoforms (*P < 0.05 compared with WT). Time constants were determined from monoexponential fits to the data. Currents recorded at voltages <0 mV were too small to determine time constants. Inset: Averaged current traces (blue, mKv2.1 + SJL-Kv8.2; black, mKv2.1 + B6-Kv8.2) recorded from 10 to 500 ms after a test pulse to 0 mV and normalized to current amplitude measured at 500 ms. (B) Voltage dependence of steady-state activation. Tail-current amplitudes were measured at −30 mV after a 2,000-ms activating pulse from −60 to +60 mV. Currents were normalized to peak amplitude and fit with Boltzmann functions. Values for activation $V_{1/2}$ were not significantly different between B6-Kv8.2 and SJL-Kv8.2.

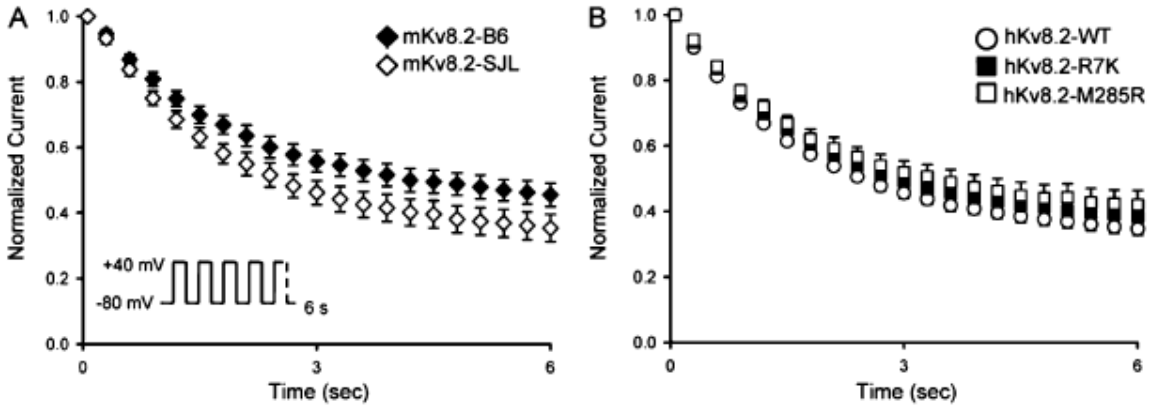

Figure 2.3 Cumulative Inactivation of Kv2.1 Channels Coexpressed with Kv8.2
Current was measured during a train of 100 depolarizing pulses to +40 mV of 40-ms duration from a holding potential of –80 mV at a frequency of 17 Hz. Currents were normalized to peak current amplitude. Plotted points correspond to means ± SEM of every fifth pulse for mouse (A) and human (B) Kv8.2 subunits coexpressed with mouse and human Kv2.1, respectively. Cumulative inactivation kinetics were estimated by monoexponential decay fit to each cell recording and averaged. No significant differences were observed.

Relative Expression of Kcnv2 in Hippocampus

Whole-brain expression of *Kcnv2* does not differ between strains B6 and SJL [149]. We further investigated strain-dependent expression in the hippocampus for three reasons: first, previous EEG studies showed that seizures in Q54 likely originate in the hippocampus [71]; second, *Kcnv2* transcripts are enriched in the hippocampus [167]; and, third, the biophysical differences described above were counterintuitive and suggested more complex physiology. RNA was isolated from dissected hippocampi of 8-wk-old B6 and SJL mice for quantitative RT-PCR (qRT-PCR) analysis. Relative *Kcnv2* expression was assessed by the $2^{-\Delta\Delta Ct}$ method normalizing to TATA binding protein using the same assay previously used for whole-brain analysis [169]. Strain SJL exhibited

threefold greater expression of hippocampal *Kcnv2* transcript relative to B6 (Fig. 2.4). The finding indicates that higher *Kcnv2* expression in hippocampus correlates with greater epilepsy severity.

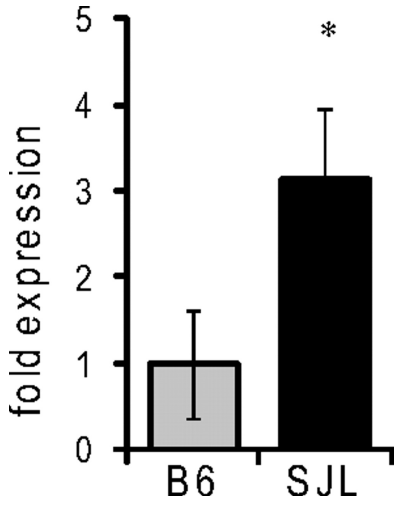

Figure 2.4 Relative Hippocampal Expression of Kcnv2
Transcript levels were measured by qRT-PCR (n = 7 per strain; *P = 0.012 compared with B6, pairwise fixed reallocation randomization test).

Transgenic Transfer of the Modified Phenotype

We evaluated the *in vivo* modifier effects of *Kcnv2* using a transgenic transfer approach, based on the prior observation that the modifier effect is a dominant trait [140]. We constructed transgenes containing the B6 or SJL *Kcnv2* coding sequence under the control of the neuron-specific enolase (NSE) promoter. This promoter drives pan neuronal expression in transgenic mice and is the same promoter that drives expression of the Q54 transgene [71, 168]. To determine the contribution of the *Kcnv2* amino acid variants, we generated

transgenic lines expressing the SJL-derived *Kcnv2* transgenes (Kcnv2-S1, Kcnv2-S2). To determine whether higher expression alone is sufficient for the severe phenotype, we generated lines carrying the B6-derived *Kcnv2* transgenes (Kcnv2-B1, Kcnv2-B2).

Transgenes were microinjected into B6 oocytes and maintained on the B6 background, ensuring a pure genetic background for experiments. The transgenic lines expressed varying amounts of *Kcnv2* transgene transcript as determined by qRT-PCR (Fig. 3A). Kv8.2 protein levels exhibited a similar trend in the transgenic lines, as determined by immunoblotting (Fig. 2.6). *Kcnv2* transgenic hemizygotes were crossed with B6.Q54 mice to generate double-transgenic Kcnv2;Q54 offspring and single-transgenic littermate controls that were phenotyped for spontaneous seizure onset and survival. For all *Kcnv2* transgenic lines, single-transgenic mice displayed no spontaneous seizures and had a normal lifespan.

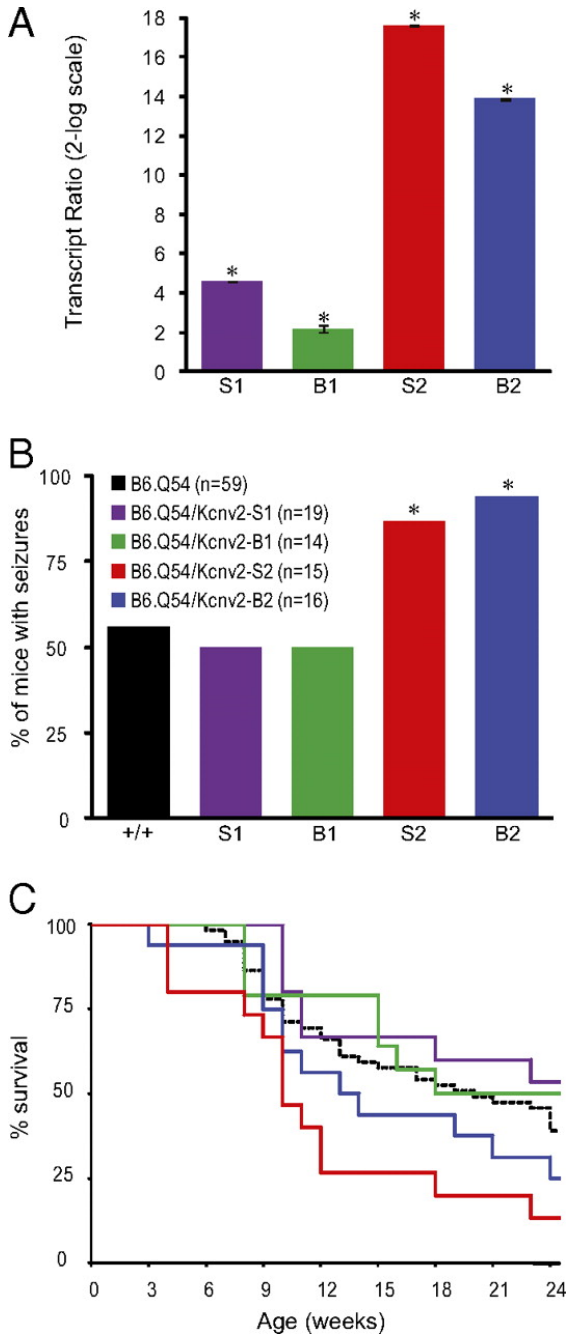

Figure 2.5 Transgenic Transfer of the Modified Phenotype in *Kcnv2*;Q54 Double Transgenic Mice

(*A*) Relative whole-brain expression of *Kcnv2* transcript measured by qRT-PCR (n = 5 per genotype; $^*P \leq 0.002$ compared with nontransgenic, pairwise fixed reallocation randomization test). (*B*) Percentage of mice exhibiting more than 1 seizure per 30 min by 6 wk of age ($^*P < 0.03$ compared with B6.Q54, Fisher's exact test). (*C*) Survival of Q54 mice carrying *Kcnv2* transgenes and single transgenic B6.Q54 littermates (dashed black line).

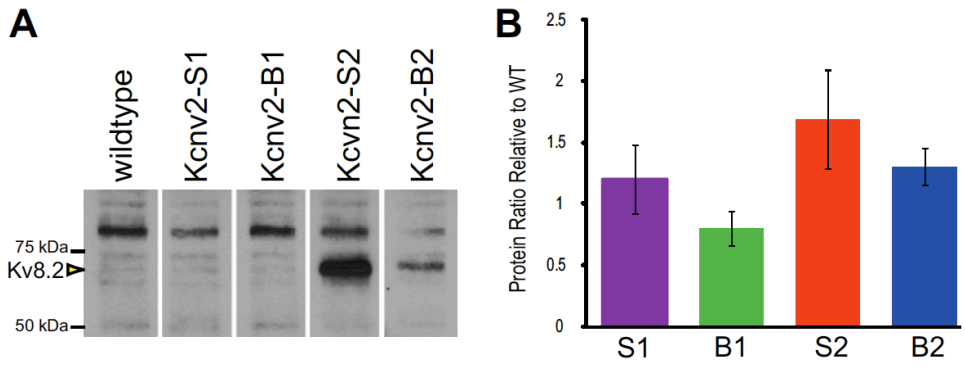

Figure 2.6 Relative Whole-brain Expression of Kv8.2 Protein in *Kcnv2* Transgenic Lines
(A) Representative immunoblot of Kv8.2 from *Kcnv2* transgenic mice and nontransgenic littermates (WT). Brain membrane proteins (25 μg) were isolated at 6 wk of age and analyzed by immunoblotting with an affinity-purified rabbit polyclonal antiserum generated against the immunogenic peptide MLKQSNERRWSLSY (ProSci Inc.). The predicted molecular weight of Kv8.2 is 64 kDa (arrowhead). Protein loading is indicated by relative intensity of the nonspecific immunoreactive band at ≈80 kDa. All lanes are from the same exposure of a single blot. Isolation of membrane proteins and Western blotting was carried out as previously described (1). (B) Quantitative analysis of Kv8.2 relative protein levels normalized to the 80-kDa band (n ≥ 3 per genotype).

Lines Kcnv2-S2 and Kcnv2-B2, with the highest levels of transgene expression, generated an increased number of Kcnv2;Q54 double-transgenic mice with seizures by 6 wk of age (Fig. 2.5 A and B). Double-transgenic mice with either the Kcnv2-S2 or Kcnv2-B2 transgenes also exhibited accelerated mortality, with 50% mortality by 10 wk and 14 wk of age, respectively, compared with B6.Q54 single-transgenic mice with 50% survival at 20 wk of age (Fig. 2.5C). Lines Kcnv2-S1 and Kcnv2-B1, with lower levels of transgene expression, did not influence the Q54 phenotype (Fig. 2.5). The level of *Kcnv2* transgene expression was strongly correlated with seizure phenotype (R^2 = 0.85) and 24-wk

survival (R^2 = 0.79), whereas amino acid sequence was not correlated with seizure phenotype (R^2 = 0.008) or survival (R^2 = 0.04). Although the precise contribution of the amino acid variants *in vivo* is unclear, elevated expression of *Kcnv2* seems to be sufficient to exacerbate the Q54 epilepsy phenotype.

Human Kcnv2 Screening

To determine whether *KCNV2* contributes to human epilepsy, we screened 209 pediatric epilepsy subjects for variants in *KCNV2* by exon amplification, conformation-sensitive gel electrophoresis (CSGE), and sequencing [172]. A number of known polymorphic coding SNPs were present in the patients, including seven synonymous SNPs and a common nonsynonymous SNP with a population minor allele frequency of 0.12 (Table 2.1). Additionally, we identified two unique nonsynonymous coding variants: R7K and M285R. These variants were not detected in 368 neurologically normal control chromosomes [National Institute of Neurological Disorders and Stroke (NINDS) Neurologically Normal Control Panels NDPT079, NDPT093]. Additionally, these variants are not present in dbSNP, nor have they been reported in resequencing projects, including the 1000 Genomes Project (http://browser.1000genomes.org/index.html) and the Baylor Ion Channel Sequencing Project (http://www.hgsc.bcm.tmc.edu/ionchannel-snpList.xsp).

Table 2.1 *KCNV2* Polymorphisms Detected in Screening of Pediatric Epilepsy Patient Samples

SNP ID	Position* (Mb)	Type	Amino acid	Major/minor alleles	Population minor allele frequency†	Flanking sequence
rs11793555	2717629	5′ UTR	−64 from AUG	G/T	0.333	CTAGAGGCAG(G/T)GAGCAGGTGA
rs7029012	2717698	5′ UTR	−42 from AUG	C/G	0.483	GGACCCCTAC(C/G)ACAGCCAGGA
Unique	2717759	Nonsyn	R7K	G/A	NA	CAGAGTGAGA(G/A)GAGACGGTCC
rs10967705	2717922	Syn	61	C/G	0.459	ACGAAGACGG(C/G)GAGGAGGAGG
rs10967709	2718498	Syn	253	A/G	0.127	TGGAGAAGCC(A/G)TTCTCCTCGG
rs12237048	2718534	Syn	265	C/G	0.415	TCGGGGTGGC(C/G)TCCAGCACCT
rs17656693	2718588	Syn	283	G/A	0.009	ACACCGTGGA(A/G)GAGATGCAGC
Unique	2718593	Nonsyn	M285R	T/G	NA	GTGGAGGAGA(T/G)GCAGCAGCAC
rs7859993	2718654	Syn	305	G/A	0.059	TGGAGCACGT(G/A)GAGATGCTGT
rs7860945	2718717	Syn	326	C/T	0.042	CCACGCCCGA(C/T)CTGAGGCGCT
rs41312842	2729475	Syn	462	C/T	0.097	GCTACGGAGA(C/T)ATGTACCCAG
rs12352254	2729686	Nonsyn	L533V	C/G	0.12	TGAGTGTTTG(C/G)TTGGAAGCAA
rs41306094	2729733	3′ UTR	+6 from stop	C/T	0.097	ATTAGTATTT(T/C)ATAGGACATG

Patient DNAs (n = 209) were screened for *KCNV2* variants by exon amplification, heteroduplex analysis, and sequencing. Two unique, nonsynonymous variants were identified (as noted) in unrelated patients and were subject to biophysical characterization. Nonsyn, nonsynonymous; NA, not available; Syn, synonymous.
*Position is based on the human GRCh37 assembly.
†Population minor allele frequencies are from dbSNP reports.

The *KCNV2*-R7K variant was identified in a patient with febrile and afebrile partial seizures starting at age 2 years (Table 2.2, patient 1). The variant was inherited from his unaffected mother. However, there is a positive family history of two paternal uncles with childhood epilepsy. R7K substitutes lysine for an evolutionarily conserved arginine in the cytoplasmic amino terminus of the Kv8.2 channel (Fig. 2.7A).

Table 2.2 Clinical Features of Epilepsy Patients with Unique, Nonsynonymous *KCNV2* Coding Variants

Patient	Seizure types	Age of onset	EEG	MRI	Treatment	Family history	*KCNV2* variant*	Inherited?
1	Partial, febrile and afebrile	2 y	Right temporal epileptiform discharges	Right temporal T2 signal changes	Spontaneous remission: seizure-free at age 10 y with no AEDs	Yes	R7K c.20G > A	Yes
2	Generalized, myoclonic, atonic	2 y	Right centrotemporal spikes; generalized abnormalities	NA	Corpus callosotomy; incomplete control with 3 AEDs	No	M285R c.854T > G	Yes

AEDs, antiepileptic drugs; NA, not available.
*GenBank accession no. BC10135.

Figure 2.7 Human *KCNV2* Variants Identified in Epilepsy Patients
(A) Evolutionary conservation of arginine 7. (B) Evolutionary conservation of methionine 285.

The *KCNV2*-M285R variant was identified in a patient with an epileptic encephalopathy with severely refractory epilepsy (Table 2.2, patient 2). There is no family history of epilepsy, and the variant was inherited from his unaffected mother. Methionine 285 is located at the extracellular face of transmembrane segment 1 and is evolutionarily invariant in homologous channels from other mammals, birds, and fish. (Fig. 2.7B).

Both patients were also screened for variants in the voltage-gated sodium channel genes *SCN1A* and *SCN2A*. No pathogenic variants were identified (Table 2.3).

Table 2.3 *SCN1A* and *SCN2A* SNPs in Patients with *KCNV2* Variants

Gene	Patient	SNP ID	SNP function	cDNA position	Amino acid	Patient genotype	Heterozygote frequency*
SCN1A	1	rs994399†	Intronic	c.965–21C > T		T/T	0.6
		rs9333574	Intronic	c.1171–9_10delTT		ΔTT/ΔTT	0.04‡
		rs7580482†	Synonymous	c.1212A > G	V404	G/G	0.4
		rs6432860†	Synonymous	c.2292T > C	V764	C/C	0.3
		rs2126152†	Intronic	c.2416–37A > C		C/C	0.3
		rs2298771†	Nonsynonymous	c.3199A > G	A1067T	A/A	0.3
	2	rs61741123	Synonymous	c.345T > C	N115	T/C	0.2
		rs994399†	Intronic	c.965–21C > T		C/T	0.6
		rs1542484	Intronic	c.1028+21T > C		T/C	0.5
		rs7580482†	Synonymous	c.1212A > G	V404	A/G	0.4
		rs7559148	Intronic	c.1662+9C > A		C/A	0.2
		rs6432860†	Synonymous	c.2292T > C	V764	C/C	0.3
		rs2126152†	Intronic	c.2416–37A > C		C/C	0.3
		rs2298771†	Nonsynonymous	c.3199A > G	A1067T	A/A	0.3
SCN2A	1	rs67198220	Intronic	c.3399–74+>insG		-/G	0.015
		rs1864885	Intronic	c.4211–31A > G		G/A	0.3
	2	Unique	Intronic	c.385+46C > A		C/A	0.004
		rs67198220	Intronic	c.3399–74+>insG		-/G	0.015
		Unique	Synonymous	c.5326C > T	L1776	C/T	NA

Patients 1 and 2 were screened for *SCN1A* and *SCN2A* mutations by amplification and sequencing of the coding exons. No pathogenic variants were identified. Patient 1 is homozygous for the most common *SCN1A* haplotype (T,G,C,C,A), whereas patient 2 is heterozygous for a rare haplotype (C,A,C,C,A) (1). NA, not available.

*Heterozygote frequencies are from dbSNP reports unless otherwise noted.

†One of five SNPs that define *SCN1A* haplotypes.

‡Heterozygote frequency from Escayg et al. (2001) A novel SCN1A mutation associated with generalized epilepsy with febrile seizures plus—and prevalence of variants in patients with epilepsy. *Am J Hum Genet* 68:866–873.

Functional Properties of Human KCNV2 Variants

We determined the functional consequences of the R7K and M285R variants engineered in human Kv8.2 by coexpressing with human Kv2.1 in CHO cells. Coexpression of Kv2.1 with either R7K or M285R Kv8.2 variants resulted in significantly greater suppression of Kv2.1-mediated current compared with wild-type Kv8.2 for voltage steps from 0 mV to +60 mV (Fig. 2.8 A and B). Furthermore, M285R, but not R7K, exhibited a significant depolarizing shift in the voltage dependence of steady-state activation and significantly greater time constants of activation (τ) measured between 0 and +30 mV (Fig. 2.8 C and D). Neither variant differed from wild-type in the magnitude of cumulative inactivation evoked by moderate-frequency pulse trains (Fig. 2.3). Thus, both variants cause enhanced Kv2.1 suppression consistent with reduced neuronal delayed rectifier

current. Furthermore, these effects are compounded by the slower kinetics and more depolarized voltage dependence of activation evoked by M285R.

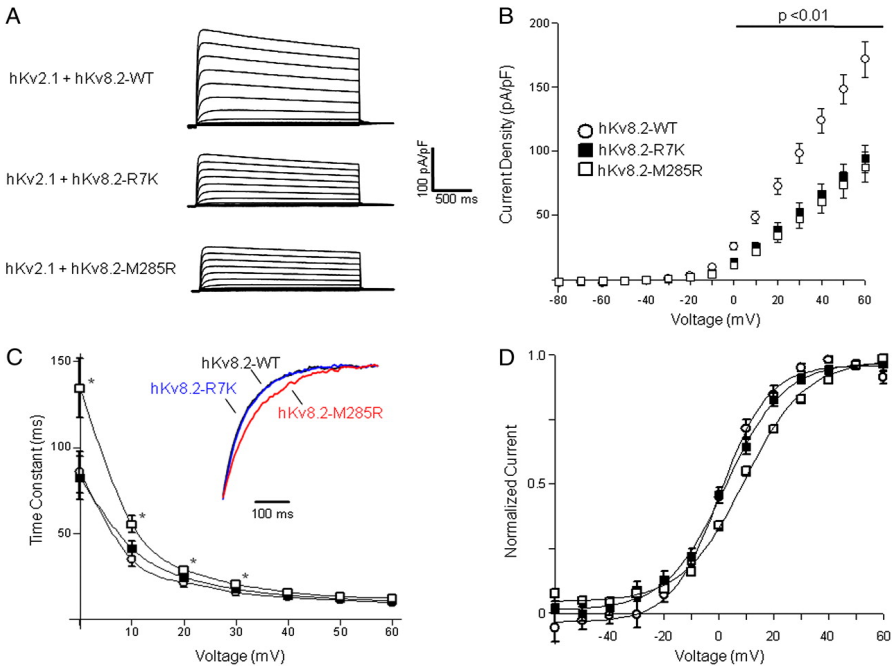

Figure 2.8 Functional Consequences of Human *KCNV2* Variants
(*A*) Averaged whole-cell current traces normalized to membrane capacitance recorded from CHO cells coexpressing human Kv2.1 with wild-type or mutant Kv8.2 (n = 7 to 8 for each condition). (*B*) Current density–voltage relationships recorded from cells coexpressing Kv2.1 with wild-type or mutant Kv8.2. Current was measured at 1,990 ms after start of the test pulse, then normalized to membrane capacitance. (*C*) Voltage dependence of activation time constants for Kv2.1 coexpressed with wild-type or mutant Kv8.2 (*P < 0.05 compared with WT). Time constants were determined from monoexponential fits to the data. Currents recorded at voltages <0 mV were too small to determine time constants. *Inset:* Averaged current traces (black, hKv8.2-WT; blue, hKv8.2-R7K; red, hKv8.2-M285R) recorded from 10 to 500 ms after a test pulse to 0 mV and normalized to current amplitude measured at 500 ms. (*D*) Voltage dependence of steady-state activation. Tail-current amplitudes were measured at −30 mV after a 2,000-ms activating pulse from −60 to +60 mV. Currents were normalized to peak amplitude and fit with Boltzmann functions. Values for activation $V_{1/2}$ were as follows: wild-type Kv8.2, 0.9 ± 1.2 mV; Kv8.2-R7K, 2.0 ± 1.6 mV (not significantly different from wild-type); and Kv8.2-M285R, 9.1 ± 1.1 mV (P < 0.01 compared with wild-type Kv8.2).

Discussion

In the present study we demonstrate important effects of *Kcnv2* variants on seizure susceptibility in humans and mice. In transgenic mice, increased expression of *Kcnv2* was sufficient to exacerbate the seizure phenotype in Q54 mice. In human epilepsy patients, we identified two unique nonsynonymous variants that exerted increased suppression of delayed rectifier potassium currents. Although both human *KCNV2* variants were inherited from an unaffected parent, they may act as susceptibility modifiers in the affected patients, as do the *Kcnv2* variants in the Q54 mouse model. Taken together, these results implicate *Kcnv2* as an important genetic factor in epilepsy.

Kcnv2 encodes the voltage-gated potassium channel subunit Kv8.2, which is a silent subunit when expressed as a homotetramer. However, when coassembled as a heterotetramer with Kv2 family members, Kv8.2 influences membrane translocation and biophysical properties of these channels [85, 86]. Kv2 channels are major contributors to delayed rectifier K+ current in hippocampal pyramidal neurons and act to dampen excitability during high-frequency stimulation [151, 156, 166]. Inclusion of Kv8.2 in heteromeric channels results in suppression of Kv2-mediated delayed rectifier potassium currents, which could impair membrane repolarization and thus predispose neurons to increased excitability.

Direct interaction between Kv8.2 and Kv2.1 channels has been demonstrated by coimmunoprecipitation in HEK293 cells [85]. The Kv8.2 and Kv2.1 subunits also show significant regional overlap in their central nervous

system expression patterns. Within the hippocampus, transcripts for both *Kcnv2* and *Kcnb1*, which encodes Kv2.1, are detected in the principal excitatory neurons of the pyramidal cell layers and the dentate gyrus [159-162, 167]. Similarly, both *Kcnv2* and *Kcnb1* are expressed in the cortex, with high levels of transcript in Layers 2/3 and 5 [159-162, 167]. This regional colocalization is consistent with an effect of Kv8.2 variants on Kv2.1 channels within cells of critical importance for seizure generation and propagation.

We had initially hypothesized that the amino acid differences between the resistant B6 and susceptible SJL strains were responsible for the divergent phenotypes [149]. Functional characterization of the Kv8.2 amino acid differences in a heterologous expression system demonstrated that the B6 isoform was more effective at suppressing Kv2.1-mediated currents. Because these channels are localized in excitatory neurons and the B6 strain is more resistant, this result was counterintuitive and suggested that the *in vivo* physiology is more complex. Therefore, we sought to test the relative contribution of expression and amino acids differences *in vivo*. Relative expression of *Kcnv2* in hippocampus was threefold greater in the susceptible SJL strain compared with B6. The *Kcnv2* gene is located in a divergent haplotype block between B6 and SJL, with a high degree of noncoding sequence variation (four SNPs/kb) that may influence *Kcnv2* transcript levels by altering the rate of transcription or mRNA stability [149]. Increased transgenic expression *in vivo* increased the severity of the seizure phenotype in Q54 mice, regardless of the amino acid sequence of the *Kcnv2* transgene. This observation supports the view that higher

expression of *Kcnv2* in strain SJL is sufficient for increased phenotype severity. Increased expression of *Kcnv2* would be predicted to decrease Kv2.1-mediated delayed rectifier potassium current, which could promote increased excitability under conditions of repetitive stimulation. In support of this mechanism, others have demonstrated that antisense knockdown of Kv2.1 in hippocampal slices resulted in increased CA1 pyramidal neuron excitability under conditions of high-frequency stimulation [151]. Thus, increased expression of *Kcnv2* alone could contribute to seizure susceptibility.

In further support of the importance of *KCNV2* in seizure pathogenesis, we identified unique nonsynonymous variants in two unrelated children with epilepsy. Functional characterization of these *KCNV2* variants, R7K and M285R, demonstrated that these variants also enhance Kv8.2-mediated suppression of Kv2.1 currents. These mutations would be predicted to decrease delayed rectifier potassium current in neurons, resulting in increased excitability under conditions of repetitive stimulation. The net effects would be similar to the effects of elevated expression of *KCNV2*. Consistent with the more severe clinical phenotype of patient 2, M285R exhibited additional kinetic defects, including a +10 mV shift in the voltage dependence of activation and slower activation kinetics. These defects are predicted to delay channel opening, which would likely further impair membrane repolarization and increase excitability. These results implicate enhanced Kv8.2 activity as a plausible genetically encoded factor in epilepsy susceptibility. Loss-of-function mutations in *KCNV2* identified in

autosomal recessive retinal cone dystrophy 3 [174-177] also implicate this channel as an important modulator of neuronal firing patterns.

Clinical severity in the two patients with *KCNV2* variants differs, ranging from relatively benign febrile and afebrile seizures in patient 1 (R7K) to severe epileptic encephalopathy in patient 2 (M285R). However, it is not uncommon for missense mutations in the same gene to result in different epilepsy types of varying severity. For example, missense mutations in *SCN1A* and *SCN2A* have been reported in patients with the benign epilepsy syndrome GEFS+, as well as in patients with the severe epileptic encephalopathy DS [44, 55]. Several factors may underlie the wide spectrum of phenotypes, including the location and nature of the amino acid substitution, divergent effects of the mutation on protein function, the genetic background of the individual, and environmental effects. Nonconservative substitution of arginine for methionine at the extracellular face of transmembrane segment 1 results in more profound biophysical defects than the conservative R7K substitution in the amino terminus. This difference in dysfunction is consistent with the difference in clinical severity. Additional resistance and susceptibility alleles at other loci are likely to contribute to the overall clinical phenotype. Although we found no evidence for interaction with mutant sodium channels in these patients, it is conceivable that the *KCNV2* variants interact with other loci to influence epilepsy susceptibility. Patient 1 (R7K) has a positive family history of two paternal uncles with childhood epilepsy. Although the R7K variant was inherited from his unaffected mother, it is possible

that there was paternal inheritance of additional genetic resistance or susceptibility factors.

Kcnv2 belongs to a group of potassium channel modulatory subunits that are electrically silent and cannot form functional homotetramers. These silent subunits form heterotetramers and modulate the properties of Kv2 and Kv3 channels, increasing the functional diversity of the channel subfamilies. This is particularly relevant for the Kv2 subfamily with only two members, Kv2.1 and Kv2.2. Targeting of modulatory subunits may offer a new therapeutic approach for fine-tuning neuronal excitability.

The interplay between ion channels contributes to overall neuronal excitability. Previous results from our laboratory and others have demonstrated genetic interactions between voltage-gated sodium, potassium, and calcium channels in mouse models of epilepsy [178-180]. The present study implicates a unique potassium channel subtype in epilepsy and suggests that variants in ion channels may act to modify the clinical phenotype in human epilepsy. This may have implications for molecular diagnostic testing and suggests that expanded ion channel screening may improve the utility of molecular testing for clinical risk assessment and disease management in epilepsy.

In summary, our results implicate *KCNV2* as a genetic modifier of epilepsy, and demonstrate that isolation of genetic modifiers in mice can lead to the identification of human epilepsy genes. Discovery of genes that influence susceptibility and disease progression will provide insight into the molecular

events of epileptogenesis, improve molecular diagnostic utility, and identify novel therapeutic targets for improved treatment of human epilepsy.

CHAPTER III

IDENTIFICATION OF KCNV2 REGULATORY REGIONS IN MOUSE

Introduction

Epilepsy is the fourth most common neurological disease in the United States behind migraine, stroke, and Alzheimer's disease, and it costs the U.S. economy approximately 12.5 billion dollars annually [6, 181]. It is a multifactorial disease, but the majority of cases have a genetic basis [35, 36]. Significant progress has been made in recent years identifying monogenic epilepsy genes. Most of the genes that have been identified encode voltage-gated ion channels or other components of neuronal signaling [44, 165].

Mutations in voltage-gated sodium channels are the leading cause of monogenic epilepsies. More than 800 mutations have been reported in *SCN1A* and the paralogous sodium channel gene *SCN2A* [55, 182, 183], resulting in a variety of human epilepsy syndromes, including BFNIS, GEFS+, and DS [44]. Variable expressivity is commonly observed among family members with inherited epilepsy-associated mutations [55]. This suggests that genetic modifiers may influence the clinical severity of monogenic epilepsies. Although monogenic epilepsies represent only 1 to 2% of genetic epilepsies [35], recent studies have shown a genetic association between monogenic epilepsy genes and epilepsy with more complex inheritance [184-186]. Therefore, identifying and characterizing modifier genes that contribute to monogenic epilepsies may

provide additional inroads into the etiology of more common epilepsy syndromes with complex inheritance.

We previously identified *Kcnv2* as a genetic modifier of the seizure phenotype of the Q54 transgenic mouse model, which carries a gain of function mutation in *Scn2a* (GAL879-881QQQ). Q54 mice have a progressive epilepsy phenotype, with focal seizures originating in the hippocampus at two months of age and eventually progressing to generalized tonic-clonic seizures. The seizures are accompanied by behavioral arrest, stereotyped repetitive behaviors, hippocampal cell loss and gliosis, and a reduced lifespan [71].

Analogous to the variable expressivity observed in humans with epilepsy-associated sodium channel mutations, the phenotype of Q54 mice varies with the genetic background of the mice. Q54 mice on the [B6 x SJL]F1.Q54 background (F1.Q54) exhibit an increased incidence of spontaneous seizures, earlier seizure onset, and decreased survival compared to Q54 mice on the B6 background. This indicates that the SJL strain contributes dominant modifier alleles that alter the severity of the epilepsy phenotype [140]. We performed genetic mapping and identified two modifier loci, *Moe1* on mouse chromosome 11 and *Moe2* on chromosome 19, that contribute to the strain-dependent phenotype variability in Q54 mice [140]. Subsequent studies identified the voltage-gated potassium channel *Kcnv2* as an epilepsy modifier gene at the *Moe2* locus [117, 149].

Kcnv2 encodes Kv8.2*,* a modulatory voltage-gated potassium channel subunit that coassembles with Kv2.1 subunits, altering membrane translocation and biophysical properties, with suppression of Kv2.1-mediated potassium

current as a net consequence [85, 86]. Kv2.1 channels, encoded by *Kcnb1* are the main contributors to delayed rectifier K^+ current in the cortex and hippocampus where they act to dampen excitability during high frequency stimulation of hippocampal pyramidal neurons [151, 156, 166]. Expression analyses reveal significant overlap between *Kcnv2* and *Kcnb1* transcripts in principal excitatory neurons of the pyramidal cell layers and dentate gyrus of the hippocampus and in layers 2/3 and 5 of the cortex [159-161, 167, 187].

Enhanced suppression of delayed rectifier potassium currents could predispose neurons to hyperexcitability by impairing membrane repolarization. Therefore, elevated expression of *Kcnv2* would be predicted to heighten neuronal excitability, especially under conditions of repetitive stimulation [117]. Consistent with this prediction, the seizure-susceptible SJL strain exhibits a threefold increase in hippocampal *Kcnv2* expression relative to the seizure-resistant B6 strain, and elevated *Kcnv2* expression is positively correlated with the phenotype severity of double transgenic mouse lines expressing Q54 with variable amounts of the *Kcnv2* transgene [117]. Hence, strain-dependent variability in *Kcnv2* expression appears to underlie its modifier effect on the Q54 phenotype.

The identification of *Kcnv2* as a genetic modifier of epilepsy by genetic mapping and candidate gene analysis suggests that regulatory sequence variation in or near the *Kcnv2* locus contributes to differences in steady-state *Kcnv2* expression between strains. A transcript's steady-state expression level is a result of the balance between its rates of transcription and degradation.

Elements controlling the rate of transcription are generally found upstream of the transcription start site (TSS) in the promoter regions of genes, while elements that determine the rate of mRNA degradation are often found in the 3' UTR.

We hypothesize that regulatory sequence variation in the promoter and/or 3' UTR of *Kcnv2* influences seizure susceptibility by altering steady-state expression levels. As a first step towards addressing our hypothesis, we sought to define the TSS, promoter, and 3' UTR organization of the full-length *Kcnv2* transcript. Using 5' RNA ligase-mediated rapid amplification of cDNA ends (RACE) analysis and an RNase protection assay (RPA), we identified the *Kcnv2* TSS and applied this knowledge to the generation of a 5' deletion series of luciferase reporter constructs to identify the core promoter region. We also employed 3' RACE analysis to define the 3' UTR organization of *Kcnv2*. The knowledge gained from these studies will inform future experiments to elucidate the effects of regulatory sequence variation on *Kcnv2* expression levels. Taken together these studies will improve our understanding of the molecular basis of the *Kcnv2* modifier effect and advance our knowledge of the mechanisms by which genetic modifiers influence epilepsy.

Methods

Sequencing of Kcnv2 Non-Coding Sequence

Overlapping PCR amplicons spanning 3.3 kb upstream and 3.3 kb downstream of the *Kcnv2* open reading frame were gel purified and Sanger sequenced. (The amplification/sequencing primers are listed in Table 3.1.) The resulting sequences were aligned to the B6 reference sequence (GRCm38) for comparison using Sequencher software (Gene Codes, Ann Arbor, MI, USA).

Table 3.1 Primer and Oligo Sequences for Sequencing, RACE, and RPA

	Primer/Oligo	Sequence (5'-3')
Sequencing	5' UTR-F1	ATATTGCCTAGAAAGTCAGTATG
	5' UTR-R1	ATCGCTCTGGAGCTTCTCTTTAC
	5' UTR-F2	TTAAAAGTAAAGAGAAGCTCCAG
	5' UTR-R2	TGTTTAGATCCTCTAGAATTTTC
	5' UTR-F3	GAAAATTCTAGAGGATCTAAAC
	5' UTR-R3	GCGGTGTTGGTTGCTCCCAGTG
	3' UTR-F1	GAGGGAACGAGGAAAGGTCAACT
	3' UTR-R1	GTTCCCAACCCTCAGTCTAAAGA
	3' UTR-F2	TGGAAGAGTAAAACCTCCTTCAC
	3' UTR-R2	TTGAGTAGGGCTCTCTGTAAGTC
	3'UTR-R3	TCATTCCCTGATGTCTGAGTTAG
	3' UTR-F4	CAAAGAATCCTGGCTTGATG
	3' UTR-R4	ATGGGACCTAGTCAACAGCA
5' RACE	5' RACE Oligo	CGACUGGAGCACGAGGACACUGACAUGGA CUGAAGGAGUAGAAA
	5' RACE-F	CGACTGGAGCACGAGGACACTGA
	5' RACE-F Nested	GGACACTGACATGGACTGAAGGAGTA
	5' RACE-R	CAGCTCGTCTCGCACCAGCAACACC
	5' RACE-R Nested	TGGCCAGGCGACCCAGGCGCGTTTT
	M13R	CAGGAAACAGCTATGAC
3' RACE	GeneRacer Oligo dT	GCTGTCAACGATACGCTACGTAACGGCATG ACAGTG$(T)_{24}$
	3' RACE-F	CCCAAACAGCACACCCTTCAGCCAAGA
	3' RACE-F Nested	TGCCCTTCCATCCATCCCCAGCTCTCTA
	3' RACE-R	CGACTGGAGCACGAGGACACTGA
	3' RACE-R Nested	TGCCCTTCCATCCATCCCCAGCTCTCTA
	M13R	GTAAAACGACGGCCAG
RPA	RPA-F	GGTGGGGAGAGACTGAACTG
	RPA-R	TTCCTGGCCTATCTCTCCTG

5' Rapid Amplification of cDNA Ends

Poly(A) RNA was isolated from total RNA (extracted from B6 and SJL eyes or whole brain with TRIzol (Life Technologies, Grand Island, NY, USA)) using the PolyAtract mRNA Isolation system (Promega, Madison, WI, USA). The poly(A) RNA was used as a template to produce RACE-ready cDNA using the the GeneRacer Kit (Invitrogen, Carlsbad, CA, USA) according to the manufacturer's protocol. Briefly, poly(A) RNA was treated with calf intestinal phosphatase to remove 5' phosphates from truncated transcripts, preventing the subsequent ligation of an RNA Oligo. The RNA was then treated with tobacco acid pyrophosphatase to remove the 5' cap structure from full-length transcripts, and an RNA Oligo (5' RACE Oligo) (Table 3.1) was ligated to the 5' end of de-capped transcripts with T4 RNA ligase. cDNA was reverse transcribed from the ligation product with SuperScript III reverse transcriptase and random hexamers (Invitrogen, Carlsbad, CA, USA). 5' cDNA ends were amplified by nested PCR with forward primers complimentary to the ligated RNA Oligo (5' RACE-F and 5'RACE-F Nested) and *Kcnv2*-specific reverse primers (5' RACE-R and 5' RACE-R Nested) (Table 3.1; Figure 3.1). The PCR product was gel-purified and cloned into the pCR4-TOPO sequencing vector (Invitrogen, Carlsbad, CA, USA) and transformed into One Shot TOP10 Competent Cells (Invitrogen, Carlsbad, CA, USA). Plasmid DNA was isolated with the QIAprep Spin Miniprep Kit (Qiagen, Germantown, MD, USA) and Sanger sequenced with the M13R primer (Table 3.1). Insert sequences were aligned to the C57BL/6J *Kcnv2* reference sequence and analyzed using Sequencher software (Gene Codes, Ann Arbor,

MI, USA) to determine the genomic location of the 5' terminus of each RACE product.

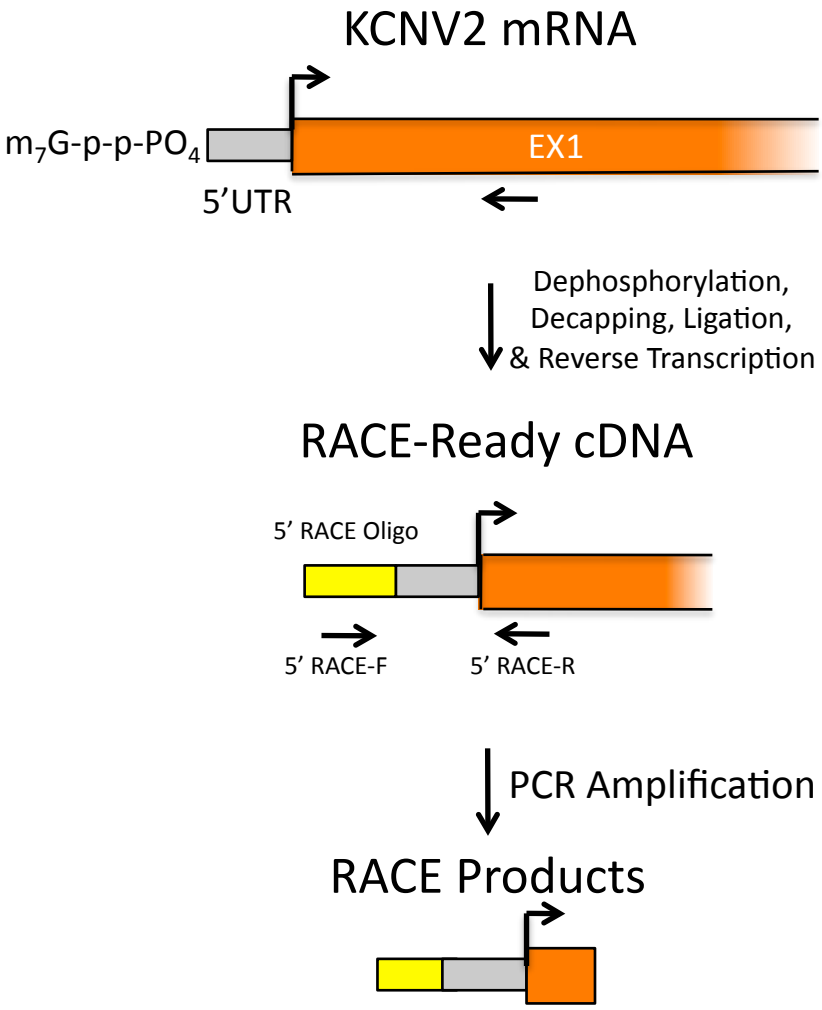

Figure 3.1 5' RACE Strategy
5' RACE products were generated using the GeneRacer Kit (Invitrogen, Carlsbad, CA, USA). RACE products were cloned into the pCR4-TOPO sequencing vector (Invitrogen, Carlsbad, CA, USA) for sequencing, and the resulting sequences were aligned to the C57BL/6J *Kcnv2* reference sequence and analyzed using Sequencher software (Gene Codes, Ann Arbor, MI, USA).

3' Rapid Amplification of cDNA Ends

Poly(A) RNA was isolated from B6 and SJL whole-brains as described above. The poly(A) RNA was used as a template to produce RACE-ready cDNA using the GeneRacer Kit (Invitrogen, Carlsbad, CA, USA) according to the manufacturer's protocol. Briefly, cDNA was reverse transcribed from poly(A) RNA with SuperScript III reverse transcriptase (Invitrogen, Carlsbad, CA, USA) using the GeneRacer Oligo dT Primer (Table 3.1). 3' cDNA ends were then amplified by nested PCR with *Kcnv2*-specific forward primers (3' RACE-F; 3' RACE-F Nested) and reverse primers complementary to the sequence of the Oligo dT Primer that was used for reverse transcription (3' RACE-R and 3' RACE-R Nested) (Table 3.1; Figure 3.2). Nested PCR products were gel-purified, cloned, and sequenced as described above to determine the genomic location of the 3' termini of each RACE product.

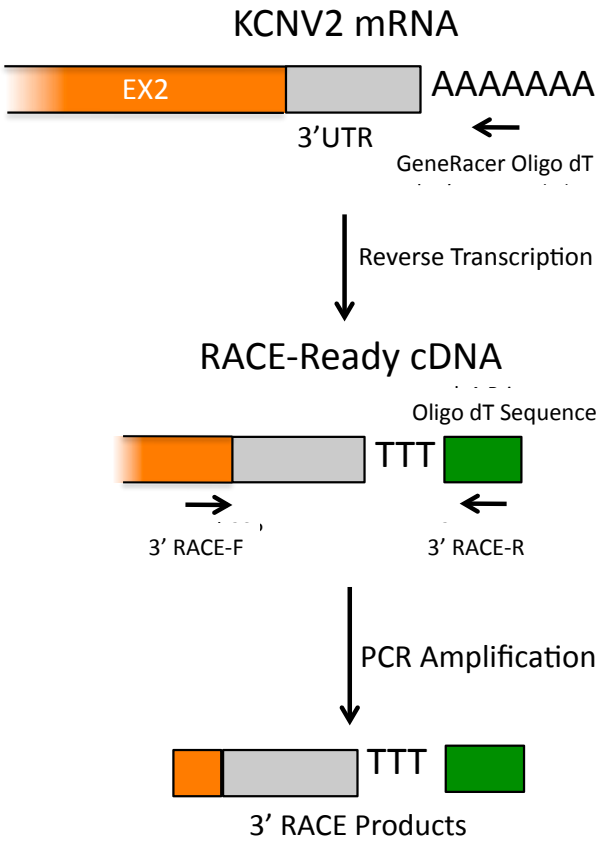

Figure 3.2 3' RACE Strategy
3' RACE products were generated with the GeneRacer Kit (Invitrogen, Carlsbad, CA, USA) and analyzed as described for 5' RACE.

Ribonuclease Protection Assay

Poly(A) RNA was isolated from B6 or SJL eyes as described above. An antisense RNA probe labeled with incorporated biotin-16-labeled-UTP (4:1 labeled:unlabeled nucleotide) and directed against the mouse *β-actin* transcript was transcribed from the T3 promoter of linearized pTRIPLEscript plasmid containing 250 bp of mouse β-actin gene (Ambion, Austin, TX, USA) using the MAXIscript In Vitro Transcription Kit (Life Technologies, Grand Island, NY, USA). For generation of an antisense RNA probe directed to overlap the predicted 5' terminus of the *Kcnv2* transcript (258 bp to 16 bp upstream of the *Kcnv2* start codon), a DNA template was PCR amplified from the B6 BAC clone RP24-537C5, containing the *Kcnv2* genomic region 63.6 kb upstream of the start codon and 37.3 kb downstream of the stop codon, with RPA-F and RPA-R primers (Table 3.1). The resulting product was cloned into the pCR4-TOPO plasmid (Invitrogen, Carlsbad, CA, USA), and the sequence was verified by Sanger sequencing. The resulting plasmid DNA was linearized by restriction enzyme digest (NotI) and used as template to transcribe the antisense RNA probe with incorporated biotin-16-labeled-UTP (4:1 labeled:unlabeled nucleotide) using the MAXIscript In Vitro Transcription Kit (Life Technologies, Grand Island, NY, USA). The full-length β-actin and *Kcnv2* probes were gel purified following electrophoresis on an 8 M urea 5% acrylamide gel, by overnight recovery in elution buffer (0.5M ammonium acetate, 1 mM EDTA , and 0.2% SDS), ethanol precipitation, and resuspension in nuclease-free water. RNA samples (0.36 μg mouse eye-derived poly(A) RNA, 10 μg torulla yeast RNA, or 1 μg mouse liver-

derived RNA) were co-precipitated with the appropriate probe (300 pg α-*Kcnv2* or 300 pg α-β-*actin*), resuspended in 10 μL of Hybridization Buffer III, denatured for 4 minutes (95° C), and hybridized overnight at 42° C. 150 μL of RNase Digestion III Buffer with or without RNaseA/RNase T1 Mix (1:100 dilution) was added to the hybridization reactions and the mixtures were incubated for 30 minutes at 37° C. Digestion reactions were inactivated by addition of 225 uL RNase Inactivation Solution III and ethanol precipitated. Protected probe fragments were resuspended in 10 uL of Gel Loading Buffer II and separated by electrophoresis through a denaturing polyacrylamide gel (5% acrylamide, 8M urea). Separated fragments were then electrolytically transferred to a positively-charged nylon membrane and visualized by chemiluminescent detection using the BrightStar BioDetect system (Ambion, Austin, TX, USA) according to the manufacturer's protocol.

Generation of Luciferase Reporter Constructs

A 7.3 kb fragment spanning -5.9 kb to +1.4 kb from the *Kcnv2* start codon was digested from RP24-537C5 B6 BAC DNA with SnaBI and SacII, gel purified, and cloned into the multiple cloning site of the pGEM-T Easy Vector (Promega, Madison, WI, USA) between the EcoRI and SacII sites. From this construct a 5.8 kb fragment corresponding to the region -5925 bp to -102 bp from the *Kcnv2* start codon was digested with ApaI and MluI, gel purified, and cloned into the multiple cloning site of the promoterless pGL3-Basic luciferase reporter vector (Promega, Madison, WI, USA) between the SmaI and MluI sites (upstream of the firefly

luciferase gene) to generate pGL3-Basic-5925. From this construct we generated a 5' deletion series of reporter constructs by excising fragments from the 5' end of the *Kcnv2* insert with restriction enzymes, gel purifying the remaining construct, and re-ligation (Figure 3.3). pGL3-Basic-2818, containing a fragment corresponding to the region -2818 bp to -102 bp from the *Kcnv2* start codon, was generated by excising the region between the MluI and SmaI sites; pGL3-Basic-1924, containing a fragment corresponding to the region -1924 bp to -102 bp from the *Kcnv2* start codon, was generated by excising the region between the two KpnI sites; and pGL3-Basic-373, containing a fragment corresponding to the region -373 bp to -102 bp from the *Kcnv2* start codon, was generated by excising the region between the PasI and MluI sites. We positioned the 3' end of all of the constructs downstream of the predicted transcription start site to account for potential downstream promoter elements (Fig. 3.3). The direction of the insert corresponding to the region -373 bp to -102 bp from the *Kcnv2* start codon was reversed by excision with KpnI and XhoI followed by a blunt-ended re-ligation of the excised fragment and insert. All of the constructs were prepped using the QIAfilter Plasmid Maxi Kit (Qiagen, Germantown, MD, USA), ammonium acetate precipitated, and verified by Sanger sequencing.

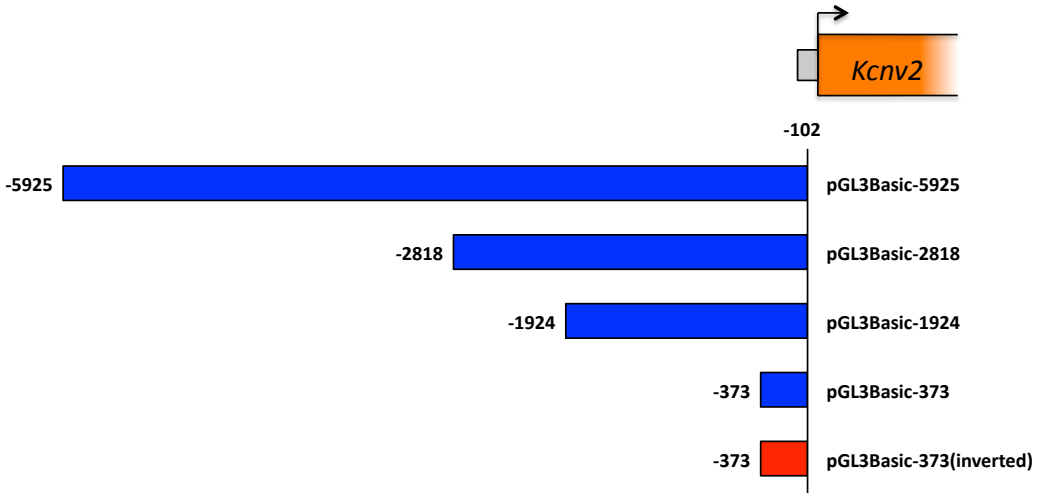

Figure 3.3 Luciferase Promoter Assay Constructs
The genomic location of each of the 5' *KCNV2* genomic fragments used in the 5' deletion series of luciferase reporter constructs are depicted in blue. The numbers represent the postion of the ends of the fragments relative to the *KCNV2* start codon (bp).

Mammalian Cell Culture

tSA201 cells were grown in 35x10 mm cell culture dishes in Dulbecco's modified Eagle's medium (DMEM, Life Technologies, Grand Island, NY, USA) supplemented with 10 % fetal bovine serum (FBS, Atlanta Biologicals, Norcross, GA, USA), 2 mm l-glutamine (Life Technologies, Grand Island, NY, USA) and penicillin (50 units ml−1)-streptomycin (50 µg ml−1) (PenStrep) (Life Technologies, Grand Island, NY, USA). Cells were maintained at 37° C and 5% CO2.

Neuro-2a cells were grown as described above in Minimum Essential Medium (MEM, Life Technologies, Grand Island, NY, USA) supplemented with 10% FBS (Atlanta Biologicals, Norcross, GA, USA) and Pen Strep (Life Technologies, Grand Island, NY, USA).

Transfection

Each pGL3 promoter-reporter vector was co-transfected with an internal control vector (phRL-TK, Promega, Madison, WI, USA) into tSA201 cells (grown to 70% confluency in 35x10mm dishes) with FuGene 6 transfection reagent (8.3 µL) (Promega, Madison, WI, USA) (10:1 mass ratio promoter-reporter:control). Cells co-transfected with a positive control vector (pGL3-Control) and phRL-TK or empty pGL3-Basic and phRL-TK were included as positive and negative controls, respectively.

Promoter Assay

One day post-transfection, each co-transfected plate of cells was spun down, resuspended in .5 mL Dulbecco's modified Eagle's medium without phenol red (Life Technologies, Grand Island, NY, USA), and used to seed quadruplicate wells of a 96-well plate (50,000 cells/well in 75 μL medium). Firefly and renilla luciferase luminescence values were assayed in the 96-well plate with the Dual-Glo Luciferase Assay System (Promega, Madison, WI, USA) according to the manufacturer's protocol on a SpectraMax M5 microplate reader (Molecular Devices, Sunnyvale, CA, USA) (integration time: 1000 ms). Background firefly and renilla luminescence values from untransfected cells (in relative luminescence units) were used for background subtraction, and the background subtracted firefly luciferase signal from each well was normalized to the background subtracted renilla signal. The normalized luminescence values were averaged for each co-transfection condition, and the averaged values were expressed as a percentage of the signal from the positive control condition (cells transfected with pGL3-Control and phRL-TK). Relative luminescence values from three independent experiments were compared by analysis of variance (ANOVA) with Fisher's protected least significant difference (PLSD) post hoc tests.

Results

Polymorphisms in the Kcnv2 Genomic Locus

In order to determine the degree and location of sequence variation between the B6 and SJL strains in the genomic regions likely to contain *cis*-regulatory elements, we sequenced the regions 3.3 kb upstream and 3.3 kb downstream of the *Kcnv2* open reading frame. We observed 11 SNPs and 4 insertions/deletions in the 3.3 kb region upstream of the start codon and 10 SNPs and 3 insertions/deletions in the predicted 3.3 kb 3' UTR (Table 3.2). Any of these sequence variants could potentially occur in *Kcnv2 cis*-regulatory elements and contribute to phenotype variability by altering *Kcnv2* steady-state expression levels.

Table 3.2 Sequence Variations Flanking the *Kcnv2* Open Reading Frame

refSNPNumber	Position	Location	Polymorphism (B6/SJL)
rs47576807	27394410	5' UTR (-2831)	A/T
rs49973767	27394423	5' UTR (-2818)	A/G
rs49032467	27394430	5' UTR (-2811)	C/G
rs50095982	27394459	5' UTR (-2782)	G/T
rs51118515	27394547	5' UTR (-2694)	A/G
rs48681962	27394550	5' UTR (-2691)	A/G
rs50151415	27394608	5' UTR (-2633)	C/T
rs51798120	27394610	5' UTR (-2631)	A/G
N/A	27394667	5' UTR (-2574)	AAGC/ΔΔΔΔ
rs48240078	27394691	5' UTR (-2550)	A/T
rs47991174	27394734	5' UTR (-2507)	C/T
N/A	27395776	5' UTR (-1465)	AGAG/ΔΔΔΔ
N/A	27396226	5' UTR (-1015)	TT/ΔΔ
N/A	27396358	5' UTR (-883)	ΔΔΔΔΔΔΔΔ/TGTGTATG
rs52438530	27396370	5' UTR (-871)	A/G
rs30714257	27408725	3' UTR (*312)	C/T
rs47646864	27409103	3' UTR (*690)	C/T
rs48939494	27409106	3' UTR (*693)	C/T
rs36353013	27409161	3' UTR (*748)	A/G

Table 3.2 Contd. Sequence Variations Flanking the *Kcnv2* Open Reading Frame

refSNPNumber	Position	Location	Polymorphism (B6/SJL)
rs30637777	27409359	3' UTR (*946)	C/T
rs31041186	27409707	3' UTR (*1294)	A/G
rs30366768	27409848	3' UTR (*1435)	A/G
rs30425376	27410172	3' UTR (*1759)	A/G
N/A	27410560	3' UTR (*2147)	A/Δ
N/A	27410569	3' UTR (*2156)	T/Δ
rs30657326	27411462	3' UTR (*3049)	C/T
rs30763819	27411668	3' UTR (*3255)	C/T
N/A	27411676	3' UTR (*3263)	Δ/T

Determination of Kcnv2 Transcription Start Site Region

To determine the location of the *Kcnv2* TSS region we performed a 5' RNA ligase-mediated rapid amplification of cDNA ends (RACE) analysis on CNS-derived cDNA from B6 and SJL mice. The 5' terminus of each RACE product represents the beginning of the *Kcnv2* transcript from which it was made. Thus, we cloned and sequenced 142 *Kcnv2* RACE products and aligned the sequences to the B6 reference sequence (GRCm38) to determine the genomic location of individual RACE products. The 5' RACE product termini aligned to a region 230-130 bp upstream of the *Kcnv2* start codon. This suggests that *Kcnv2* transcription occurs from any of several sites dispersed over a 100 bp TSS region at this location (Figure 3.4). This location is consistent with available RNA-

seq data as well as TSS predictions from the Ensembl and UCSC genome databases (GRCm38) (Fig. 3.5) [188, 189].

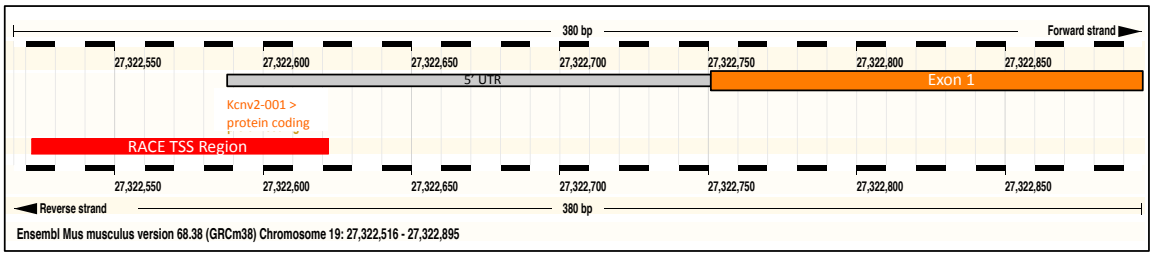

Figure 3.4 5' RACE Summary
Summary of 5' RACE data. The RACE TSS Region (in red) represents the genomic location of the region in which the 5' termini of RACE products aligned. The gray and orange bars represent the *Kcnv2* 5' UTR and coding sequence, respectively, as predicted in Ensembl. (Modified from from www.ensembl.org (GRCm38 & h37)).

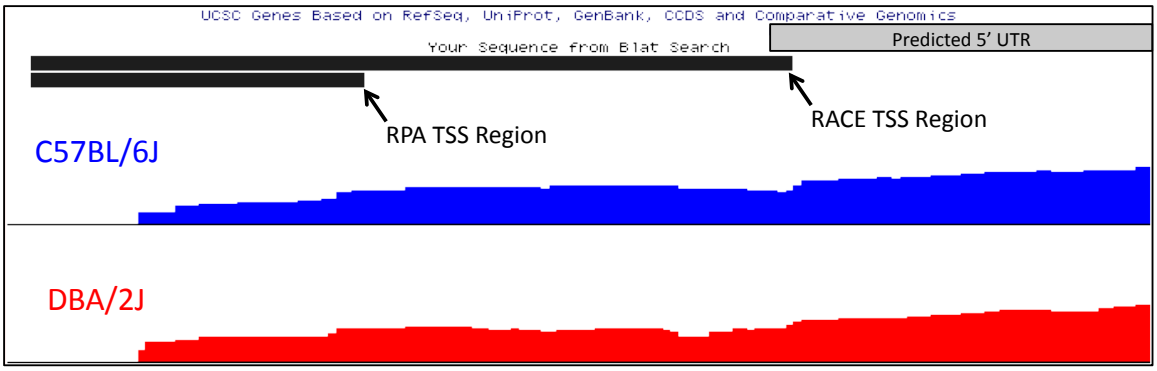

Figure 3.5 Convergence of RACE, RPA, and RNA-seq Data
Alignment of *Kcnv2* TSS regions as predicted by RACE, RPA, and RNA-seq data from C57BL/6J and DBA/2J mouse strains (available in genenetwork.org). DBA/2J and SJL share a similar haplotype in this genomic region. Gray bar represents the TSS predicted in the UCSC Genome Browser (GRCm38). (Modified from UCSCbrowser.genenetwork.org.)

Next, to independently confirm the location of the *Kcvn2* TSS, we performed a ribonuclease protection assay on eye-derived mRNA from B6 and SJL mice with an anti-sense RNA probe directed against the 5' end of the predicted *Kcnv2* transcript (-274 to -17 bp upstream of the start codon). Inferring from the genomic location of the full-length *Kcnv2* probe and the size of the protected probe fragments, which ranged from ~215 bp to ~190 bp, the assay suggested that the *Kcnv2* transcription start site region is located approximately 230-205 bp upstream of the *Kcnv2* start codon (Figure 3.6), which is consistent with both the 5' RACE data and available RNA-seq data from genenetworks.org (Figure 3.5) [190].

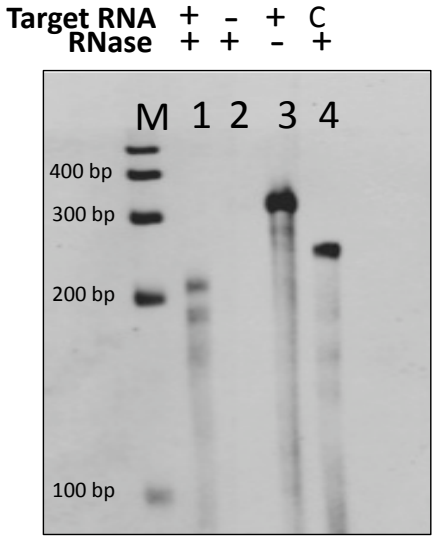

Full length α-sense probe = 258 bp
Full length probe + vector = 323 bp
B-actin probe = 245 bp

Lane M – RNA Century Plus Marker

Lane 1 – *Kcnv2* probe + sample mRNA (experimental lane)

Lane 2 – no target control

Lane 3 – no Rnase control

Lane 4 – β-actin probe + mouse liver RNA (positive control lane)

Figure 3.6 RNase Protection Assay
Protected probe fragments were separated by electrophoresis and visualized by chemiluminescence. Lane M: RNA Century-Plus Marker. Lane 1: *Kcnv2* probe hybridized with sample mRNA from mouse retina. Lane 2: Fully digested *Kcnv2* probe (no target control). Lane 3: Full-length *Kcnv2* probe w/ 105 bp of flanking vector (no Rnase control). Lane 4: β-actin probe hybridized with RNA from mouse liver (positive control).

Identification of Kcnv2 Core Promoter Region

To identify the *Kcnv2* core promoter, we cloned genomic fragments upstream of the *Kcnv2* TSS region into a promoterless luciferase reporter vector (pGL3Basic, Promega, Madison, WI, USA) to generate a 5' deletion series of promoter-reporter constructs (Figure 3.3). We transiently transfected each construct into a human-derived cell line (tsA201) with a renilla luciferase-expressing control vector (phRL-TK) and compared the resulting promoter activities using the Dual-Glo Luciferase Assay System (Promega, Madison, WI, USA). The reporter construct containing the *Kcnv2* genomic fragment corresponding to the region 373-102 bp upstream of the *Kcnv2* start codon exhibited significantly greater renilla-normalized firefly luciferase activity than the empty pGL3-Basic vector. This activity was abolished when the sequence was inverted in the reporter construct (Figure 3.7). These results suggest that the *Kcnv2* core promoter, which we operationally defined as the minimal genomic sequence necessary to produce a basal level of promoter activity, is contained within the region 373-102 bp upstream of the *Kcnv2* start codon. Additionally, we observed significant differences in the luciferase activities exhibited by the promoter-reporter constructs containing upstream *Kcnv2* sequence, which suggests that the corresponding regions may contain additional cis-regulatory elements that influence *Kcnv2* transcription. We also tested the constructs in a mouse neuroblastoma-derived cell line (Neuro-2a), but we did not observe luciferase signal from any of the *Kcnv2*-derived constructs (data not shown). This suggests that *Kcnv2* may be actively repressed in this cell line.

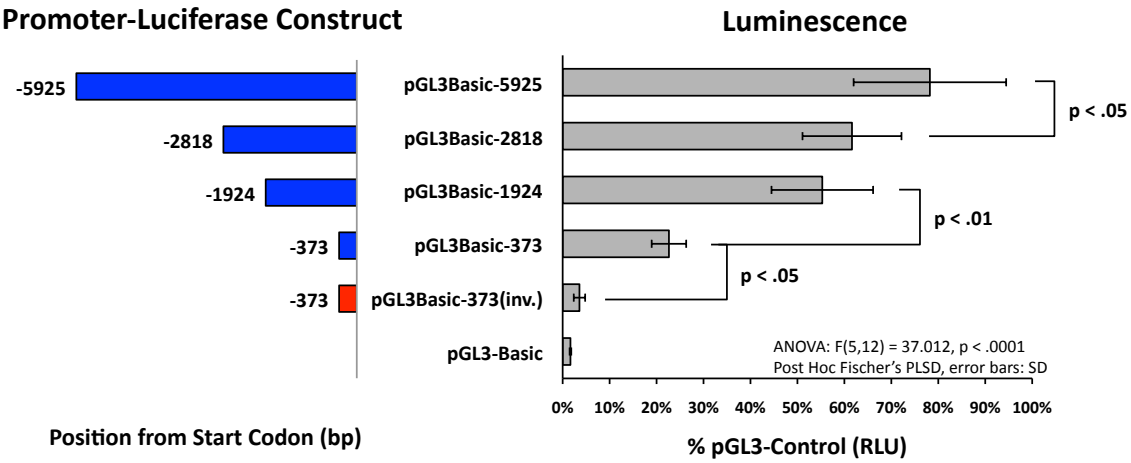

Figure 3.7 Luciferase Promoter Assay
Data are from three independent experiments, each with four technical replicates per condition. Firefly luciferase signals (relative luminescence units) from each well were background subtracted and normalized to renilla. The normalized values were averaged for each condition (four replicates / condition) and expressed as a percentage of the signal from the positive control vector (pGL3-Control).

Determination of 3' Untranslated Region Organization

To determine the organization of the *Kcnv2 3' UTR*, we performed a 3' RACE analysis on *Kcnv2* RACE products generated from B6 and SJL-derived cDNA. The RACE products were cloned, sequenced, and analyzed as described for the 5' RACE analysis to determine the genomic location of the 3' termini of each RACE product, which represents the 3' end of the *Kcnv2* transcript from which it was derived. Consistent with the predicted transcript in the Ensembl and UCSC genome databases (GRCm38), the 3' termini of the RACE products (n = 15 alignments) aligned to a region located 3193-3284 bp downstream of the *Kcnv2* stop codon (Figure 3.8) [188, 189].

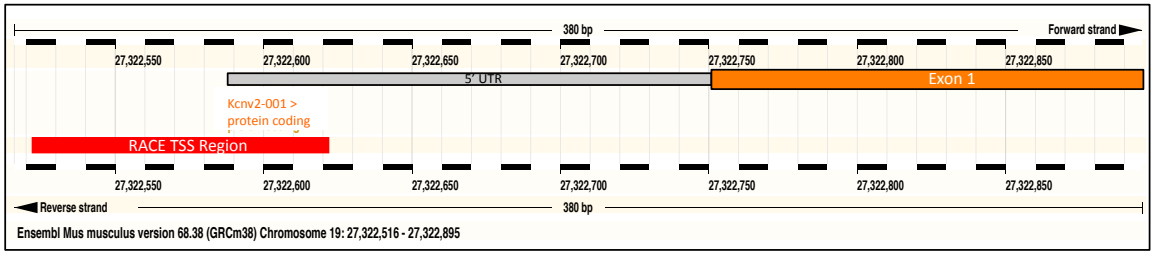

Figure 3.8 5' RACE Summary
Summary of 5' RACE data. The RACE TSS Region (in red) represents the genomic location of the region in which the 5' termini of RACE products aligned. The gray and orange bars represent the *Kcnv2* 5' UTR and coding sequence, respectively, as predicted in Ensembl. (Modified from www.ensembl.org (GRCm38 & h37)).

Discussion

Our previous studies suggested that *Kcnv2* expression differences may underlie the strain differences in the epilepsy phenotype of Q54 mice. We hypothesized that regulatory sequence variation in the promoter and/or 3' UTR of *Kcnv2* influences seizure susceptibility by altering steady-state expression levels. Consistent with our hypothesis, regulatory variants with a relatively small effect on mRNA expression have been shown to modify complex clinical phenotypes in a number of diseases including cystic fibrosis, type 1 diabetes, female diarrhea predominant irritable bowel syndrome, and epilepsy [191-195].

Kcnv2 is located on mouse chromosome 19 in a divergent haplotype block between B6 and SJL [149]. We observed a high degree of sequence variation between the B6 and SJL strains in the genomic regions flanking the *Kcnv2* open reading frame, where *cis*-regulatory elements are likely to be located. Variation in cis-regulatory elements in the promoter region could affect the rate of *Kcnv2* transcription by altering transcription factor binding sites, and variation in the 3'

UTR could disrupt binding sites for regulatory proteins and miRNAs that influence mRNA degradation.

As an initial step towards identifying *Kcnv2* *cis*-regulatory elements that influence strain differences in *Kcnv2* expression, we sought to define the *Kcnv2* core promoter and 3' UTR regions. Because the promoter region lies upstream of the TSS, we first identified the *Kcnv2* TSS region by two independent methods, RACE analysis and RPA. Both the 5' RACE and RNase protection assays suggested the *Kcnv2* TSS region is located 230-130 bp upstream of the *Kcnv2* start codon. Thus, it appears that *Kcnv2*, which does not have a TATA box, is transcribed from multiple TSS dispersed over ~100 bp region. This observation is consistent with other TATA-less genes, which tend to be transcribed from a nondescript 50-100 bp region rather than from a single, defined nucleotide [196, 197]. Neither assay indicated the presence of any 5' non-coding exons, and the suggested TSS region location is consistent with RNA-seq data [190] and predicted transcripts in the Ensembl and UCSC genome databases (GRCm38) [188, 189]. The convergence of 5' RACE and RNase protection assay data with available bioinformatic data suggests that we correctly defined the location of the *Kcnv2* TSS region.

We used this information to generate a 5' deletion series of luciferase reporter constructs to identify the *Kcnv2* core promoter. The reporter construct containing the insert corresponding to the region 373-102 bp upstream of the *Kcnv2* start codon exhibited a basal level of luciferase activity, which suggests that the *cis*-factors necessary for the proper initiation of transcription are

contained within this region. Consistent with the directional activity of a promoter, reversing the orientation of the insert in the reporter vector abolished its activity. These observations suggest that the *Kcnv2* core promoter lies within the region 373-102 bp upstream of the *Kcnv2* start codon. We also observed significant differences in the luciferase activities of the promoter-reporter constructs containing additional *Kcnv2* upstream sequence. This suggests that the region upstream from the *Kcnv2* core promoter may contain proximal promoter elements that influence *Kcnv2* expression. In the future, these regulatory elements can be identified by comparing the luciferase activities of parallel B6 and SJL-derived reporter constructs in cultured hippocampal neurons.

To determine the organization of the *Kcnv2* 3' UTR, we performed a 3' RACE assay. The results of this assay suggest that the 3' UTR extends between 3193-3284 bp downstream of the *Kcnv2* stop codon. This location is consistent with the predicted 3' UTR in the Ensembl and UCSC genome databases (GRCm38). Additionally, there is a consensus polyadenylation sequence located 3256 bp downstream from the *Kcnv2* stop codon, which further supports the results of the RACE assay. Thus, it is likely that we correctly defined the 3' terminal region of the *Kcnv2* transcript. However, it should be noted that interpretation of the 3' RACE results is complicated by the presence of a genomic 21 bp poly-A tract immediately downstream from the predicted 3' UTR. It is possible that this poly-A tract acts as an erroneous binding site for the GeneRacer Oligo dT primer used to reverse transcribe the cDNA from which the RACE products were amplified. This would result in truncated RACE products.

An RNase protection assay with an antisense RNA probe directed against the 3' end of the *Kcnv2* transcript would further validate the results of the RACE assay.

In the future, the effect of 3' UTR sequence variation between strains on the rate of mRNA degradation could be determined by treating cultured hippocampal neurons from B6xSJL.F1 mice with Actinomycin-D to inhibit transcription. An allele specific qRT-PCR could then be performed on samples taken at various timepoints after treatment to compare the relative amounts of remaining B6 or SJL-derived *Kcnv2* transcript. If it is determined that there are allelic differences in mRNA degradation, replacing specific regions of the B6-derived 3' UTR with SJL-derived sequence in reporter constructs could help to identify the regulatory elements responsible.

The aforementioned studies are focused on the *Kcnv2* promoter and 3' UTR regions. While these regions are likely to contain *cis*-regulatory elements that influence *Kcnv2* expression, it is possible that distal enhancers or silencers also act to influence *Kcnv2* expression. If sequence variation in *cis*-regulatory elements within the promoter and/or 3' UTR regions fails to account for the strain differences in *Kcnv2* expression, it may be necessary to investigate more distal regions for potential *Kcnv2* regulatory elements.

In the present studies we defined the regions where *Kcnv2 cis*-regulatory elements are likely to be located. These studies will provide the foundation for future studies to determine the effect of sequence variation in these regions on *Kcnv2* expression. Together, these studies will help determine the molecular

basis of the *Kcnv2* modifier effect and advance our knowledge of the mechanisms by which genetic modifiers influence epilepsy.

CHAPTER IV

DE NOVO KCNB1 MUTATIONS IN EPILEPTIC ENCEPHALOPATHY*

Introduction

Epileptic encephalopathies are a heterogeneous group of severe childhood-onset epilepsies characterized by refractory seizures, neurodevelopmental impairment, and poor prognosis [26]. The developmental trajectory is normal prior to seizure onset, after which cognitive and motor delays become apparent. Ongoing epileptiform activity adversely affects development and contributes to functional decline. Therefore, early diagnosis and intervention may improve long-term outcomes [198-200].

Recently, there has been significant progress in identifying genes responsible for epileptic encephalopathies, and *de novo* mutations have been reported in approximately a dozen genes, including *SCN1A*, *SCN2A*, *SCN8A*, *KCNQ2*, *HCN1, GABRA1*, *GABRB3*, *STXBP1*, *CDKL5*, *CHD2*, *SYNGAP1*, and *ALG13* [60, 201-204]. The majority of mutations reported are in genes encoding voltage-gated ion channels, neurotransmitter receptors and synaptic proteins. There is considerable phenotype heterogeneity, with mutations in the same gene resulting in different clinical presentations, as well as locus heterogeneity, with mutations in different genes resulting in the same syndrome. Further, epileptic

* Modified from: Torkamani, A., et al., De Novo KCNB1 Mutations in Epileptic Encephalopathy. Ann Neurol, 2014.

encephalopathy genes have substantial overlap with genes responsible for other neurodevelopmental disorders, including autism and intellectual disability [205-207].

Due to the considerable phenotype and locus heterogeneity, it is difficult to predict appropriate candidate genes for testing in a particular patient. Therefore hypothesis-free approaches such as whole exome sequencing (WES) or whole genome sequencing (WGS) may be useful for uncovering causative variations in epileptic encephalopathies of unknown etiology. We aimed to identify the underlying genetic cause of epileptic encephalopathy in the proband by WES and WGS of a family quartet.

Materials and Methods

Study Subjects

Study participants included ID9, parents ID9F and ID9M, and an unaffected sister ID9S. Adults provided written informed consent, with additional assent by ID9 and ID9S, under a protocol approved by the Scripps institutional review board. Consent for release of medical information for individual 2 was obtained from the parents. Clinical details are below and summarized in Table 4.1.

Table 4.1 Clinical Features in Three Individuals with Epileptic Encephalopathy and *KCNB1* Missense Mutations

Individual	Current Age (sex)	Age of onset	Seizure types	Seizure control with anti-epileptic therapies? (treatments)	Developmental Delay	Brain MRI
ID9	9 yo (female)	4 yrs	Tonic-clonic; Tonic; Atonic; Focal; Focal with secondary generalization	No (Topiramate, clobazam, levitiracetam, Depakote, carbamazepine, trileptal, lacosamide, clonazepam, oxcarbazepine)	Yes (motor and language)	Subtle volume loss in left hippocampus
2	7 yo (male)	8 mos	Tonic-clonic; Atonic; Focal; Infantile spasms	No (ACTH, Topiramate, Depakote, pyridoxine; ketogenic diet)	Yes (motor and language)	normal
3 (Coriell ND27062)	5 yo (female)	0 yrs	Tonic-clonic; Atonic; Focal dyscognitive Atypical absence; Infantile spasms;	unknown	Yes (unspecified)	normal

Table 4.1 Contd.

Individual	EEG	Other	Family history of epilepsy	Presumed causal variant	Amino Acid Change	Predicted Consequence Provean (score) SIFT (score) Polyphen2 (score)
ID9	Mild diffuse slowing and abundant bi-hemispheric multifocal epileptiform discharges	Hypotonia; Strabismus; Migraine;	No	Chr20: 47991056 G/T	S347R	Deleterious (-4.996) Damaging (0.003) Probably Damaging (0.995)
2	Hypsarrhythmia; diffuse polyspikes, diffuse polyspike-wave, right temporal spike and wave, left occipital spikes and series of bursts of diffuse polyspikes	Hypotonia Strabismus; Tremulousness; Non-verbal; Stereotyped handwringing movements; In-turning of feet	No	Chr20: 47990962 C/T	G379R	Deleterious (-7.926) Damaging (0.000) Probably Damaging (1.000)
3 (CoriellND27062)	unspecified	Cerebral palsy	Yes (Absence epilepsy in great uncle)	Chr20: 47990976 G/A	T374I	Deleterious (-5.945) Damaging (0.000) Probably Damaging (0.999)

Individual ID9 is a 9-year-old female with epileptic encephalopathy, hypotonia, developmental delays, cognitive impairment, and intermittent agitation. Pre- and perinatal histories were unremarkable, although hypotonia and excessive somnolence were noted early. Motor milestones were delayed, with sitting at 9 months, walking at 20 months, and persistent clumsiness. Language acquisition was delayed with regression at age 18 months. Motor, language and behavior have fluctuated but overall there has been forward developmental progress. Onset of generalized tonic-clonic seizures (GTCS) was at 4.75 years of age, although behavioral manifestations likely representing other seizure types were present earlier. Multiple seizure seimiologies were reported including rare GTCS, head drops, and more common facial twitching with drooling, eye fluttering, gagging, vomiting and stiffening. Rare GTCS are controlled with levetiracetam and clonazepam, but other seizure types have been poorly controlled with multiple therapies that were ineffective or limited by side effects (Table 4.1). In addition, the patient experiences sumatriptan-responsive migrainous episodes consisting of headache, abdominal discomfort, photophobia and lethargy.

Brain MRI showed subtle asymmetric volume loss in left hippocampus. Recent seven day video-EEG monitoring revealed mild diffuse slowing and abundant bi-hemispheric multifocal epileptiform discharges more prominent in right temporal and midparietal regions. Electroclinical seizures began in the left hemisphere, with two in centro-parietal areas and one without clear localization. Magnetoencephalography showed frequent epileptiform spikes during sleep (648

spikes observed over 50 minutes), with frequent trains of spikes. Source modeling showed epileptiform spike activity arising from bilateral posterior perisylvian regions. The first cluster of spikes (~55%) originated from the anterior-inferior aspect of the left parietal lobe, extending to the left superior temporal gyrus. The second cluster of spikes (~45%) originated from the right temporal-parietal junction. No propagations were observed.

Muscle biopsy showed type 1 fiber predominance with mild generalized hypertrophy. There was slight elevation of plasma guanidinoacetate 2.5 (0.3-2.1 μM) but not in the range typically associated with disease. There was mild elevation of cerebrospinal fluid (CSF) pyruvate with normal lactate [2.06 (0.5-2.2 mM)/147 (0-75 μM)]. CSF 5-methyltetrahydrofolate was mildly reduced 36 (40-128 nM). Folinic acid therapy has had unclear impact. Extensive additional work-up was normal and included: karyotype, fragile X and Angelman syndrome testing, comparative genomic hybridization (CGH) Oligo-SNP Array, mitochondrial DNA Southern blot and mitochondrial DNA sequencing, plasma acylcarnitine, creatine phosphokinase (CPK), uric acid, biotinidase, ammonia, Vitamin B12, folate, homocysteine, folate receptor antibodies, lymphocyte pyruvate dehydrogenase activity, urine organic acids, urine creatine and guanidinoacetate, CSF glucose, protein, amino acids, neurotransmitter metabolite levels and pterins, muscle carnitine, CoQ10, and electron transport chain complex analysis.

Individual 2 presented as a 2-yr-10-month male with poor seizure control, developmental delay, absent speech, stereotyped handwringing movements, and

progressive in-turning of feet requiring orthotic support. Prenatal and perinatal histories were normal. Development plateaued at 6 months and seizures began at 8 months of age, with hypsarrythmic EEG for which he was treated with ACTH. Although seizures were resistant to conventional treatment (Table 4.1), a gluten/casein/sugar/starch-free diet begun at 2.5 years of age resulted in seizure reduction to 3/day despite marked spike activity demonstrable on EEG. At 4 years of age, seizures worsened and L-carnitine was added with subsequent amelioration. At 5 years of age, EEG was persistently abnormal with epileptiform discharges of multifocal origin including bursts of diffuse polyspikes, diffuse polyspike-wave, right temporal spike and wave, left occipital spikes and diffuse polyspike bursts lasting up to 4 minutes. Brain MRI studies at 9 months did not show structural, neuronal migration, or white matter abnormalities. He began walking at 2.5 years, and is presently interactive socially, though nonverbal. Extensive additional work-up was normal (Table 4.1). Genetic testing for mutations associated with *SCN1A*, *MECP2*, *CDKL5*, *FOXG1*, *ARX*, Fragile X, Pitt-Hopkins and Angelman syndromes were negative. Tests for plasma and cerebrospinal fluid (CSF) amino acid concentrations, urine organic acid levels, CSF neurotransmitter levels, lysosomal enzymes, very long chain fatty acids (VLCFA), neuronal ceroid lipfuscinosis (NCL) 1 & 2, urine sulfocysteine, congenital disorders of glycosylation (CDG), and oligo array were all normal. Clinical WES was performed by GeneDx and reported variants were confirmed by Sanger sequencing.

Individual 3 (Coriell ND27062) was ascertained by the Epilepsy Phenome/Genome Project [208] as part of a patient cohort with infantile spasms and/or Lennox-Gastaut syndrome [60]. Seizure onset occurred during the first year of life and seizure types include tonic-clonic, atypical absence, atonic, infantile spasms and focal dyscognitive (Table 4.1). EEG findings were unspecified, while imaging studies were reported as normal.

Whole Exome, Whole Genome Sequencing, Variant Calling, and Filtration

Genomic DNA was extracted from blood using the QiaAmp system (Qiagen, Valencia, CA). Enriched exome libraries were prepared using the SureSelect XT enrichment system (Agilent, Santa Clara, CA). WES was performed on an Illumina HiSeq2500 instrument with indexed, 100-bp, paired-end sequencing. Reads were mapped to the hg19 reference genome using BWA [209], variant calling and quality filtration was performed using GATK best practices variant quality score recalibration [210-212]. Mean coverage of 97 to 124-fold was achieved for each subject with 94-95% of the target exome covered by >10 reads (Table 4.2). Libraries for low-pass WGS were prepared using the NEBNext DNA Library Prep System (New England Biolabs, Ipswich, MA). WGS was performed on an Illumina HiSeq2500 with 100-bp indexed, paired-end sequencing. Mean coverage of 4 to 7-fold was achieved for each subject with ~64.3% of the genome covered by >5 reads (Table 4.2). Copy number variants (CNVs) were identified by CNVNator [213].

Table 4.2 Whole Exome and Whole Genome Sequencing Coverage

	Whole Exome Sequencing		Whole Genome Sequencing	
Sample	**Coverage (Mean)**	**% Target Exome with at least 10 Reads**	**Coverage (Mean)**	**% Genome Redundancy of 5 Reads**
ID9 – Proband	109	94.5%	4.1	37.9%
ID9F – Father	109	94.6%	6.0	66.7%
ID9M – Mother	124	94.9%	6.9	75.2%
ID9M – Sister	97	94.2%	7.2	77.4%

Variant annotation was performed using the Scripps Genome Annotation and Distributed Variant Interpretation Server (SG-ADVISER) (http://genomics.scripps.edu/ADVISER/) as previously described [214]. A series of filters were applied to derive a set of candidate disease-causing variants (Table 4.3): (1) population-based filtration removed variants present at >1% allele frequency in the HapMap [215] or 1,000 Genomes [216], NHLBI Exome Sequencing Project (http://evs.gs.washington.edu/EVS/), or Scripps Wellderly populations (individuals over the age of 80 with no common chronic conditions sequenced on the Complete Genomics platform); (2) annotation-based filtration removed variants in segmental duplication regions that are prone to produce false positive variant calls due to mapping errors [217]; (3) functional impact-based filtration retained only variants that are non-synonymous, frameshift, nonsense, or affect canonical splice-site donor/acceptor sites, and (4) inheritance-based filters removed variants not present in the trio in a manner consistent with affectation status. Following filtering, retained variants were confirmed by Sanger sequencing.

Table 4.3 WES Variant Filtration for Individual ID9

Variant Type	# in Family
Total Variants	101,797
Rare Variants (<1% allele frequency)	18,475
Not in Segmental Duplication	13,463
Nonsynonymous, Truncating, or Splice Site	1,053
***De Novo* Inheritance**	2
Homozygous or Compound Heterozygous Inheritance	3

Locus Specific Mutation Rate Estimate

The *KCNB1* locus specific mutation rate was determined as described [218]. Human and chimpanzee alignments of the protein coding portion of exons and intronic essential splice sites were considered. The *KCNB1* mutation rate per site is 2.71×10^{-3} differences per bp of aligned sequence. Assuming a divergence time of 12 million years between chimpanzee and human and a 25 year average generation time, the *KCNB1* locus specific mutation rate per site per generation is 5.65×10^{-9}. The probability of observing *de novo* mutation events was estimated using the Poisson distribution:

$$PX; \mu = [(e-\mu)(\mu X)]/X!$$

where X is the number of *de novo* events observed and μ is the average number of *de novo* events based on the locus specific mutation rate.

Plasmids and Cell Transfection

Mutations were introduced into full-length human $K_V2.1$ cDNA engineered in plasmid pIRES2-Ds-Red-MST [117] by QuikChange mutagenesis (Agilent). Wildtype human $K_V2.1$ cDNA was subcloned into the pIRES2-smGFP expression vector. Expression of wildtype and mutant $K_V2.1$ in CHO-K1 cells was achieved by transient transfection using FUGENE-6 (Roche) and 0.5 µg of total cDNA (1:1 mass ratio). Expression of wildtype alone was achieved by transfection with pIRES2-smGFP-WT-$K_V2.1$ plus empty pIRES2-DsRed-MST, while expression of mutant alone was performed with pIRES2-DsRed-MST-mutant-$K_V2.1$ and empty pIRES2-smGFP. Co-expression of mutant and wildtype was achieved by co-transfection with pIRES2-smGFP-WT-$K_V2.1$ and pIRES2-DsRed-MST-mutant-$K_V2.1$ or pIRES2-dsRed-MST-WT-$K_V2.1$. Following transfection cells were incubated for 48 hours before use in experiments.

Cell Surface Biotinylation

Proteins on the surface of CHO-K1 cells transfected with wildtype and/or mutant $K_V2.1$ were labeled with cell membrane-impermeable Sulfo-NHS-Biotin (Thermo Scientific). Following quenching with 100 mM glycine, cells were lysed and centrifuged. Supernatant was collected and an aliquot was retained as the total protein fraction. Biotinylated surface proteins (100 µg per sample) were recovered from the remaining supernatant by incubation with strepavidin-agarose beads (Thermo Scientific) and eluted in Laemmli sample buffer. Total (1 µg per lane) and surface fractions were analyzed by Western blotting using mouse anti-

$K_V2.1$ (1:500; NeuroMab, clone K89/34), mouse anti-transferrin receptor (1:500; Invitrogen, #13-6800), rabbit anti-calnexin (H70)(1:250; Santa Cruz, sc-11397) primary antibodies, and peroxidase-conjugated mouse anti-rabbit IgG (1:100,000 Jackson ImmunoResearch) and goat anti-mouse IgG (1:50,000, Jackson ImmunoResearch) secondary antibodies. Blots were probed for each protein in succession, stripping in between with Restore Western Blot Stripping Buffer (Pierce). Western blot analysis was performed in triplicate on samples from three independent transfections. The order of anti-$K_V2.1$and anti-transferrin receptor antibodies was alternated, with transferrin receptor probed first in two of three experiments. Selectivity of biotin labeling for cell surface was confirmed by probing with calnexin following detection of $K_V2.1$ and transferrin receptor. Calnexin signal was consistently present in total protein lanes and absent in surface fraction lanes. Densitometry was performed using NIH ImageJ software. To control for protein loading, $K_V2.1$ bands were normalized to the corresponding transferrin receptor band. For each genotype, the normalized values were then expressed as a ratio of surface:total expression. Normalized total, surface and surface:total ratios were compared between genotypes using one-way ANOVA.

Electrophysiology

Whole cell patch-clamp recordings were performed as described [117], except recording solutions were altered to achieve appropriate voltage-control. The external solution contained (in mM): 132 XCl [where X is Na^+ except when molar substitution for K^+, Rb^+ or N-methyl-D-glucamine ($NMDG^+$) is indicated in

the figure], 4.8 KCl, 1.2 $MgCl_2$, 2 $CaCl_2$, 10 glucose, and 10 HEPES, pH 7.4. The internal solution contained (in mM): 20 K-aspartate, 90 NMDG-Cl, 1 $MgCl_2$, 1 $CaCl_2$, 11 EGTA, 10 HEPES, and 5 K_2ATP, pH 7.3. When cells expressing mutant channels alone or co-expressed with wildtype $K_V2.1$ ($K_V2.1$-WT) were held at -80 mV, they exhibited large currents that prevented adequate voltage control. Therefore, a holding potential of -30 mV was used for experiments. Whole cell currents were measured from -80 to +60 mV (in 10 mV, 500 msec long steps) from a holding potential of -30 mV followed by a 500 msec step to 0 mV (tail currents). Voltage-dependence of activation was evaluated from tail currents measured 10 msec after stepping to 0 mV from -40mV to +30mV and fit to the Boltzmann equation. Kinetic analysis of activation rate was performed by exponential fit of the first 50 msec of current induced after a voltage step from the holding potential.

For cation selectivity experiments, recording solutions were altered as follows: sucrose dilution was performed by adding 300 mM sucrose solution 10:1 (v/v) to the external solution described above. For determining permeability ratios, the internal solution was modified to contain (in mM): 110 K-aspartate, 1 $MgCl_2$, 1 $CaCl_2$, 11 EGTA, 10 HEPES, and 5 K_2ATP, pH 7.3 and equimolar replacement of extracellular sodium with the monovalent cations K^+, Rb^+ and $NMDG^+$. The permeability ratio (P_X/P_{Na}) was calculated from measured reversal potentials (E_{rev}) according to the following equation [73]:

$$E_{rev} = (RT/F) \ln(P_x[X^+]_o / PK^+[Na^+]_i$$

where R is the gas constant, T is absolute temperature, F is Faraday's constant, X^+ is the monovalent cation in the extracellular solution, and P_X is permeability of the X^+ cation.

Data for each experimental condition were collected from ≥3 transient transfections, and analyzed and plotted using Clampfit (Molecular Devices) and Graphpad Prism5 (Graphpad Software). Currents were normalized for membrane capacitance and shown as mean ± SEM, and number of cells used for each experimental condition is listed in Table 4.5. Statistical significance was determined using unpaired Student's t test (Graphpad). P values are provided in the figures or figure legends.

Results

We employed WES (~100X coverage) and WGS (~5X coverage) of the proband (ID9), unaffected father (ID9F), unaffected mother (ID9M), and unaffected sister (ID9S) to identify the molecular cause of an epileptic encephalopathy. Filtering of WES variants was done under the assumption that disease in ID9 was the result of a heterozygous *de novo* mutation, but we also considered simple and compound recessive models. Variants discovered by WES were processed through a series of population-, variant annotation-, functional-impact-, and inheritance-based filters, to identify a set of candidate disease-causing variants (Table 4.3).

Table 4.4 Inheritance of Validated Candidate Variants in Individual ID9

Gene	ID1 Status	Amino Acid Change	WES Genotype				Predicted Consequence		
			ID9	ID9F	ID9M	ID9S	Provean	SIFT	Polyphen 2
KCNB1	*de-novo*	S347R	01	00	00	00	deleterious (-4.996)	damaging (0.003)	probably damaging (0.995)
MLST8	*de-novo*	Q302R	01	00	00	00	neutral (-2.12)	tolerated (0.203)	benign (0.114)
HRNBP3	homozygous	Y5H	11	01	01	00	deleterious (-3.54)	damaging (0.000)	benign (0.446)
NLRP1	compound heterozygous	V939M	01	00	01	01	neutral (-2.08)	damaging (0.006)	probably damaging (0.982)
		R834C	10	01	00	00	neutral (-0.46)	tolerated (0.216)	benign (0.000)
BAHCC1	compound heterozygous	A941T	01	00	01	01	neutral (-1.38)	tolerated (0.215)	benign (0.009)
		E1990K	10	01	00	00	neutral (-0.91)	tolerated (0.168)	possibly damaging (0.900)

Genotypes: 0 – reference allele, 1 – alternate allele

Sequence coverage and detailed variant data are presented in Table 4.2. CNVs were also interrogated by WGS, however, no CNVs consistent with disease segregation were identified. This process identified *de novo* missense variants in 2 candidate genes, *KCNB1* and *MLST8* (Table 4.4). Under other genetic models, we identified a homozygous missense variant in *HRNBP3* and compound heterozygous variants in *NLRP1* and *BAHCC1* (Table 4.4). Of all the identified variants, the *KCNB1* variant was deemed the most likely candidate based on the *de novo* inheritance pattern, the function of *KCNB1* and its relationship to other epilepsy genes, and the predicted deleterious consequence on protein function by multiple algorithms (Table 4.4). *KCNB1* encodes the alpha subunit of the $K_V2.1$ voltage-gated potassium channel, a delayed rectifier potassium channel that is an important regulator of neuronal excitability. The

S347R variant is located in the pore domain that is necessary for ion selectivity and gating (Figs. 4.1 & 4.2).

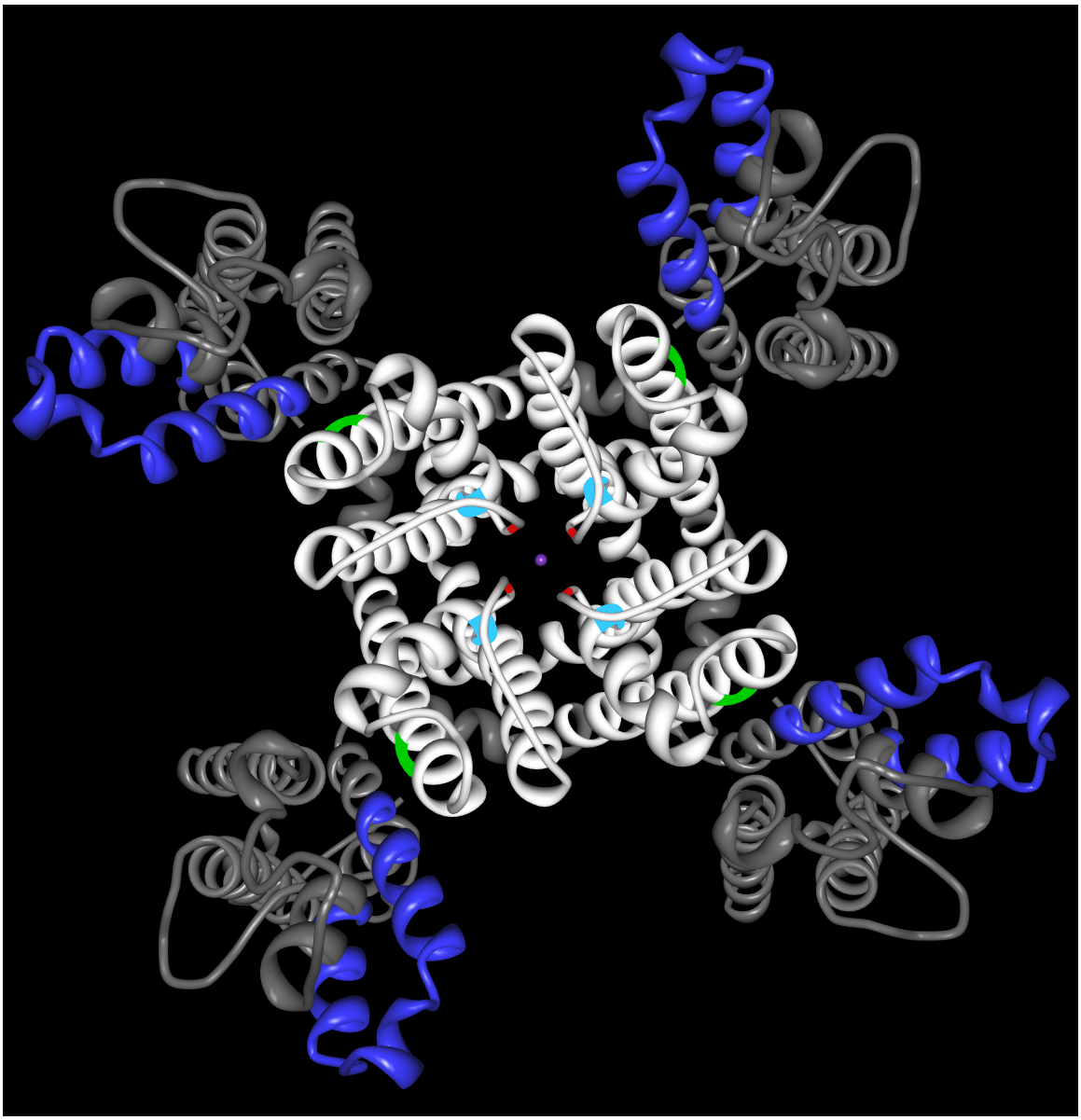

Figure 4.1 Location of K_V2.1 Mutations Mapped onto the Crystal Structure of a K_V2.1/K_v1.2 Chimera
Extracellular side of channel tetramer. S347 (green) lies at the interface between the voltage sensor (blue) and pore (white) domains. T374 (teal) lies adjacent to the selectivity filter, while G379 (red) lies in the selectivity filter (PDB 29R9)[219]

We identified two additional unrelated patients with epileptic encephalopathy and *de novo* missense variants in *KCNB1* discovered by WES. Individual 2 presented with a sporadic epileptic encephalopathy of unknown cause (Table 4.1). After a series of negative genetic and metabolic tests, he was referred for clinical WES. From that analysis it was determined that he had a single *de novo* missense variant in *KCNB1*. The variant G379R, located in the selectivity filter of $K_V2.1$, was predicted to be deleterious by functional impact algorithms (Figs. 4.1 & 4.2; Table 4.1). Additional inherited variants included a heterozygous splice site mutation in the *NPC2* gene (IVS4+1 G>A) inherited from his unaffected father and a variant of unknown significance in *GRIN2A* (A1276G) inherited from his unaffected mother. Neither of these transmitted variants was thought to be causative for principal phenotypes of individual 2, although they may contribute by modifying the overall expression of the clinical phenotype. Inheritance of NPC type 2 is generally recessive, and the clinical phenotype of individual 2 was not consistent with NPC type 2. The *GRIN2A* A1276G variant is a known SNV that was inherited from the unaffected mother and exists in the general population (0.1% MAF in European Americans). A1276G is a conservative substitution in an alternatively spliced portion of the *GRIN2A* gene at a position that does not show a high degree of evolutionary conservation and was predicted to be benign by multiple functional impact algorithms (Provean: neutral (-0.78); SIFT: tolerated (0.284; Polyphen2: benign (0.376)).

Individual 3 was recently reported as part of an epileptic encephalopathy exome sequencing study by the Epi4K consortium [60]. She presented with

early-onset epileptic encephalopathy and cerebral palsy (Table 4.1). A *de novo* missense variant in *KCNB1* was reported for individual 3, with no additional *de novo* variants reported [60]. The variant T374I is located in the pore domain of $K_V2.1$ and was predicted to be deleterious by functional impact algorithms (Fig. 4.1; Table 4.1).

Given the locus-specific mutation rate of *KCNB1* ($5.65x10^{-9}$ mutation rate/base/generation), the probability of identifying three independent mutations is low ($P<1.1x10^{-13}$), providing statistical evidence that these variants may be pathogenic. The altered residues show a very high degree of evolutionary conservation (Fig. 4.2), with T374 and G379 being invariant through the ancestral KcsA bacterial potassium channel. Further, all three *KCNB1* variants are located in the functionally important pore domain of the $K_V2.1$ channel protein. Serine 347 is located in the pre-pore transmembrane segment and threonine 374 is located in the pore helix. Glycine 379 is part of the critical "GYG" motif that defines the potassium selectivity filter (Figs. 4.1 & 4.2).

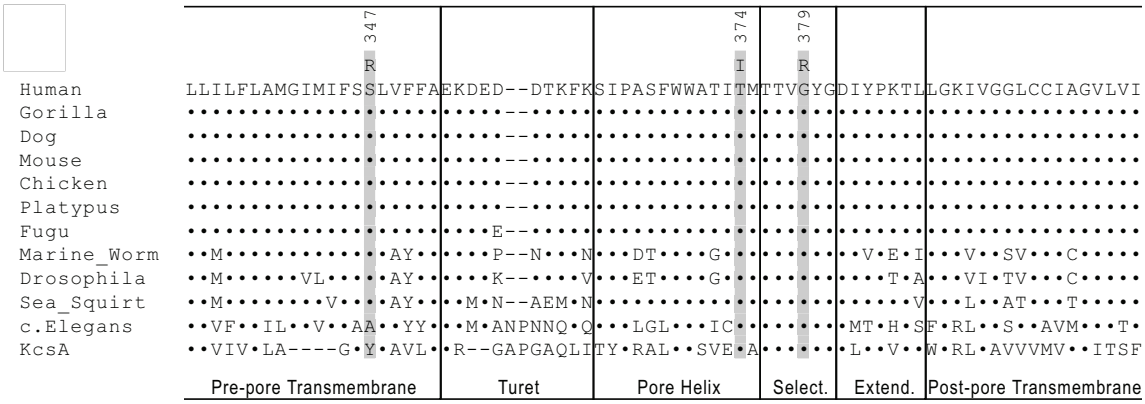

Figure 4.2 Evolutionary Conservation of $K_V2.1$
Multiple Alignment of $K_V2.1$ Species Orthologs. Mutated amino acids are shaded and functional sub-domains of the pore region are indicated (Clustal Omega) [220].

Effects of the *KCNB1* variants on $K_V2.1$ channel function were evaluated following transient expression in CHO-K1 cells. Expression of each mutant in CHO-K1 cells resulted in total and cell surface expression similar to the wildtype channel, with no significant genotype-dependent differences in total ($F_{3,8}$=1.767, p=0.213), surface ($F_{3,8}$=0.017, p=0.997) and surface:total ($F_{3,8}$=0.266, p=0.848) expression of $K_V2.1$. This indicates that the mutations do not interfere with protein expression or trafficking of channels to the cell surface (Fig. 4.3).

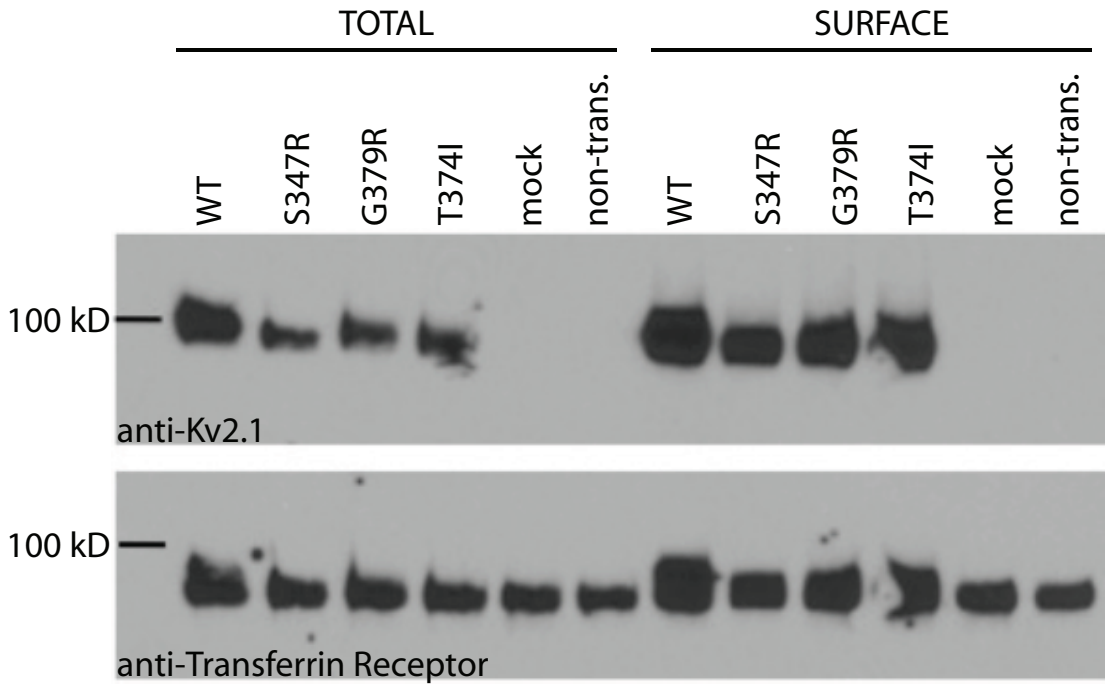

Figure 4.3 $K_V2.1$ Cell Surface Expression
Mutant $K_V2.1$ proteins are expressed and trafficked to the cell surface. Cell surface expression was measured using cell surface biotinylation of CHO-K1 cells transfected with wildtype or mutant $K_V2.1$. Total and surface fractions of $K_V2.1$ were detected with anti-$K_V2.1$ antibody. Endogenous transferrin receptor levels were measured as a loading control.

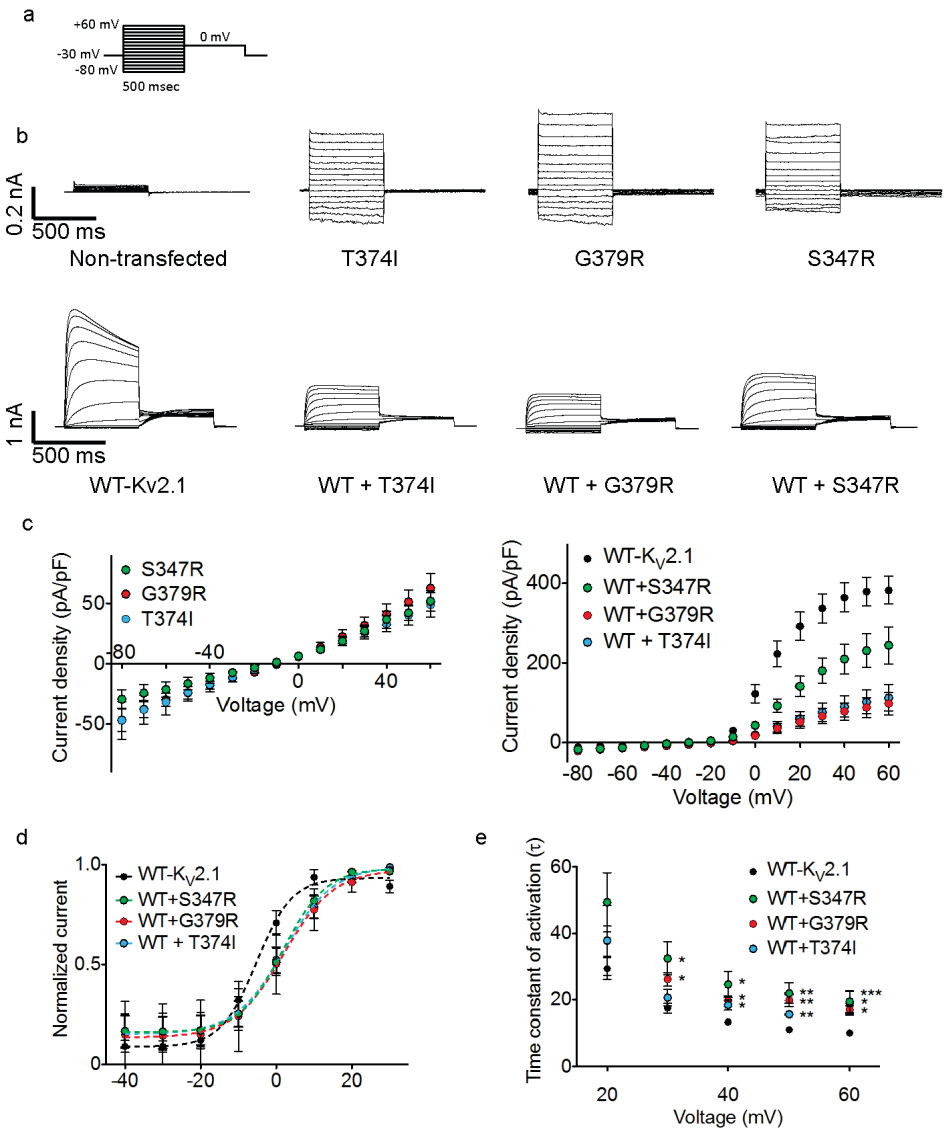

Figure 4.4 Functional Consequence of K_V2.1 Mutations
(**a**) CHO-K1 cells were held at -30mV and whole cell currents were recorded from -80 to +60 mV in 10 mV steps for 500 msec followed by a 500ms step to 0mV to record tail currents. (**b**) Average whole-cell current traces recorded from non-transfected CHO-K1 cells and CHO-K1 cells transiently expressing wild-type or mutant (G379R, S347R, T374I) K_V2.1 channels, or co-expressing wild-type plus mutant channels. (**c**) Current density–voltage relationships measured from CHO-K1 cells expressing mutant, wild-type, or co-expressing wild-type and mutant K_V2.1 channels. Currents were normalized to cell capacitance (pF). (**d**) Voltage dependence of steady-state activation. Tail currents were normalized to peak amplitude and fit with Boltzmann function. Biophysical parameters of voltage-dependence are detailed in Table 3.5. (**e**) The time constant of activation was determined from exponential fit of individual current traces.

Expression of K_V2.1-WT resulted in large voltage-dependent potassium currents with characteristic outward rectification and late inactivation (Fig. 4.4b-c). In contrast, expression of each of the three mutants yielded small currents with linear current-voltage relationships (Fig. 4.4b-c). These aberrant currents were blocked by gadolinium (Gd^{3+}), strongly suggesting that the currents are pore-mediated (Fig. 4.5).

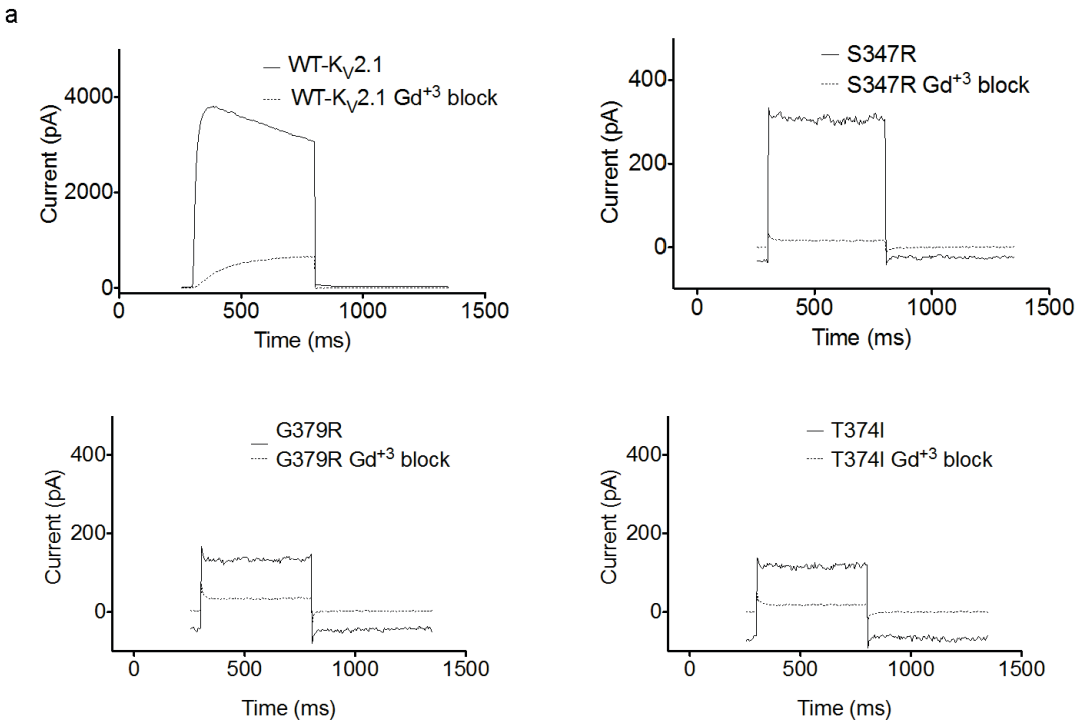

Figure 4.5 GdCl3 Block of Mutant K_V2.1 Channels
Representative traces of control and Gd+3 block at +60 mV of wild-type (86±2.1%, n=5) or mutant channels (S347R (94±3.7%, n=3), G379R (79±4.2%, n=4), T374I (94±2.5%, n=3)).

Based upon the external and internal K^+ concentrations used in these experiments, the theoretical reversal potential (E_{rev}) for K^+-selective currents is -47 mV. Expression of the mutant channels produced currents with depolarized E_{rev} (S347R: -23.2±4.8 mV; G379R -14.0±4.5 mV; T374I -16.5±5.5 mV) indicating that the mutations affect ion selectivity. To test ion selectivity, the external solution was diluted 1:10 with 300 mM sucrose. Under these conditions, a depolarizing shift in E_{rev} would indicate anion selectivity, while a hyperpolarizing shift would indicate cation selectivity. Dilution of the extracellular solution produced a hyperpolarizing shift in E_{rev} confirming the current conducted was cation-selective (Fig. 4.6). Changes in cation selectivity were determined by measuring changes in E_{rev} following molar replacement of extracellular sodium with monovalent cations. All three mutants exhibited loss of K^+ selectivity, with K^+/Na^+ permeability ratios of 0.9 (Fig. 4.6; Table 4.5) compared to the reported 14:1 ratio for K_V2.1-WT [221].

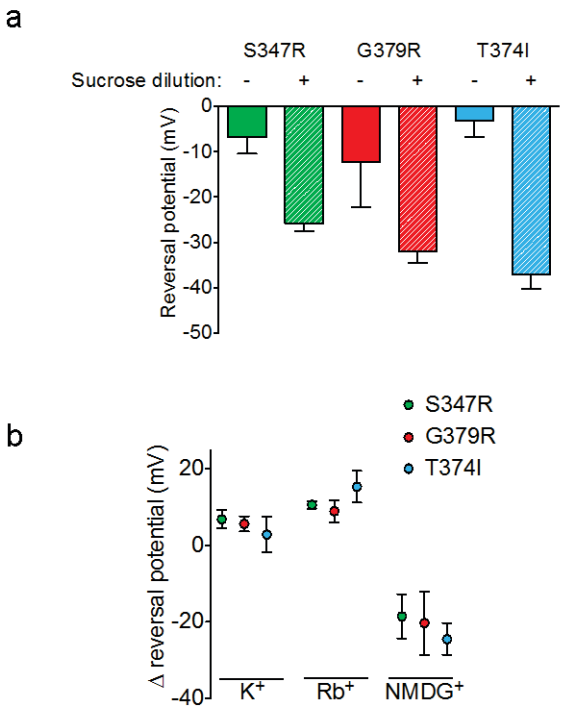

Figure 4.6 Ion Selectivity of Mutant K_V2.1 Channels
(a) Reversal potentials were determined by linear fit to y=mx+b in control bath and after bath was diluted 10-fold in 300mM sucrose solution. (b) Change in reversal potential after equimolar substitution of extracellular monovalent Na^+.

Table 4.5 Biophysical Properties of Voltage-dependence of Activation for Wild-type and Mutant K_V2.1 Channels

	Mean $V_{1/2}$ ± S.E.M.	Slope factor ± S.E.M.	*n*
Kv2.1-WT	-4.1 ± 1.5	4.4 ± 0.4	12
Kv2.1-WT + G379R	1.3 ± 2.0 *	5.2 ± 0.6	8
Kv2.1-WT + S347R	2.8 ± 1.6 *	5.9 ± 0.5	8
Kv2.1-WT + T374I	1.9 ± 1.5 *	5.7 ± 0.2	7

To investigate the effects of the mutant channels in a heterozygous background, we co-expressed each mutant with K_V2.1-WT channel and compared to the wildtype channel expressed alone. Co-expression of K_V2.1-WT with T374I, S347R, or G379R resulted in reduced current measured at test potentials ranging from 0 to +60 mV (Fig. 4.4c), depolarizing shifts in the voltage-dependence of steady-state activation (Fig. 4.4d; Table 4.5; Fig. 4.7), and greater time constants of activation (τ) measured from +30 to +60 mV test potentials (Fig. 4.4e; Fig. 4.7). The observed changes in kinetic parameters suggest that the mutant and wild-type subunits can form heterotetrameric channels.

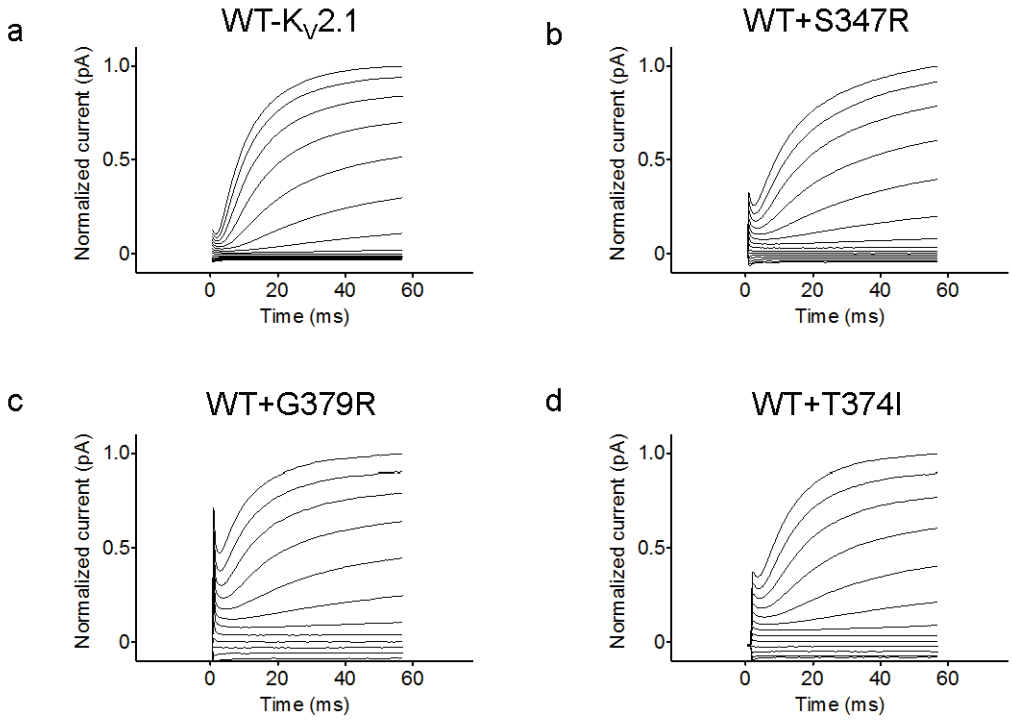

Figure 4.7 Expanded View of Whole-cell Current Traces for Evaluation of Activation Kinetics of Wild-type K_V2.1 Channel Alone or Co-expressed with Mutant Channels

Expanded view of the first 50 msec of whole-cell currents following voltage change from -80mV to +60mV and normalized to peak current recorded from CHO-K1 cells transiently expressing K_V2.1-WT (a) or co-expressing wild-type and mutant Kv22.1 channels ((b) G379R, (c) S347R, (d) T374I).

Discussion

Co-occurrence of *de novo* variants in *KCNB1* in three independent patients with overlapping clinical phenotypes that include epileptic encephalopathy with associated cognitive and motor dysfunction provides strong genetic evidence that the *KCNB1* variants are likely pathogenic. Further evidence for a pathogenic effect of the *KCNB1* mutations comes from functional studies of mutant $K_V2.1$ channels. All three mutations, located within the pore domain of $K_V2.1$, resulted in channels with similar dysfunctional features.

Previous studies demonstrated that mutations in the pore region can result in altered ion selectivity [79, 82-84]. Consistent with this, each $K_V2.1$ mutant exhibited voltage-independent, non-selective cation currents. When co-expressed with wildtype channels, all $K_V2.1$ mutants induced depolarizing shifts in the voltage-dependence of activation and reduced current density at more depolarized voltages. Further, co-expression of the $K_V2.1$ mutants with wildtype channels resulted in inward currents in the voltage range where $K_V2.1$ channels are normally closed, as evidenced by large inward currents observed when using a holding potential of -80 mV. These gain-of-function and dominant-negative functional defects are predicted to result in depolarized resting membrane potential and impaired membrane repolarization, with increased cellular excitability as a net consequence.

$K_V2.1$ is the main contributor to delayed rectifier potassium current in pyramidal neurons of the hippocampus and cortex [151-155]. Delayed rectifier potassium current is critical for membrane repolarization under conditions of

repetitive stimulation and acts to dampen high frequency firing. Reduction of delayed rectifier potassium current by *Kcnb1* deletion in mice results in reduced thresholds to induced seizures, but not spontaneous seizures [222]. This suggests that loss of $K_V2.1$ function predisposes neuronal networks to hyperactivity, resulting in a modest increase in seizure risk. In contrast, our results demonstrate that gain-of-function and dominant-negative effects result in epileptic encephalopathy. A similar phenomenon is observed with *KCNQ2* wherein heterozygous loss-of-function mutations result in benign familial neonatal seizures, while mutations with dominant-negative effects result in epileptic encephalopathy [126]. This suggests that variable functional defects resulting from different mutations in the same gene contribute to the pleiotropic effects observed for genes associated with neurodevelopmental disorders.

In summary, our genetic and functional evidence identify mutation of *KCNB1* as a cause of epileptic encephalopathy. This expands the considerable locus heterogeneity associated with epileptic encephalopathies [60, 201], suggesting that clinical exome sequencing may be useful for molecular diagnosis. Rapid genetic diagnosis is beneficial for appropriate disease management and may improve long-term outcomes in epileptic encephalopathies [198-200].

CHAPTER V

DISCUSSION

Summary

Rationale

Epilepsy is a common neurological disease that affects more than 50 million people worldwide [4]. The U.S. spends more than 12.5 billion dollars annually on epilepsy associated medical expenditures [181]. However, more than one-third of epilepsy patients do not have effective treatments for their epilepsy [20]. Although many factors contribute to epilepsy, the majority of epilepsy cases have an underlying genetic cause [35, 36].

The vast majority of heritable epilepsies are thought to be due to complex interactions between multiple genes, with only 1-2% attributed to single genes [35]. Nevertheless, identifying the genes involved in monogenic epilepsies can help to elucidate the etiology of more complex epilepsies. Many genes responsible for monogenic epilepsies have been identified in recent years. Most of these genes encode components of neuronal signaling, including voltage-gated ion channels [35, 44, 165].

Mutations in voltage-gated sodium channels are the leading cause of monogenic epilepsies. Over 900 mutations have been identified in the voltage-

gated sodium channels *SCN1A* and *SCN2A* [55]. These mutations are associated with a number of epilepsy syndromes including febrile seizures, BFNIS, GEFS+, Lennox-Gastaut, DS, and Ohtahara syndrome [35, 42-44, 55-60, 64, 67-70]. Family members who inherit identical mutations in voltage-gated sodium channels often exhibit variable phenotypes, which suggests that genetic variation at modifier loci may contribute to epilepsy phenotypes [42, 136, 223]. Identifying and characterizing genetic modifiers of epilepsy can lead to a better understanding of the pathogenic mechanisms underlying epilepsy, and genetic modifiers may represent novel therapeutic targets for the treatment of epilepsy. Our lab previously identified the voltage-gated potassium channel subunit, *Kcnv2*, as a candidate modifier of epilepsy in the Q54 transgenic mouse model of epilepsy by genetic mapping and candidate gene analysis [140, 149].

Validation of Kcnv2 as a Genetic Modifier of Epilepsy

Chapter II detailed experiments to validate *Kcnv2* as a genetic modifier of epilepsy. We initially hypothesized that amino acid differences in Kv2.1 between the B6 and SJL strains would result in functional changes in the protein that would account for the disparate phenotypes. However, when we co-expressed either the B6 or SJL-derived Kv8.2 with Kv2.1 in CHO cells and performed whole-cell patch clamp recordings, we did not observe any such functional differences.

To determine whether differences in *Kcnv2* expression might contribute to the divergent phenotypes, we measured *Kcnv2* transcript levels in the

hippocampus, the origin of seizures in the Q54 mice, and observed a threefold increase in hippocampal *Kcnv2* expression in the seizure susceptible SJL mouse strain relative to the resistant B6 strain. We then tested the *Kcnv2* modifier effect *in vivo* using a transgenic transfer approach and observed a positive correlation between increased expression of the *Kcnv2* transgene and phenotype severity in multiple lines of Kcnv2;Q54 double-transgenic mice. Consistent with the functional analysis in CHO cells, there was not a significant correlation between the amino acid sequence of the *Kcnv2* transgene and the phenotype. These results indicate that increased *Kcnv2* expression is sufficient to exacerbate the seizure phenotype of Q54 mice and implicate *Kcnv2* as a modifier of the Q54 phenotype. Additionally, they suggest that sequence variation in *Kcnv2 cis*-regulatory regions may underlie the modifier effect. Furthermore, the validation of *Kcnv2* as a quantitative modifier substantiates the utility of our approach for identifying genetic modifiers and emphasizes the potential impact of genetic variation in non-coding regions of the genome on disease susceptibility.

Identification and Characterization Kcnv2 Variants in Pediatric Epilepsy Patients

Also detailed in Chapter II is the identification of two unique *KCNV2* variants (R7K and M285R) in pediatric epilepsy patients, both of which occur in highly conserved residues and, when co-expressed with Kv2.1 in CHO cells, result in increased suppression of Kv2.1-mediated delayed-rectifier potassium

current. This effect would be predicted to result in a hyperexcitable phenotype and is consistent with the predicted consequence of *Kcnv2* overexpression in mice. The M285R variant, which occurred in the more severely affected patient, exhibited additional kinetic defects that would be predicted to delay channel opening. These observations suggest that the variants might contribute to the epilepsy phenotype of the patients. Both variants were inherited from an unaffected parent, suggesting that *KCNV2* may interact with other genetic loci to influence epilepsy susceptibility. Although neither patient carried any pathogenic variants in *SCN1A* or *SCN2A*, it is possible that inherited genetic variation at other loci contributes to the phenotype. Together, these findings suggest that genetic variation in *KCNV2* may contribute to human epilepsy, further validating *KCNV2* as an epilepsy gene. Additionally, they implicate suppression of delayed rectifier potassium current as a potential factor contributing to epilepsy susceptibility. The identification of *KCNV2* variants in human patients supports the idea that modifier genes identified in mice can provide clues into the etiology of human disease and highlights the value of identifying genetic modifiers in mice.

Identification of Kcnv2 Regulatory Regions in Mouse

Based on the observation that *Kcnv2* acts as a quantitative modifier of the Q54 phenotype we hypothesized that sequence variation between the resistant B6 strain and the susceptible SJL strain in *Kcnv2 cis*-regulatory regions may influence epilepsy susceptibility by affecting steady-state expression. As the

promoter and 3' UTR are the regions most likely to contain *cis*-regulatory elements, we sought to define these regions as a first step towards addressing our hypothesis. Because promoter regions of genes lie immediately upstream of the transcription start site, we first identified the *Kcnv2* promoter using two independent methods, RNA ligase mediated rapid amplification of cDNA ends (RACE) and RNase protection assay (RPA). The results of both methods were in agreement with each other and with bioinformatic data available from multiple databases, suggesting that the RACE and RPA-defined transcription start site region was accurate.

We next used the information from the RACE and RPA assays to design a 5' deletion series of luciferase reporter vectors containing sequence corresponding to the genomic region upstream of the *Kcnv2* transcription start site to define the core promoter region. Our luciferase based promoter assays suggested that the *Kcnv2* core promoter is contained within the region 373-102 bp upstream of the *Kcnv2* start codon. Variation in luciferase expression between the constructs containing *Kcnv2* genomic inserts extending in the 5' direction suggested that the regions upstream of the core promoter contain additional proximal promoter elements that may contribute to variability in *Kcnv2* transcription levels. We proposed future studies to determine whether sequence variation in these elements contributes to *Kcnv2* expression differences between the B6 and SJL strains.

Additionally, we performed a 3' RACE assay to determine the 3' UTR organization of *Kcnv2*. Our data suggested that the *Kcvn2* 3' UTR extends 3193-

3284 bp downstream of the *Kcnv2* stop codon. This data is consistent with the predicted 3' UTR in the Ensembl and UCSC genomic databases (GRCm38). However, there is a 21 bp poly-A tract in the genomic sequence immediately downstream from the location where the longest 3' RACE product termini align. Because the GeneRacer Oligo dT primer used to generate the RACE products was designed to bind to the mRNA poly-A tail, the genomic poly-A tract could act as an erroneous binding site for the primer. This would result in prematurely truncated 3' RACE products, which would suggest that the 3'UTR is shorter than it actually is. For this scenario to occur, the efficiency of either the primer binding to or reverse transcription from the erroneous site would have to be greater than from the actual poly-A tail. Otherwise, there would also be longer 3' RACE products than the ones that we observed. This was not the case. Nor were there longer transcripts identified in the genomic databases. Thus, it is unlikely that the poly-A tract influenced our data. Nonetheless, the 3' RACE data should be confirmed by RPA. Future studies will determine whether sequence variation in the 3' UTR contributes to *Kcnv2* expression differences between the B6 and SJL strains. We also proposed future studies to determine the *in vivo* effects of regulatory sequence variation between the B6 and SJL strains on seizure susceptibility in Q54 mice.

The identification of *Kcnv2* regulatory regions provides the foundation for the proposed future studies to determine the effects of regulatory sequence variation in these regions on *Kcnv2* transcription rates and mRNA stability. Taken together, these studies will help to elucidate the molecular mechanism of the

Kcnv2 modifier effect, advancing our knowledge of how genetic modifiers contribute to epilepsy, and potentially revealing novel therapeutic targets for the treatment of epilepsy.

Identification of de novo KCNB1 Mutations in Patients with Epileptic Encephalopathy

In Chapter IV we describe the identification of three *de novo* missense *KCNB1* mutations in three patients with overlapping epileptic encephalopathy phenotypes with cognitive and motor dysfunction by whole exome sequencing. All three mutations occurred in the pore-forming region of *KCNB1* and resulted in similar patterns of $K_v2.1$ dysfunction in a heterologous expression system, including both gain-of-function and dominant-negative defects. These defects included voltage-independent, non-selective cation currents, and when co-expressed with wild-type channels, depolarizing shifts in voltage-dependence of activation, reduced current density at depolarized voltages, and inward currents at more hyperpolarized voltages. Taken together, these defects would be predicted to result in a depolarized resting membrane potential and impaired membrane repolarization, both of which would contribute to a net increase in cellular excitability. The overlapping phenotypic features of the patients and the similar functional characteristics exhibited by each of the variants strongly suggest that the mutations are pathogenic. The mechanism by which each of the

variants contributes to hyperexcitability appears to be similar as each variant occurs in the pore-forming region of the channel and results in similar gain-of-function and dominant negative effects on channel function. The phenotype associated with these variants is more severe than the phenotype displayed by *Kcnb1* homozygous knock out mice, which have increased susceptibility to induced seizures but no spontaneous seizure activity [222]. This suggests that the phenotypic outcome of *KCNB1* mutations is dependent upon the functional consequence of the mutation. This is consistent with the pleiotropy exhibited by other genes associated with epilepsy [126, 224]. These results implicate *KCNB1* in epileptic encephalopathy and further support the importance of delayed rectifier potassium current in the regulation of neuronal excitability. Furthermore, these studies emphasize the value of WES for identifying candidate genes in patients with idiopathic epilepsies. This approach is more cost effective than the current practice of sequencing individual genes or small panels of known epilepsy genes and holds a greater potential for discovery of novel epilepsy genes.

Future Directions

Effects of Promoter Sequence Variation on Kcnv2 Expression

As an initial step towards determining whether sequence variation in *Kcnv2 cis*-regulatory regions influences seizure susceptibility by altering steady-state expression levels, we defined the *Kcnv2* promoter and 3' UTR regions, where *cis*-regulatory elements are likely to be located. The next step is to determine whether sequence variation in these regions affects *Kcnv2* expression levels. Our sequencing identified 11 SNPs (Chapter III), and there are an additional 36 imputed SNPs between the B6 and SJL strains in the genomic region corresponding to our promoter-luciferase reporter constructs (Fig. 5.1) [225]. To determine whether this sequence variation contributes to differences in *Kcnv2* expression levels, a parallel 5' deletion series of SJL-derived luciferase reporter constructs can be generated, and the resulting luciferase activities can be compared to the corresponding B6-derived constructs. If any two corresponding B6 and SJL-derived constructs exhibit differences in luciferase activity, then the corresponding genomic region is likely to contain sequence variation in one or more *cis*-regulatory elements that influences *Kcnv2* expression.

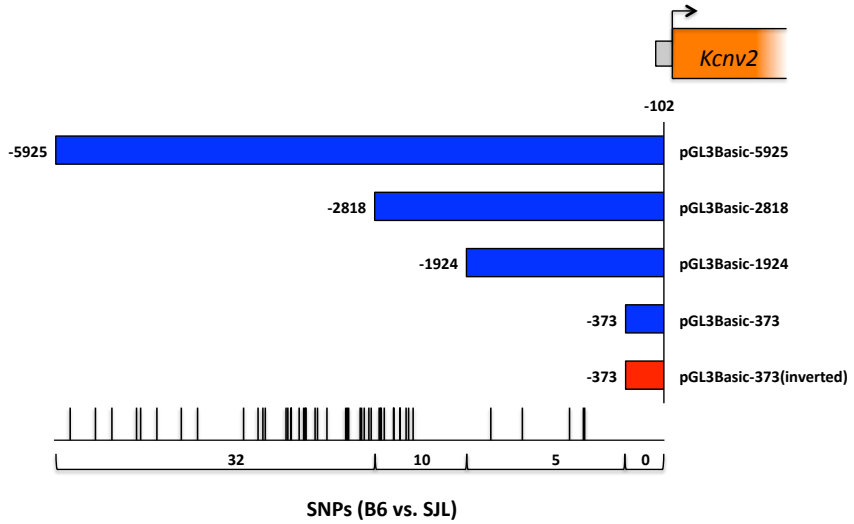

Figure 5.1 Location of *Kcnv2* Upstream SNPs
The location of sequenced and imputed SNPs between the B6 and SJL strains relative to the genomic location of promoter construct insert sequences (shown to scale). Then number of SNPs contained within each insert is shown below.

It is possible that multiple regulatory elements with opposing effects on *Kcnv2* transcription exist within the region being tested. Testing multiple constructs within the 5' deletion series should help to identify these elements, but it may be necessary to create additional constructs to evaluate the opposing elements independently. Furthermore, our data suggested that *Kcnv2* expression is actively repressed in the mouse brain-derived Neuro-2a cell line (Chapter III). To circumvent this problem and to ensure that all of the relevant trans-regulatory elements are expressed, the comparison of B6 and SJL-derived constructs should be performed in hippocampal neurons cultured from B6xSJL.F1 mice.

Effects of 3' UTR Sequence Variation on Kcnv2 Expression

To determine whether sequence variation in the 3' UTR affects mRNA stability, cultured hippocampal neurons from B6xSJL.F1 mice can be treated with Actinomycin-D to arrest transcription, and RNA samples can be taken at various time points after treatment and used as a template for an allele-specific qRT-PCR to determine if there are differences in stability between transcripts from the B6 and SJL *Kcnv2* alleles. If the *Kcnv2* mRNA degradation rates vary between strains, then the qRT-PCR data should show a more precipitous drop off in mRNA levels between time-points for one of the strains, and the ratio of B6:SJL *Kcnv2* mRNA will deviate from the expected 1:1 ratio. If there are differences in *Kcnv2* transcription between strains, then mRNA from untreated cells will also deviate from the expected 1:1 ratio. In this case, the data from each time point will need to be normalized to the ratio from untreated cells.

In vivo Evaluation of Selected Regulatory Regions

If the aforementioned *in vitro* studies suggest that sequence variation in the promoter and/or 3' UTR affects steady-state *Kcnv2* expression, then these effects can be evaluated *in vivo* in transient transgenic mice. The B6 BAC clone RP24-537C5 contains the *Kcnv2* open reading frame plus 63.6 kb upstream of the start codon and 37.3 kb downstream of the stop codon. Homologous recombination could be used to replace the B6-derived regulatory regions of interest with SJL-derived sequence. Additionally, the *Kcnv2* open reading frame could be replaced with a luciferase reporter gene, allowing transgene-derived

transcripts to be easily distinguished from endogenous *Kcnv2* transcripts. The effects of replacing the B6 sequence with SJL sequence on *Kcnv2* expression levels could then be monitored using qRT-PCR to compare luciferase transcript expression between transient transgenic mice expressing the B6-derived transgene with or without SJL-derived sequence in the potential regulatory regions of interest. Any regions that exhibit a large effect on *Kcnv2* steady-state expression when replaced with SJL-derived sequence could be further evaluated for effects on seizure susceptibility by using CRISPR technology to generate B6 Q54 mice with the region of interest replaced by SJL-derived sequence.

Circadian Regulation of Kcnv2

There is a well-documented reciprocal interaction between sleep and epilepsy [226]. Interestingly, a recent study shows that blood levels of *KCNV2* expression fluctuate with circadian cycles in humans [227]. Evidence that *Kcnv2* may be circadian regulated in mice comes from the presence of a predicted *Rora2* (a component of the mammalian circadian clock) [228, 229] binding site in the promoter region that is conserved in both mouse and human [230] and the presence of an *miR96* (a light regulated, neurosensory miRNA expressed in hair and photreceptor cells) [231] binding site in the 3' UTR [232, 233]. Intriguingly, there is a SNP between the B6 and SJL strains in the predicted *miR96* binding site. Given that *Kcnv2* expression levels contribute to epilepsy susceptibility, it may be worthwhile to determine if *Kcnv2* expression is circadian regulated in the hippocampus of Q54 mice by performing qRT-PCR on hippocampal RNA isolated

at multiple time points throughout a 48-hour period. If the data suggests that *Kcnv2* is circadian regulated, then time of day would need to be controlled for in any future experiments in which *Kcnv2* expression is a dependent variable. Furthermore, if *Kcnv2* is circadian regulated, then any *cis*-regulatory elements associated with circadian regulation (e.g. the *Rora2* and *miR96* binding sites) and in which there is sequence variation between B6 and SJL could be prioritized for further examination.

Knock-in Mouse Models of KCNB1 Mutations

The studies described in Chapter IV showed that mutations in *KCNB1* resulting in both gain-of-function and loss-of-function effects on Kv2.1 mediated potassium current are associated with severe epileptic encephalopathy. Mice lacking Kv2.1 (*Kcnb1*$^{-/-}$) have reduced thresholds to induced seizures, but they do not have spontaneous seizures [222]. This suggests that the phenotypic consequences of the gain-of-function and dominant-negative mutations we described are inherently different and more severe than a simple loss of Kv2.1-mediated current by *Kcnb1* deletion. To test this hypothesis and to better understand how these variants contribute to the epilepsy phenotype, CRISPR technology could be used to introduce each of the human mutations described in Chapter IV into mice, and the phenotypes of these mice could be compared to the phenotype of *Kcnb1* knockout mice. If the hypothesis is correct, then the mice harboring the human mutations will have a more severe phenotype than the knockout mice. The generation of the knock-in mice would also allow us to

perform additional experiments to evaluate the effects of the mutations on network hyperexcitability, as well as cognitive and motor function.

Small Molecule Screen for Specific Inhibitors of Kv2.1/Kv8.2 Mediated Potassium Current

Given the importance of Kv2.1/Kv8.2-mediated delayed-rectifier potassium current in regulating neuronal excitability and its effect on epilepsy susceptibility, a pharmalogical modulator of K_v2.1/Kv8.2 mediated potassium current would be a valuable tool. There is a paucity of pharmalogical agents that specifically target potassium channels. The anticonvulsant drug ezogabine (retigabine) interacts with K_v7.2/K_v7.3 subunit containing potassium channels to activate M-current and reduce neuronal excitability, but there are currently no specific inhibitors or activators of delayed rectifier potassium current. Such a tool would allow investigators to differentiate between Kv2.1/Kv8.2-mediated current and other endogenous potassium currents when performing *ex vivo* electrophysiological recordings. These recordings could be used to study the contribution of delayed rectifier potassium current to the overall excitability of both excitatory and inhibitory neurons in the hippocampus and cortex to better understand the physiological consequences of genetic mutations that might alter the current. Additionally, this tool could be used to study the effects of altering delayed rectifier potassium current on seizure susceptibility *in vivo*. Furthermore, such a molecule could be a candidate for further development and testing as a potential therapy for the treatment of epilepsy. Thus, a small molecule screen to discover

a specific inhibitor/activator of Kv2.1/Kv8.2 mediated potassium current would be a worthwhile endeavor.

Significance

This dissertation outlined: the validation of *Kcnv2* as a quantitative modifier of epilepsy in mice; the identification of *KCNV2* variants in pediatric epilepsy patients; the determination of *Kcnv2* regulatory regions; and the identification of *KCNB1* mutations in individuals with epileptic encephalopathy. Taken together, these studies contribute to our understanding of epilepsy by adding *KCNV2* and *KCNB1* to the growing catalogue of genes associated with epilepsy and highlight the importance of delayed-rectifier potassium current in governing neuronal excitability. More generally, these studies demonstrate both the utility of mouse models for identifying genetic modifiers of epilepsy and the potential for genetic modifiers to elucidate underlying disease mechanisms, possibly leading to more effective treatment strategies for patients.

References

1. Fisher, R.S., et al., *Epileptic seizures and epilepsy: definitions proposed by the International League Against Epilepsy (ILAE) and the International Bureau for Epilepsy (IBE).* Epilepsia, 2005. **46**(4): p. 470-2.
2. Fisher, R.S., et al., *ILAE official report: a practical clinical definition of epilepsy.* Epilepsia, 2014. **55**(4): p. 475-82.
3. England, M.J., et al., *Epilepsy across the spectrum: promoting health and understanding. A summary of the Institute of Medicine report.* Epilepsy Behav, 2012. **25**(2): p. 266-76.
4. Leonardi, M. and T.B. Ustun, *The global burden of epilepsy.* Epilepsia, 2002. **43 Suppl 6**: p. 21-5.
5. de Boer, H.M., M. Mula, and J.W. Sander, *The global burden and stigma of epilepsy.* Epilepsy Behav, 2008. **12**(4): p. 540-6.
6. World Health Organization., *International classification of functioning, disability and health : ICF*2001, Geneva: World Health Organization. iii, 299 p.
7. Institute of Medicine (U.S.). Committee on the Public Health Dimensions of the Epilepsies. and M.J. England, *Epilepsy across the spectrum : promoting health and understanding*2012, Washington, D.C.: National Academies Press. xxix, 537 p.
8. Murray, C.J.L., et al., *The global burden of disease : a comprehensive assessment of mortality and disability from diseases, injuries, and risk factors in 1990 and projected to 2020*. Global burden of disease and injury series1996, Cambridge, Mass.: Published by the Harvard School of Public Health on behalf of the World Health Organization and the World Bank ; Distributed by Harvard University Press. xxxii, 990 p.
9. Sander, J.W., *The epidemiology of epilepsy revisited.* Curr Opin Neurol, 2003. **16**(2): p. 165-70.
10. MacDonald, B.K., et al., *The incidence and lifetime prevalence of neurological disorders in a prospective community-based study in the UK.* Brain, 2000. **123 (Pt 4)**: p. 665-76.
11. Hauser, W.A., J.F. Annegers, and W.A. Rocca, *Descriptive epidemiology of epilepsy: contributions of population-based studies from Rochester, Minnesota.* Mayo Clin Proc, 1996. **71**(6): p. 576-86.
12. Hesdorffer, D.C., et al., *Estimating risk for developing epilepsy: a population-based study in Rochester, Minnesota.* Neurology, 2011. **76**(1): p. 23-7.
13. Shafer, P.O. and C. Begley, *The Human and Economic Burden of Epilepsy.* Epilepsy Behav, 2000. **1**(2): p. 91-92.
14. Gaitatzis, A., M.R. Trimble, and J.W. Sander, *The psychiatric comorbidity of epilepsy.* Acta Neurol Scand, 2004. **110**(4): p. 207-20.

15. Wilner, A.N., et al., *Common comorbidities in women and men with epilepsy and the relationship between number of comorbidities and health plan paid costs in 2010.* Epilepsy Behav, 2014. **32**: p. 15-20.
16. Deboer, H., M. Mula, and J. Sander, *The global burden and stigma of epilepsy.* Epilepsy & Behavior, 2008. **12**(4): p. 540-546.
17. Lhatoo, S.D., et al., *Mortality in epilepsy in the first 11 to 14 years after diagnosis: multivariate analysis of a long-term, prospective, population-based cohort.* Ann Neurol, 2001. **49**(3): p. 336-44.
18. Lee, B.I. and K. Heo, *Epilepsy: new genes, new technologies, new insights.* Lancet Neurol, 2014. **13**(1): p. 7-9.
19. Fazel, S., et al., *Premature mortality in epilepsy and the role of psychiatric comorbidity: a total population study.* Lancet, 2013. **382**(9905): p. 1646-54.
20. Annegers, J.F., W.A. Hauser, and L.R. Elveback, *Remission of seizures and relapse in patients with epilepsy.* Epilepsia, 1979. **20**(6): p. 729-37.
21. Jensen, F.E., *Epilepsy as a spectrum disorder: Implications from novel clinical and basic neuroscience.* Epilepsia, 2011. **52 Suppl 1**: p. 1-6.
22. Camfield, P. and C. Camfield, *Epileptic syndromes in childhood: clinical features, outcomes, and treatment.* Epilepsia, 2002. **43 Suppl 3**: p. 27-32.
23. Engel, J., Jr., *Report of the ILAE classification core group.* Epilepsia, 2006. **47**(9): p. 1558-68.
24. *Proposal for revised classification of epilepsies and epileptic syndromes. Commission on Classification and Terminology of the International League Against Epilepsy.* Epilepsia, 1989. **30**(4): p. 389-99.
25. McTague, A. and J.H. Cross, *Treatment of epileptic encephalopathies.* CNS Drugs, 2013. **27**(3): p. 175-84.
26. Berg, A.T., et al., *Revised terminology and concepts for organization of seizures and epilepsies: report of the ILAE Commission on Classification and Terminology, 2005-2009.* Epilepsia, 2010. **51**(4): p. 676-85.
27. Khan, S. and R. Al Baradie, *Epileptic encephalopathies: an overview.* Epilepsy Res Treat, 2012. **2012**: p. 403592.
28. Engel, J., Jr., *A proposed diagnostic scheme for people with epileptic seizures and with epilepsy: report of the ILAE Task Force on Classification and Terminology.* Epilepsia, 2001. **42**(6): p. 796-803.
29. Peljto, A.L., et al., *Familial risk of epilepsy: a population-based study.* Brain, 2014. **137**(Pt 3): p. 795-805.
30. Prasad, D.K., U. Satyanarayana, and A. Munshi, *Genetics of idiopathic generalized epilepsy: an overview.* Neurol India, 2013. **61**(6): p. 572-7.
31. Berkovic, S.F., et al., *Epilepsies in twins: genetics of the major epilepsy syndromes.* Ann Neurol, 1998. **43**(4): p. 435-45.
32. Inouye, E., *Observations on forty twin index cases with chronic epilepsy and their co-twins.* J Nerv Ment Dis, 1960. **130**: p. 401-16.
33. Corey, L.A., et al., *The occurrence of epilepsy and febrile seizures in Virginian and Norwegian twins.* Neurology, 1991. **41**(9): p. 1433-6.
34. Sillanpaa, M., et al., *Genetic factors in epileptic seizures: evidence from a large twin population.* Acta Neurol Scand, 1991. **84**(6): p. 523-6.

35. Weber, Y.G. and H. Lerche, *Genetic mechanisms in idiopathic epilepsies.* Dev Med Child Neurol, 2008. **50**(9): p. 648-54.
36. Nicita, F., et al., *The genetics of monogenic idiopathic epilepsies and epileptic encephalopathies.* Seizure, 2012. **21**(1): p. 3-11.
37. Kjeldsen, M.J., et al., *Genetic and environmental factors in epilepsy: a population-based study of 11900 Danish twin pairs.* Epilepsy Res, 2001. **44**(2-3): p. 167-78.
38. Biervert, C., et al., *A potassium channel mutation in neonatal human epilepsy.* Science, 1998. **279**(5349): p. 403-6.
39. Charlier, C., et al., *A pore mutation in a novel KQT-like potassium channel gene in an idiopathic epilepsy family.* Nat Genet, 1998. **18**(1): p. 53-5.
40. Singh, N.A., et al., *A novel potassium channel gene, KCNQ2, is mutated in an inherited epilepsy of newborns.* Nat Genet, 1998. **18**(1): p. 25-9.
41. Wallace, R.H., et al., *Febrile seizures and generalized epilepsy associated with a mutation in the Na+-channel beta1 subunit gene SCN1B.* Nat Genet, 1998. **19**(4): p. 366-70.
42. Escayg, A., et al., *Mutations of SCN1A, encoding a neuronal sodium channel, in two families with GEFS+2.* Nat Genet, 2000. **24**(4): p. 343-5.
43. Claes, L., et al., *De Novo Mutations in the Sodium-Channel Gene SCN1A Cause Severe Myoclonic Epilepsy of Infancy.* The American Journal of Human Genetics, 2001. **68**(6): p. 1327-1332.
44. Meisler, M.H. and J.A. Kearney, *Sodium channel mutations in epilepsy and other neurological disorders.* Journal of Clinical Investigation, 2005. **115**(8): p. 2010-2017.
45. Baulac, S., et al., *First genetic evidence of GABA(A) receptor dysfunction in epilepsy: a mutation in the gamma2-subunit gene.* Nat Genet, 2001. **28**(1): p. 46-8.
46. Haug, K., et al., *Mutations in CLCN2 encoding a voltage-gated chloride channel are associated with idiopathic generalized epilepsies.* Nat Genet, 2003. **33**(4): p. 527-32.
47. Escayg, A., et al., *Coding and noncoding variation of the human calcium-channel beta4-subunit gene CACNB4 in patients with idiopathic generalized epilepsy and episodic ataxia.* Am J Hum Genet, 2000. **66**(5): p. 1531-9.
48. Steinlein, O.K., et al., *A missense mutation in the neuronal nicotinic acetylcholine receptor alpha 4 subunit is associated with autosomal dominant nocturnal frontal lobe epilepsy.* Nat Genet, 1995. **11**(2): p. 201-3.
49. Catterall, W.A., *From ionic currents to molecular mechanisms: the structure and function of voltage-gated sodium channels.* Neuron, 2000. **26**(1): p. 13-25.
50. Guy, H.R. and P. Seetharamulu, *Molecular model of the action potential sodium channel.* Proc Natl Acad Sci U S A, 1986. **83**(2): p. 508-12.
51. Hirschberg, B., et al., *Transfer of twelve charges is needed to open skeletal muscle Na+ channels.* J Gen Physiol, 1995. **106**(6): p. 1053-68.
52. Heinemann, S.H., et al., *Calcium channel characteristics conferred on the sodium channel by single mutations.* Nature, 1992. **356**(6368): p. 441-3.

53. Trimmer, J.S. and K.J. Rhodes, *Localization of voltage-gated ion channels in mammalian brain.* Annu Rev Physiol, 2004. **66**: p. 477-519.
54. Hu, W., et al., *Distinct contributions of Na(v)1.6 and Na(v)1.2 in action potential initiation and backpropagation.* Nat Neurosci, 2009. **12**(8): p. 996-1002.
55. Meisler, M.H., J.E. O'Brien, and L.M. Sharkey, *Sodium channel gene family: epilepsy mutations, gene interactions and modifier effects.* The Journal of Physiology, 2010. **588**(11): p. 1841-1848.
56. Fujiwara, T., et al., *Mutations of sodium channel alpha subunit type 1 (SCN1A) in intractable childhood epilepsies with frequent generalized tonic-clonic seizures.* Brain, 2003. **126**(Pt 3): p. 531-46.
57. Mantegazza, M., et al., *Identification of an Nav1.1 sodium channel (SCN1A) loss-of-function mutation associated with familial simple febrile seizures.* Proc Natl Acad Sci U S A, 2005. **102**(50): p. 18177-82.
58. Lossin, C., *A catalog of SCN1A variants.* Brain Dev, 2009. **31**(2): p. 114-30.
59. Parihar, R. and S. Ganesh, *The SCN1A gene variants and epileptic encephalopathies.* J Hum Genet, 2013. **58**(9): p. 573-80.
60. Allen, A.S., et al., *De novo mutations in epileptic encephalopathies.* Nature, 2013. **501**(7466): p. 217-21.
61. Kearney, J.A., et al., *Recurrent de novo mutations of SCN1A in severe myoclonic epilepsy of infancy.* Pediatr Neurol, 2006. **34**(2): p. 116-20.
62. Yu, F.H., et al., *Reduced sodium current in GABAergic interneurons in a mouse model of severe myoclonic epilepsy in infancy.* Nat Neurosci, 2006. **9**(9): p. 1142-9.
63. Miller, A.R., et al., *Mapping genetic modifiers of survival in a mouse model of Dravet syndrome.* Genes Brain Behav, 2014. **13**(2): p. 163-72.
64. Ogiwara, I., et al., *Nav1.1 Localizes to Axons of Parvalbumin-Positive Inhibitory Interneurons: A Circuit Basis for Epileptic Seizures in Mice Carrying an Scn1a Gene Mutation.* Journal of Neuroscience, 2007. **27**(22): p. 5903-5914.
65. Han, S., et al., *Autistic-like behaviour in Scn1a+/- mice and rescue by enhanced GABA-mediated neurotransmission.* Nature, 2012. **489**(7416): p. 385-90.
66. Mistry, A.M., et al., *Strain- and age-dependent hippocampal neuron sodium currents correlate with epilepsy severity in Dravet syndrome mice.* Neurobiol Dis, 2014. **65**: p. 1-11.
67. Kamiya, K., et al., *A nonsense mutation of the sodium channel gene SCN2A in a patient with intractable epilepsy and mental decline.* J Neurosci, 2004. **24**(11): p. 2690-8.
68. Liao, Y., et al., *SCN2A mutation associated with neonatal epilepsy, late-onset episodic ataxia, myoclonus, and pain.* Neurology, 2010. **75**(16): p. 1454-8.
69. Ito, M., et al., *Seizure phenotypes of a family with missense mutations in SCN2A.* Pediatr Neurol, 2004. **31**(2): p. 150-2.

70. Shi, X., et al., *Missense mutation of the sodium channel gene SCN2A causes Dravet syndrome.* Brain and Development, 2009. **31**(10): p. 758-762.
71. Kearney, J.A., et al., *A gain-of-function mutation in the sodium channel gene Scn2a results in seizures and behavioral abnormalities.* Neuroscience, 2001. **102**(2): p. 307-17.
72. Kile, K.B., N. Tian, and D.M. Durand, *Scn2asodium channel mutation results in hyperexcitability in the hippocampus in vitro.* Epilepsia, 2008. **49**(3): p. 488-499.
73. Hille, B., *Ion channels of excitable membranes*. 3rd ed2001, Sunderland, Mass.: Sinauer. xviii, 814 p., 8 p. of plates.
74. Misonou, H. and J.S. Trimmer, *Determinants of voltage-gated potassium channel surface expression and localization in Mammalian neurons.* Crit Rev Biochem Mol Biol, 2004. **39**(3): p. 125-45.
75. Levitan, I.B., *Modulation of ion channels by protein phosphorylation. How the brain works.* Adv Second Messenger Phosphoprotein Res, 1999. **33**: p. 3-22.
76. Stuhmer, W., et al., *Structural parts involved in activation and inactivation of the sodium channel.* Nature, 1989. **339**(6226): p. 597-603.
77. Heginbotham, L., T. Abramson, and R. MacKinnon, *A functional connection between the pores of distantly related ion channels as revealed by mutant K+ channels.* Science, 1992. **258**(5085): p. 1152-5.
78. Doyle, D.A., et al., *The structure of the potassium channel: molecular basis of K+ conduction and selectivity.* Science, 1998. **280**(5360): p. 69-77.
79. Dibb, K.M., et al., *Molecular basis of ion selectivity, block, and rectification of the inward rectifier Kir3.1/Kir3.4 K(+) channel.* J Biol Chem, 2003. **278**(49): p. 49537-48.
80. Morais-Cabral, J.H., Y. Zhou, and R. MacKinnon, *Energetic optimization of ion conduction rate by the K+ selectivity filter.* Nature, 2001. **414**(6859): p. 37-42.
81. Zhou, Y., et al., *Chemistry of ion coordination and hydration revealed by a K+ channel-Fab complex at 2.0 A resolution.* Nature, 2001. **414**(6859): p. 43-8.
82. Choi, M., et al., *K+ channel mutations in adrenal aldosterone-producing adenomas and hereditary hypertension.* Science, 2011. **331**(6018): p. 768-72.
83. Heginbotham, L., et al., *Mutations in the K+ channel signature sequence.* Biophys J, 1994. **66**(4): p. 1061-7.
84. Navarro, B., et al., *Nonselective and G betagamma-insensitive weaver K+ channels.* Science, 1996. **272**(5270): p. 1950-3.
85. Ottschytsch, N., et al., *Obligatory heterotetramerization of three previously uncharacterized Kv channel alpha-subunits identified in the human genome.* Proc Natl Acad Sci U S A, 2002. **99**(12): p. 7986-91.

86. Czirjak, G., Z.E. Toth, and P. Enyedi, *Characterization of the heteromeric potassium channel formed by kv2.1 and the retinal subunit kv8.2 in Xenopus oocytes.* J Neurophysiol, 2007. **98**(3): p. 1213-22.
87. Coetzee, W.A., et al., *Molecular diversity of K+ channels.* Ann N Y Acad Sci, 1999. **868**: p. 233-85.
88. Christie, M.J., et al., *Heteropolymeric potassium channels expressed in Xenopus oocytes from cloned subunits.* Neuron, 1990. **4**(3): p. 405-11.
89. Isacoff, E.Y., Y.N. Jan, and L.Y. Jan, *Evidence for the formation of heteromultimeric potassium channels in Xenopus oocytes.* Nature, 1990. **345**(6275): p. 530-4.
90. McCormack, K., et al., *Shaker K+ channel subunits from heteromultimeric channels with novel functional properties.* Biochem Biophys Res Commun, 1990. **171**(3): p. 1361-71.
91. Ruppersberg, J.P., et al., *Heteromultimeric channels formed by rat brain potassium-channel proteins.* Nature, 1990. **345**(6275): p. 535-7.
92. Weiser, M., et al., *Differential expression of Shaw-related K+ channels in the rat central nervous system.* J Neurosci, 1994. **14**(3 Pt 1): p. 949-72.
93. Sheng, M., et al., *Presynaptic A-current based on heteromultimeric K+ channels detected in vivo.* Nature, 1993. **365**(6441): p. 72-5.
94. Wang, H., et al., *Heteromultimeric K+ channels in terminal and juxtaparanodal regions of neurons.* Nature, 1993. **365**(6441): p. 75-9.
95. Hugnot, J.P., et al., *Kv8.1, a new neuronal potassium channel subunit with specific inhibitory properties towards Shab and Shaw channels.* EMBO J, 1996. **15**(13): p. 3322-31.
96. Salinas, M., et al., *Modes of regulation of shab K+ channel activity by the Kv8.1 subunit.* J Biol Chem, 1997. **272**(13): p. 8774-80.
97. Salinas, M., et al., *New modulatory alpha subunits for mammalian Shab K+ channels.* J Biol Chem, 1997. **272**(39): p. 24371-9.
98. Patel, A.J., M. Lazdunski, and E. Honore, *Kv2.1/Kv9.3, a novel ATP-dependent delayed-rectifier K+ channel in oxygen-sensitive pulmonary artery myocytes.* EMBO J, 1997. **16**(22): p. 6615-25.
99. Stocker, M., M. Hellwig, and D. Kerschensteiner, *Subunit assembly and domain analysis of electrically silent K+ channel alpha-subunits of the rat Kv9 subfamily.* J Neurochem, 1999. **72**(4): p. 1725-34.
100. Post, M.A., G.E. Kirsch, and A.M. Brown, *Kv2.1 and electrically silent Kv6.1 potassium channel subunits combine and express a novel current.* FEBS Lett, 1996. **399**(1-2): p. 177-82.
101. Kramer, J.W., et al., *Modulation of potassium channel gating by coexpression of Kv2.1 with regulatory Kv5.1 or Kv6.1 alpha-subunits.* Am J Physiol, 1998. **274**(6 Pt 1): p. C1501-10.
102. D'Adamo, M.C., et al., *K(+) channelepsy: progress in the neurobiology of potassium channels and epilepsy.* Front Cell Neurosci, 2013. **7**: p. 134.
103. Assaf, S.Y. and S.H. Chung, *Release of endogenous Zn2+ from brain tissue during activity.* Nature, 1984. **308**(5961): p. 734-6.

104. Browne, D.L., et al., *Episodic ataxia/myokymia syndrome is associated with point mutations in the human potassium channel gene, KCNA1.* Nat Genet, 1994. **8**(2): p. 136-40.
105. Guan, D., et al., *Expression and biophysical properties of Kv1 channels in supragranular neocortical pyramidal neurones.* J Physiol, 2006. **571**(Pt 2): p. 371-89.
106. Adelman, J.P., et al., *Episodic ataxia results from voltage-dependent potassium channels with altered functions.* Neuron, 1995. **15**(6): p. 1449-54.
107. D'Adamo, M.C., et al., *Episodic ataxia type-1 mutations in the hKv1.1 cytoplasmic pore region alter the gating properties of the channel.* EMBO J, 1998. **17**(5): p. 1200-7.
108. Zuberi, S.M., et al., *A novel mutation in the human voltage-gated potassium channel gene (Kv1.1) associates with episodic ataxia type 1 and sometimes with partial epilepsy.* Brain, 1999. **122 (Pt 5)**: p. 817-25.
109. Geiger, J.R. and P. Jonas, *Dynamic control of presynaptic Ca(2+) inflow by fast-inactivating K(+) channels in hippocampal mossy fiber boutons.* Neuron, 2000. **28**(3): p. 927-39.
110. Cusimano, A., M. Cristina D'Adamo, and M. Pessia, *An episodic ataxia type-1 mutation in the S1 segment sensitises the hKv1.1 potassium channel to extracellular Zn2+.* FEBS Lett, 2004. **576**(1-2): p. 237-44.
111. Imbrici, P., et al., *Episodic ataxia type 1 mutations in the KCNA1 gene impair the fast inactivation properties of the human potassium channels Kv1.4-1.1/Kvbeta1.1 and Kv1.4-1.1/Kvbeta1.2.* Eur J Neurosci, 2006. **24**(11): p. 3073-83.
112. Imbrici, P., et al., *Episodic ataxia type 1 mutation F184C alters Zn2+-induced modulation of the human K+ channel Kv1.4-Kv1.1/Kvbeta1.1.* Am J Physiol Cell Physiol, 2007. **292**(2): p. C778-87.
113. Heilstedt, H.A., et al., *Loss of the potassium channel beta-subunit gene, KCNAB2, is associated with epilepsy in patients with 1p36 deletion syndrome.* Epilepsia, 2001. **42**(9): p. 1103-11.
114. Kalachikov, S., et al., *Mutations in LGI1 cause autosomal-dominant partial epilepsy with auditory features.* Nat Genet, 2002. **30**(3): p. 335-41.
115. Morante-Redolat, J.M., et al., *Mutations in the LGI1/Epitempin gene on 10q24 cause autosomal dominant lateral temporal epilepsy.* Hum Mol Genet, 2002. **11**(9): p. 1119-28.
116. Singh, B., et al., *A Kv4.2 truncation mutation in a patient with temporal lobe epilepsy.* Neurobiol Dis, 2006. **24**(2): p. 245-53.
117. Jorge, B.S., et al., *Voltage-gated potassium channel KCNV2 (Kv8.2) contributes to epilepsy susceptibility.* Proceedings of the National Academy of Sciences, 2011. **108**(13): p. 5443-5448.
118. Keller, D.I., et al., *Characterization of novel KCNH2 mutations in type 2 long QT syndrome manifesting as seizures.* Can J Cardiol, 2009. **25**(8): p. 455-62.

119. Omichi, C., Y. Momose, and S. Kitahara, *Congenital long QT syndrome presenting with a history of epilepsy: misdiagnosis or relationship between channelopathies of the heart and brain?* Epilepsia, 2010. **51**(2): p. 289-92.
120. Tu, E., et al., *Post-mortem review and genetic analysis of sudden unexpected death in epilepsy (SUDEP) cases.* Brain Pathol, 2011. **21**(2): p. 201-8.
121. Zamorano-Leon, J.J., et al., *KCNH2 gene mutation: a potential link between epilepsy and long QT-2 syndrome.* J Neurogenet, 2012. **26**(3-4): p. 382-6.
122. Brown, D.A. and P.R. Adams, *Muscarinic suppression of a novel voltage-sensitive K+ current in a vertebrate neurone.* Nature, 1980. **283**(5748): p. 673-6.
123. Delmas, P. and D.A. Brown, *Pathways modulating neural KCNQ/M (Kv7) potassium channels.* Nat Rev Neurosci, 2005. **6**(11): p. 850-62.
124. Hahn, A. and B.A. Neubauer, *Sodium and potassium channel dysfunctions in rare and common idiopathic epilepsy syndromes.* Brain Dev, 2009. **31**(7): p. 515-20.
125. Singh, N.A., et al., *KCNQ2 and KCNQ3 potassium channel genes in benign familial neonatal convulsions: expansion of the functional and mutation spectrum.* Brain, 2003. **126**(Pt 12): p. 2726-37.
126. Orhan, G., et al., *Dominant-negative effects of KCNQ2 mutations are associated with epileptic encephalopathy.* Ann Neurol, 2014. **75**(3): p. 382-94.
127. Miceli, F., et al., *Genotype-phenotype correlations in neonatal epilepsies caused by mutations in the voltage sensor of K(v)7.2 potassium channel subunits.* Proc Natl Acad Sci U S A, 2013. **110**(11): p. 4386-91.
128. Schroeder, B.C., et al., *Moderate loss of function of cyclic-AMP-modulated KCNQ2/KCNQ3 K+ channels causes epilepsy.* Nature, 1998. **396**(6712): p. 687-90.
129. Watanabe, H., et al., *Disruption of the epilepsy KCNQ2 gene results in neural hyperexcitability.* J Neurochem, 2000. **75**(1): p. 28-33.
130. Singh, N.A., et al., *Mouse models of human KCNQ2 and KCNQ3 mutations for benign familial neonatal convulsions show seizures and neuronal plasticity without synaptic reorganization.* J Physiol, 2008. **586**(14): p. 3405-23.
131. Cooper, E.C., *Potassium Channels (including KCNQ) and Epilepsy.* 2012.
132. Main, M.J., et al., *Modulation of KCNQ2/3 potassium channels by the novel anticonvulsant retigabine.* Mol Pharmacol, 2000. **58**(2): p. 253-62.
133. Alekov, A., et al., *A sodium channel mutation causing epilepsy in man exhibits subtle defects in fast inactivation and activation in vitro.* J Physiol, 2000. **529 Pt 3**: p. 533-9.
134. Raol, Y.H., et al., *A KCNQ channel opener for experimental neonatal seizures and status epilepticus.* Ann Neurol, 2009. **65**(3): p. 326-36.
135. Wallace, R.H., et al., *Mutant GABA(A) receptor gamma2-subunit in childhood absence epilepsy and febrile seizures.* Nat Genet, 2001. **28**(1): p. 49-52.

136. Baulac, S., et al., *A Second Locus for Familial Generalized Epilepsy with Febrile Seizures Plus Maps to Chromosome 2q21-q33.* The American Journal of Human Genetics, 1999. **65**(4): p. 1078-1085.
137. Tan, E.H., et al., *Generalized epilepsy with febrile seizure plus (GEFS+) spectrum: Novel de novo mutation of SCN1A detected in a Malaysian patient.* J Pediatr Neurosci, 2012. **7**(2): p. 123-5.
138. Shi, X., et al., *Missense mutation of the sodium channel gene SCN2A causes Dravet syndrome.* Brain Dev, 2009. **31**(10): p. 758-62.
139. Wang, J.W., et al., *Prevalence of SCN1A mutations in children with suspected Dravet syndrome and intractable childhood epilepsy.* Epilepsy Res, 2012. **102**(3): p. 195-200.
140. Bergren, S.K., et al., *Genetic modifiers affecting severity of epilepsy caused by mutation of sodium channelScn2a.* Mammalian Genome, 2005. **16**(9): p. 683-690.
141. Kearney, J.A., *Genetic modifiers of neurological disease.* Curr Opin Genet Dev, 2011. **21**(3): p. 349-53.
142. Giess, R., et al., *Early onset of severe familial amyotrophic lateral sclerosis with a SOD-1 mutation: potential impact of CNTF as a candidate modifier gene.* Am J Hum Genet, 2002. **70**(5): p. 1277-86.
143. Carrasquillo, M.M., et al., *Genetic variation in PCDH11X is associated with susceptibility to late-onset Alzheimer's disease.* Nat Genet, 2009. **41**(2): p. 192-8.
144. Rubinsztein, D.C., et al., *Genotypes at the GluR6 kainate receptor locus are associated with variation in the age of onset of Huntington disease.* Proc Natl Acad Sci U S A, 1997. **94**(8): p. 3872-6.
145. Au, K.S., C.H. Ward, and H. Northrup, *Tuberous sclerosis complex: disease modifiers and treatments.* Curr Opin Pediatr, 2008. **20**(6): p. 628-33.
146. Cantrell, V.A., et al., *Interactions between Sox10 and EdnrB modulate penetrance and severity of aganglionosis in the Sox10Dom mouse model of Hirschsprung disease.* Hum Mol Genet, 2004. **13**(19): p. 2289-301.
147. Owens, S.E., et al., *Genome-wide linkage identifies novel modifier loci of aganglionosis in the Sox10Dom model of Hirschsprung disease.* Human Molecular Genetics, 2005. **14**(11): p. 1549-1558.
148. Garred, P., et al., *Association of mannose-binding lectin gene heterogeneity with severity of lung disease and survival in cystic fibrosis.* J Clin Invest, 1999. **104**(4): p. 431-7.
149. Bergren, S.K., E.D. Rutter, and J.A. Kearney, *Fine mapping of an epilepsy modifier gene on mouse Chromosome 19.* Mammalian Genome, 2009. **20**(6): p. 359-366.
150. Misonou, H., D.P. Mohapatra, and J.S. Trimmer, *Kv2.1: A Voltage-Gated K+ Channel Critical to Dynamic Control of Neuronal Excitability.* NeuroToxicology, 2005. **26**(5): p. 743-752.
151. Du, J., et al., *Frequency-dependent regulation of rat hippocampal somato-dendritic excitability by the K+ channel subunit Kv2.1.* J Physiol, 2000. **522 Pt 1**: p. 19-31.

152. Guan, D., et al., *Kv2 subunits underlie slowly inactivating potassium current in rat neocortical pyramidal neurons.* J Physiol, 2007. **581**(Pt 3): p. 941-60.
153. Guan, D., et al., *Postnatal development of A-type and Kv1- and Kv2-mediated potassium channel currents in neocortical pyramidal neurons.* J Neurophysiol, 2011. **105**(6): p. 2976-88.
154. Guan, D., W.E. Armstrong, and R.C. Foehring, *Kv2 channels regulate firing rate in pyramidal neurons from rat sensorimotor cortex.* J Physiol, 2013. **591**(Pt 19): p. 4807-25.
155. Liu, P.W. and B.P. Bean, *Kv2 channel regulation of action potential repolarization and firing patterns in superior cervical ganglion neurons and hippocampal CA1 pyramidal neurons.* J Neurosci, 2014. **34**(14): p. 4991-5002.
156. Mohapatra, D.P., et al., *Regulation of intrinsic excitability in hippocampal neurons by activity-dependent modulation of the KV2.1 potassium channel.* Channels (Austin), 2009. **3**(1): p. 46-56.
157. Misonou, H., et al., *Regulation of ion channel localization and phosphorylation by neuronal activity.* Nat Neurosci, 2004. **7**(7): p. 711-8.
158. Allen, P. and Allen Institute for Brain Science., *Allen brain atlas*, 2004, Allen Institute for Brain Science: Seattle, Wash.
159. Hwang, P.M., et al., *A novel K+ channel with unique localizations in mammalian brain: molecular cloning and characterization.* Neuron, 1992. **8**(3): p. 473-81.
160. Hwang, P.M., et al., *Contrasting immunohistochemical localizations in rat brain of two novel K+ channels of the Shab subfamily.* J Neurosci, 1993. **13**(4): p. 1569-76.
161. Lein, E.S., et al., *Genome-wide atlas of gene expression in the adult mouse brain.* Nature, 2007. **445**(7124): p. 168-76.
162. Maletic-Savatic, M., N.J. Lenn, and J.S. Trimmer, *Differential spatiotemporal expression of K+ channel polypeptides in rat hippocampal neurons developing in situ and in vitro.* J Neurosci, 1995. **15**(5 Pt 2): p. 3840-51.
163. Hauser, W.A., J.F. Annegers, and L.T. Kurland, *Incidence of epilepsy and unprovoked seizures in Rochester, Minnesota: 1935-1984.* Epilepsia, 1993. **34**(3): p. 453-68.
164. Programme for Neurological Diseases and Neuroscience., et al., *Atlas : epilepsy care in the world, 2005*2005, Geneva: Programme for Neurological Diseases and Neuroscience, Department of Mental Health and Substance Abuse, World Health Organization. 91 p.
165. Turnbull, J., et al., *Sacred disease secrets revealed: the genetics of human epilepsy.* Human Molecular Genetics, 2005. **14**(17): p. 2491-2500.
166. Murakoshi, H. and J.S. Trimmer, *Identification of the Kv2.1 K+ channel as a major component of the delayed rectifier K+ current in rat hippocampal neurons.* J Neurosci, 1999. **19**(5): p. 1728-35.
167. Allen Mouse Brain Atlas [Internet]. *Seattle, WA): Allen Institute for Brain Science. 2009. Available from: http://www.brain-map.org*.

168. Forss-Petter, S., et al., *Transgenic mice expressing beta-galactosidase in mature neurons under neuron-specific enolase promoter control.* Neuron, 1990. **5**(2): p. 187-97.
169. Livak, K.J. and T.D. Schmittgen, *Analysis of relative gene expression data using real-time quantitative PCR and the 2(-Delta Delta C(T)) Method.* Methods, 2001. **25**(4): p. 402-8.
170. Pfaffl, M.W., G.W. Horgan, and L. Dempfle, *Relative expression software tool (REST) for group-wise comparison and statistical analysis of relative expression results in real-time PCR.* Nucleic Acids Res, 2002. **30**(9): p. e36.
171. Vanoye, C.G., et al., *Distinct subdomains of the KCNQ1 S6 segment determine channel modulation by different KCNE subunits.* J Gen Physiol, 2009. **134**(3): p. 207-17.
172. Plummer, N.W., et al., *Exon organization, coding sequence, physical mapping, and polymorphic intragenic markers for the human neuronal sodium channel gene SCN8A.* Genomics, 1998. **54**(2): p. 287-96.
173. Hamill, O.P., et al., *Improved patch-clamp techniques for high-resolution current recording from cells and cell-free membrane patches.* Pflugers Arch, 1981. **391**(2): p. 85-100.
174. Ben Salah, S., et al., *Novel KCNV2 mutations in cone dystrophy with supernormal rod electroretinogram.* Am J Ophthalmol, 2008. **145**(6): p. 1099-106.
175. Thiagalingam, S., et al., *Novel mutations in the KCNV2 gene in patients with cone dystrophy and a supernormal rod electroretinogram.* Ophthalmic Genet, 2007. **28**(3): p. 135-42.
176. Wissinger, B., et al., *Cone dystrophy with supernormal rod response is strictly associated with mutations in KCNV2.* Invest Ophthalmol Vis Sci, 2008. **49**(2): p. 751-7.
177. Wu, H., et al., *Mutations in the gene KCNV2 encoding a voltage-gated potassium channel subunit cause "cone dystrophy with supernormal rod electroretinogram" in humans.* Am J Hum Genet, 2006. **79**(3): p. 574-9.
178. Glasscock, E., et al., *Masking epilepsy by combining two epilepsy genes.* Nat Neurosci, 2007. **10**(12): p. 1554-8.
179. Kearney, J.A., et al., *Severe epilepsy resulting from genetic interaction between Scn2a and Kcnq2.* Hum Mol Genet, 2006. **15**(6): p. 1043-8.
180. Martin, M.S., et al., *The voltage-gated sodium channel Scn8a is a genetic modifier of severe myoclonic epilepsy of infancy.* Hum Mol Genet, 2007. **16**(23): p. 2892-9.
181. Yoon, D., et al., *Economic impact of epilepsy in the United States.* Epilepsia, 2009. **50**(10): p. 2186-91.
182. SCN1A Variant Database [Internet], *Antwerp, Belgium): VIB Department of Molecular Genetics. 2008.* http://www.molgen.vib-ua.be/SCN1AMutations/Home/Default.cfm.
183. Claes, L.R., et al., *The SCN1A variant database: a novel research and diagnostic tool.* Hum Mutat, 2009. **30**(10): p. E904-20.

184. Epilepsies, I.L.A.E.C.o.C., *Genetic determinants of common epilepsies: a meta-analysis of genome-wide association studies.* Lancet Neurol, 2014. **13**(9): p. 893-903.
185. Kasperaviciute, D., et al., *Epilepsy, hippocampal sclerosis and febrile seizures linked by common genetic variation around SCN1A.* Brain, 2013. **136**(Pt 10): p. 3140-50.
186. Guo, Y., et al., *Two-stage genome-wide association study identifies variants in CAMSAP1L1 as susceptibility loci for epilepsy in Chinese.* Hum Mol Genet, 2012. **21**(5): p. 1184-9.
187. Maletic-Savatic, M., R. Malinow, and K. Svoboda, *Rapid dendritic morphogenesis in CA1 hippocampal dendrites induced by synaptic activity.* Science, 1999. **283**(5409): p. 1923-7.
188. Flicek, P., et al., *Ensembl 2012.* Nucleic Acids Res, 2012. **40**(Database issue): p. D84-90.
189. Kent, W.J., et al., *The human genome browser at UCSC.* Genome Res, 2002. **12**(6): p. 996-1006.
190. Wang, J., R.W. Williams, and K.F. Manly, *WebQTL: web-based complex trait analysis.* Neuroinformatics, 2003. **1**(4): p. 299-308.
191. Chen, J.-M., et al., *Genomic rearrangements in inherited disease and cancer.* Seminars in Cancer Biology, 2010. **20**(4): p. 222-233.
192. Knight, J.C., *Regulatory polymorphisms underlying complex disease traits.* Journal of Molecular Medicine, 2004. **83**(2): p. 97-109.
193. Kapeller, J., et al., *First evidence for an association of a functional variant in the microRNA-510 target site of the serotonin receptor-type 3E gene with diarrhea predominant irritable bowel syndrome.* Human Molecular Genetics, 2008. **17**(19): p. 2967-2977.
194. Collaco, J.M. and G.R. Cutting, *Update on gene modifiers in cystic fibrosis.* Current Opinion in Pulmonary Medicine, 2008. **14**(6): p. 559-566.
195. Nakayama, T., et al., *Deletions of SCN1A 5' genomic region with promoter activity in Dravet syndrome.* Hum Mutat, 2010. **31**(7): p. 820-9.
196. Sandelin, A., et al., *Mammalian RNA polymerase II core promoters: insights from genome-wide studies.* Nat Rev Genet, 2007. **8**(6): p. 424-36.
197. Frith, M.C., et al., *A code for transcription initiation in mammalian genomes.* Genome Res, 2008. **18**(1): p. 1-12.
198. Berg, A.T., T. Loddenkemper, and C.B. Baca, *Diagnostic delays in children with early onset epilepsy: impact, reasons, and opportunities to improve care.* Epilepsia, 2014. **55**(1): p. 123-32.
199. Brunklaus, A., et al., *The clinical utility of an SCN1A genetic diagnosis in infantile-onset epilepsy.* Dev Med Child Neurol, 2013. **55**(2): p. 154-61.
200. Hirose, S., et al., *SCN1A testing for epilepsy: application in clinical practice.* Epilepsia, 2013. **54**(5): p. 946-52.
201. Carvill, G.L., et al., *Targeted resequencing in epileptic encephalopathies identifies de novo mutations in CHD2 and SYNGAP1.* Nat Genet, 2013. **45**(7): p. 825-30.

202. O'Brien, J.E. and M.H. Meisler, *Sodium channel SCN8A (Nav1.6): properties and de novo mutations in epileptic encephalopathy and intellectual disability.* Front Genet, 2013. **4**: p. 213.
203. Nava, C., et al., *De novo mutations in HCN1 cause early infantile epileptic encephalopathy.* Nat Genet, 2014. **46**(6): p. 640-5.
204. Veeramah, K.R., et al., *Exome sequencing reveals new causal mutations in children with epileptic encephalopathies.* Epilepsia, 2013. **54**(7): p. 1270-81.
205. O'Roak, B.J., et al., *Sporadic autism exomes reveal a highly interconnected protein network of de novo mutations.* Nature, 2012. **485**(7397): p. 246-50.
206. Rauch, A., et al., *Range of genetic mutations associated with severe non-syndromic sporadic intellectual disability: an exome sequencing study.* Lancet, 2012. **380**(9854): p. 1674-82.
207. Sanders, S.J., et al., *De novo mutations revealed by whole-exome sequencing are strongly associated with autism.* Nature, 2012. **485**(7397): p. 237-41.
208. Abou-Khalil, B., et al., *The epilepsy phenome/genome project.* Clin Trials, 2013. **10**(4): p. 568-86.
209. Li, H. and R. Durbin, *Fast and accurate short read alignment with Burrows-Wheeler transform.* Bioinformatics, 2009. **25**(14): p. 1754-60.
210. McKenna, A., et al., *The Genome Analysis Toolkit: a MapReduce framework for analyzing next-generation DNA sequencing data.* Genome Res, 2010. **20**(9): p. 1297-303.
211. DePristo, M.A., et al., *A framework for variation discovery and genotyping using next-generation DNA sequencing data.* Nat Genet, 2011. **43**(5): p. 491-8.
212. Van der Auwera, G.A., et al., *From FastQ Data to High-Confidence Variant Calls: The Genome Analysis Toolkit Best Practices Pipeline*, in *Current Protocols in Bioinformatics*2002, John Wiley & Sons, Inc.
213. Abyzov, A., et al., *CNVnator: an approach to discover, genotype, and characterize typical and atypical CNVs from family and population genome sequencing.* Genome Res, 2011. **21**(6): p. 974-84.
214. Chen, Y.Z., et al., *Gain-of-function ADCY5 mutations in familial dyskinesia with facial myokymia.* Ann Neurol, 2014. **75**(4): p. 542-9.
215. Altshuler, D.M., et al., *Integrating common and rare genetic variation in diverse human populations.* Nature, 2010. **467**(7311): p. 52-8.
216. Abecasis, G.R., et al., *An integrated map of genetic variation from 1,092 human genomes.* Nature, 2012. **491**(7422): p. 56-65.
217. Bailey, J.A., et al., *Recent segmental duplications in the human genome.* Science, 2002. **297**(5583): p. 1003-7.
218. O'Roak, B.J., et al., *Multiplex targeted sequencing identifies recurrently mutated genes in autism spectrum disorders.* Science, 2012. **338**(6114): p. 1619-22.
219. Long, S.B., et al., *Atomic structure of a voltage-dependent K+ channel in a lipid membrane-like environment.* Nature, 2007. **450**(7168): p. 376-82.

220. Sievers, F., et al., *Fast, scalable generation of high-quality protein multiple sequence alignments using Clustal Omega.* Mol Syst Biol, 2011. **7**: p. 539.
221. Consiglio, J.F., P. Andalib, and S.J. Korn, *Influence of pore residues on permeation properties in the Kv2.1 potassium channel. Evidence for a selective functional interaction of K+ with the outer vestibule.* J Gen Physiol, 2003. **121**(2): p. 111-24.
222. Speca, D.J., et al., *Deletion of the Kv2.1 delayed rectifier potassium channel leads to neuronal and behavioral hyperexcitability.* Genes Brain Behav, 2014. **13**(4): p. 394-408.
223. Moulard, B., et al., *Identification of a New Locus for Generalized Epilepsy with Febrile Seizures Plus (GEFS+) on Chromosome 2q24-q33.* The American Journal of Human Genetics, 1999. **65**(5): p. 1396-1400.
224. Meisler, M.H. and J.A. Kearney, *Sodium channel mutations in epilepsy and other neurological disorders.* J Clin Invest, 2005. **115**(8): p. 2010-7.
225. Blake, J.A., et al., *The Mouse Genome Database: integration of and access to knowledge about the laboratory mouse.* Nucleic Acids Res, 2014. **42**(Database issue): p. D810-7.
226. Derry, C.P. and S. Duncan, *Sleep and epilepsy.* Epilepsy Behav, 2013. **26**(3): p. 394-404.
227. Moller-Levet, C.S., et al., *Effects of insufficient sleep on circadian rhythmicity and expression amplitude of the human blood transcriptome.* Proc Natl Acad Sci U S A, 2013. **110**(12): p. E1132-41.
228. Kamphuis, W., et al., *Circadian expression of clock genes and clock-controlled genes in the rat retina.* Biochem Biophys Res Commun, 2005. **330**(1): p. 18-26.
229. Sato, T.K., et al., *A functional genomics strategy reveals Rora as a component of the mammalian circadian clock.* Neuron, 2004. **43**(4): p. 527-37.
230. Loots, G.G. and I. Ovcharenko, *rVISTA 2.0: evolutionary analysis of transcription factor binding sites.* Nucleic Acids Res, 2004. **32**(Web Server issue): p. W217-21.
231. Griffiths-Jones, S., et al., *miRBase: tools for microRNA genomics.* Nucleic Acids Res, 2008. **36**(Database issue): p. D154-8.
232. Wang, X. and I.M. El Naqa, *Prediction of both conserved and nonconserved microRNA targets in animals.* Bioinformatics, 2008. **24**(3): p. 325-32.
233. Wang, X., *miRDB: a microRNA target prediction and functional annotation database with a wiki interface.* RNA, 2008. **14**(6): p. 1012-7.